A SCALED APPROACH FOR IMPROVED HUMAN-ELEPHANT RELATIONSHIPS: MODELING DRIVERS OF CONFLICT IN NORTHWESTERN ZIMBABWE

by

KATHERINE ELIZABETH MARKHAM

(Under the Direction of MARGUERITE MADDEN)

ABSTRACT

Humans and wildlife are increasingly coming into contact with each other in interactions that are often adverse. Understanding such interactions requires ascertaining how patterns and processes operate at multiple scales. Conservation science's understanding of broad ecological patterns and theories is constructed by examining local patterns and principles. Consequently, it is imperative wildlife coexistence be investigated at multiple scales to identify the most appropriate spatial and temporal resolutions for local contexts. In the region south of Victoria Falls, Zimbabwe, humans and elephants contend for space and resources amid seasonal fluctuations. Erratic precipitation and harsh growing conditions magnify this competition. The overarching goal of this research is to ameliorate human-elephant relations using geospatial analysis. This work uses geospatial analysis with scale acting as the pivotal nexus and conceptual framework. Following a review of methods for scaling remotely sensed data, land cover is classified at multiple spatial resolutions and different seasons to understand the spatial and temporal scale necessary for documenting changes in vegetation condition. Machine learning is used to model where conflict occurs and to determine which environmental and anthropogenic factors are most important for human-elephant conflict modeling in this region. In contrast to regions such as Hwange National Park in Zimbabwe and protected areas in Botswana and Kenya, little has been published about human-elephant conflict in this specific region. Findings engender

greater precision in conflict mitigation efforts and enhance our scientific understanding of scaling processes and human-elephant relations.

INDEX WORDS: Human-wildlife conflict, landscape ecology, geospatial analysis, machine learning, remote sensing

A SCALED APPROACH FOR IMPROVED HUMAN-ELEPGANT RELATIONSHIPS: MODELING DRIVERS OF CONFLICT IN NORTHWESTERN ZIMBABWE

by

KATHERINE ELIZABETH MARKHAM

BS, The George Washington University, 2011

MA, University of Victoria, 2014

MS, Clark University, 2017

A Dissertation Submitted to the Graduate Faculty of The University of Georgia in Partial Fulfillment of the Requirements for the Degree

DOCTOR OF PHILOSOPHY

ATHENS, GEORGIA

2023

A SCALED APPROACH FOR IMPROVED HUMAN-ELEPGANT RELATIONSHIPS: MODELING DRIVERS OF CONFLICT IN NORTHWESTERN ZIMBABWE

by

KATHERINE ELIZABETH MARKHAM

Major Professor:	Marguerite Madden
Committee:	Sergio Bernardes
	Andrew Grundstein
	Ferrell (Loki) Osborn
	Xiaobai (Angela) Yao

Electronic Version Approved:

Ron Walcott
Vice Provost for Graduate Education and Dean of the Graduate School
The University of Georgia
August 2023

DEDICATION

Dedicated to human-elephant conflict victims and their families and loved ones.

ACKNOWLEDGEMENTS

I would like to express my sincere gratitude to Marguerite Madden for her exceptional guidance and support throughout this project. One of the most intelligent but also one of the kindest women I know, she has played a crucial role in helping me organize my ideas and enhance their coherence. Marguerite has broadened and deepened my understanding of ecology and geospatial analysis. Always prioritizing the needs of her students, Marguerite allows her students to learn and grow in their own way. I am truly thankful to her for taking a chance on me.

I am also deeply thankful to the members of my committee for their unwavering support and guidance. Each one of them has contributed significantly to my knowledge and growth, and their critiques have always been delivered with compassion and kindness, while also maintaining high standards of rigor. I have eagerly anticipated every comment and feedback I received from them. After facing some ableist experiences in my academic journey, it is heartening to know that exceptional individuals like Marguerite Madden, Sergio Bernardes, Angela Yao, Andy Grundstein, and Loki Osborn are sharing their wisdom with emerging scholars and practitioners. Their support allowed me to truly make the most of my PhD.

I owe a tremendous gratitude to Zimbabwe Parks & Wildlife, the Hwange Rural District Council, and Connected Conservation for generously providing the data that enabled my study on human-elephant conflict. I extend a special thank you to Malvern Karidozo and all the enumerators and staff at Connected Conservation: Prince Mike Zhuwakinyu, Elmon Ndlovu, Robert Tonderai Sachikonye, Busani Ngwenya, Dzingai Zilimbile, Courage Neo Ncube, and Khumbulani Moyo.

I am indebted to Malvern Karidozo, Bill Langbaurer, and Andrea Presotto, as well as Marguerite Madden and Loki Osborn, for allowing me to participate in their elephant group meetings. These meetings were instrumental in shaping my ideas. Without the expertise and experience shared during those meetings, I would not have been able to develop my research questions.

I would like to express my appreciation to Kunwar Singh for introducing me to Marguerite Madden and suggesting that I do a review on scaling approaches for remotely sensed data. His encouragement and support have been invaluable throughout the past few years. I also extend my thanks to Kunwar for his patience and kindness in assisting me. He has truly been an exceptional mentor and embodies the type of scholarly mentorship and leadership that we need more of.

I am grateful to Amy Frazier for being an outstanding co-author and a pleasure to work with. Much of my understanding of scaling is owed to her scholarship and research.

I would also like to thank Ryan Slapikas and Austin Stone for their invaluable assistance whenever I encountered programming challenges and their willingness to listen when I needed to vent.

I would also like to express my gratitude to UGA's Disability Resource Center (DRC) for their dedication to ableism, their gatekeeping efforts, and the discrimination I received. From the ableist policies, to the poorly and, in some cases, entirely unqualified staff, most of my experiences with the DRC underscored the importance of proactively incorporating accessibility measures and fostering a mindset focused on justice. I earned this PhD despite the ableism I encountered at the DRC.

Finally, I would like to extend my deepest appreciation to my parents for their unwavering support and encouragement. Their belief in me and my dreams has been an incredible motivation and has persisted for nine years of graduate school across multiple institutions. Their desire for me to earn this degree has matched my own, if not surpassed it.

These acknowledgements solely reflect my thoughts and experiences and not those of my committee members, lab, co-authors, or UGA.

TABLE OF CONTENTS

1 INTRODUCTION AND LITERATURE REVIEW

As humans exert tremendous pressures on the planet and biodiversity declines (Newbold et al., 2015; Waters et al., 2016), the relationships humans have with the environment and with wildlife grow increasingly strained and complex. The scale at which human activities encroach into wildlife habitat, the recovery of previously declining wildlife populations, and environmental changes collectively accelerate conflicts between humans and wildlife (Treves, 2008). Contentious relations between wildlife and humans are becoming more pervasive (Madden, 2004; Thouless et al., 2016; Young et al., 2010). For humans to coexist with wildlife in a world where the two more frequently come into contact in antithetical ways, we need to incorporate local and context-specific studies (Gregory, 2000; Knight et al., 2006). This includes data that are inherently nuanced and affected by land use change, human culture, local policies, national policies, colonialism and its legacies (Dickman, 2010). In conservation science, the goal is often to scale from local to regional and regional to local in terms of conservation solutions, methods, predictions, models, etc. Optimal solutions for human-wildlife coexistence for one region should be applicable to other regions so general patterns can be discerned and simplified (Madden, 2004). Our understanding of larger patterns and theories in conservation science is composed of local patterns and trends; thus, our approach should study these phenomena at multiple scales.

To demonstrate this multi-scalar approach, in this dissertation, I examine human-elephant conflict around Victoria Falls, Zimbabwe. I aim to expand our understanding of human-elephant conflicts (e.g. geographical, ecological, etc.), and then to substantiate if patterns in other countries apply to northwestern Zimbabwe. Questions of scale underscore throughout. Chapter Two reviews scaling methods for remotely sensed data to show how scaling data permeates landscape-scale wildlife studies.

Chapter Three examines land cover in the Victoria Falls region to discern whether temporal and spatial resolution of remotely sensed imagery resolution potentially occlude or complicate land cover classification. Chapter Four models human-elephant conflict to determine which underlying spatial factors are most germane to predicting conflict so we may actively prevent and mitigate its effects. Finally, Chapter 5 summarizes results and presents conclusions.

Large carnivores perhaps present the most obvious risk to human life, but mega herbivores can also pose a significant danger. In situations where these large animals perceive a threat or are defending their offspring, encounters might turn deadly for humans. Large appetites, space requirements, and general resource needs accompany the impressive body size of these creatures. African elephants (*Loxodonta africana*), the largest extant land animal on the planet, spend most of the day browsing and grazing (Laursen & Bekoff, 1978; Owen-Smith, 1988; Shannon et al., 2008). They resort to crop raiding when highly preferred, cultivated foods are ripe and when natural vegetation health declines (Osborn, 2004; Tsalyuk et al., 2019). As such, elephants are arguably the greatest threat to African farmers (Mwamidi et al., 2012; Parker et al., 2007). Elephants do not have a mating season (calves are born every 3-5 years) and females form herds with their young whereas adult males form bachelor groups or range as individuals (Laws et al., 1975; Moss & Poole, 1983). Bachelor herds and individual male elephants are potentially more likely to be involved with conflict, as studies have found they increase the amount of time spent in developed areas with increasing elephant density (Fortin et al., 2022). Males are more likely to select anthropogenic habitat when compared to females (Fortin et al., 2022). It has also been hypothesized that females are less willing to risk venturing to anthropogenic habitat to protect their calves (Chiyo et al., 2011). Nonetheless, mothers will protect their young from humans if they feel threatened.

Any progress toward alleviating conflict between humans and wildlife requires a synthesis of local and context-specific studies, especially nuanced data. Again, this is why multi-scalar approaches

are essential. Human-wildlife studies occur within a matrix of related academic disciplines, including political ecology, environmental anthropology, wildlife biology, and landscape ecology. As most relevant to my argument here, landscape ecology is the science of the relationships between spatial-temporal patterns and ecological processes at a multitude of scales (J. Wu, 2013). It is an interdisciplinary field focusing on broad-scale ecological issues and their pattern-process relationships. Studies of land use and land cover change, landscape conservation, and animal movement all fall under the umbrella of landscape ecology. The spatial patterns of landscapes are described by landscape metrics, including patch density, dominance index, mean patch size, and others. Central to landscape ecology are the concepts of scale and scaling, which have been identified as key research priorities (Meentemeyer, 1989; J. Wu & Hobbs, 2002). Scale can greatly affect studies of landscape change (Lausch & Herzog, 2002). Conservation science and wildlife management are thus closely linked to landscape ecology through the landscape disturbances humans create, the patches wildlife navigate and inhabit, and the landscapes humans transform.

1 General background and historical context

Zimbabwe is a landlocked South African country with a GDP of $33.83 billion US dollars where 42.5% of its land is devoted to agricultural purposes, the majority of which is pasture ("Zimbabwe," 2023). It is bordered by Botswana to the west, Zambia to the north, Mozambique to the east, and South Africa to the south (Figure 1.1A). The country is divided into ten provinces, which are further subdivided into 59 districts. Zimbabwe's roughly 385,000 km^2 of land contains substantial biocultural diversity. Mosi-oa-Tunya, or Victoria Falls as it is known to most, is the largest waterfall on earth and one of the seven natural wonders of the world. It is located between Zimbabwe and Zambia. Just south of the waterfalls is the city of Victoria Falls. It is in the Matabeleland North Province in the Hwange District (Figure 1.1B).

The study region (Figure 1.1C) falls within the Matabeleland North Province in Zimbabwe; the following background on climate, land use and land cover, and relevant policies are focused on this province and on Zimbabwe.

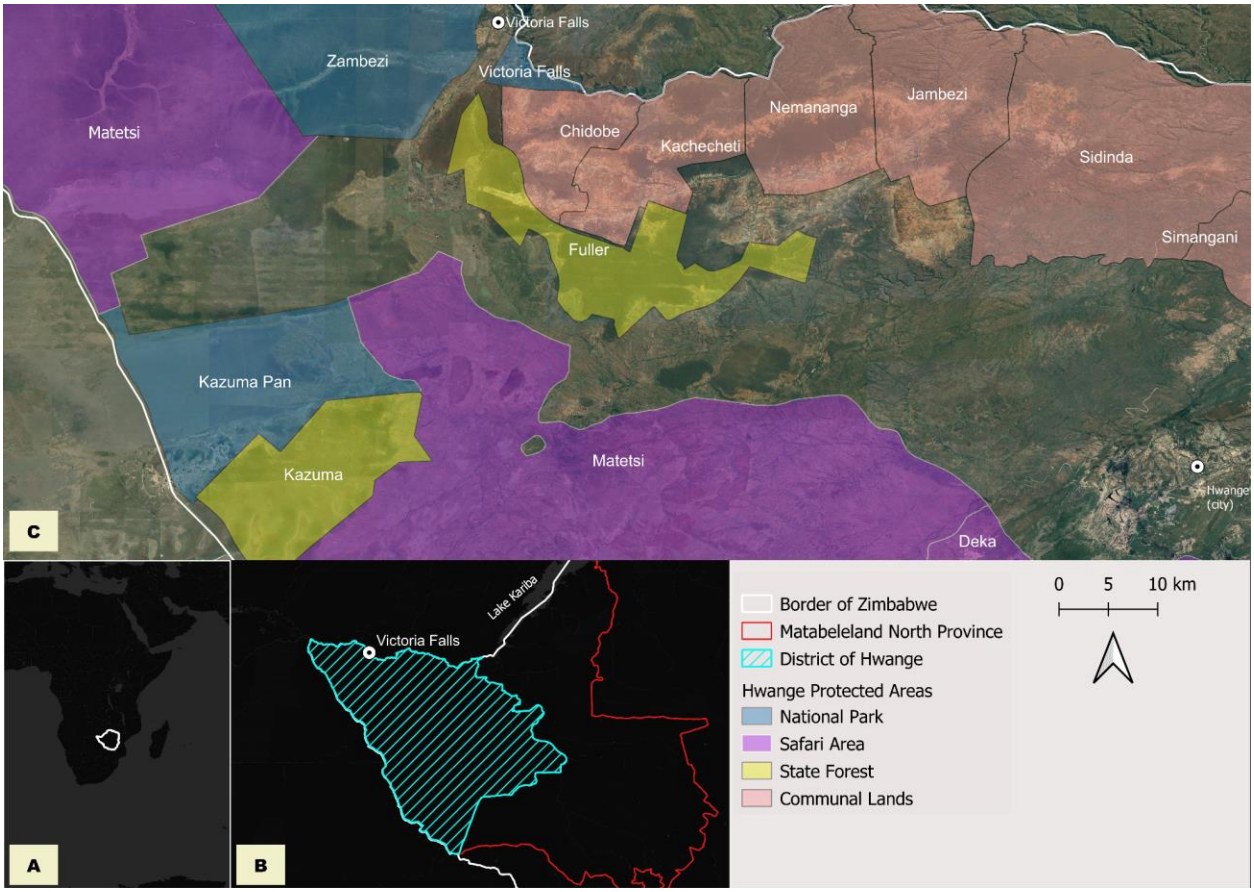

Figure 1.1. Insert map A shows Zimbabwe within the African continent. Map B shows the Matabeleland North Province outlined in red, the Hwange District is indicated by light blue lines, and the city of Victoria Falls indicated by a white circle centered around a black dot. The Zambezi River spans the northern border of Zimbabwe and flows eastward into Lake Kariba. In Map C, Protected areas are labeled by name and their type identified by color. The cities of Victoria Falls and Hwange are indicated by white circles encasing a black dot. Satellite imagery is provided by Google.

Zimbabwe's northern border with Zambia is divided by the Zambezi River. Visitors flock to Mosi-oa-Tunya either from the city of Victoria Falls in Zimbabwe or from the larger city of Livingstone, in Zambia. The degree of human modification in this region of Zimbabwe is significantly less than what is observed for Livingstone across the river in Zambia; human populations are concentrated in Victoria Falls and in the communal lands to the south. Hwange is further subdivided into wards, of which there are 20 Rural District Wards (see Appendix A) governed by the Rural District Councils as well as wards for the urban areas of Victoria Falls and Hwange.

The Zimbabwean landscape cannot be understood without recognizing its complicated socio-political context due to colonial and neoliberal influences. After declaring independence from Britain in 1965, Rhodesia entered a period of internal war before establishing itself as "Zimbabwe" in 1980. The country transitioned from a state-led approach to a market-based economic approach subscribed by the International Monetary Fund (Murisa, 2010). This strategy sought to redistribute land and use it productively for farmers and national development (Geza, 1986). This market-based approach and internal corruption led to a decline in social services, an increase in unemployment, and 60% of the country's population living on less than $1USD per day eight years later (Murisa, 2010; Richardson, 2005). In the 1980s, roughly 8,000 white commercial farmers owned 15.5 million hectares and 6,000 African farmers held 1.4 million hectares of small-scale farms; 700,000 indigenous occupied the remaining 16.4 million hectares, the majority of which was comparatively less fertile and drier land (Sachikonye, 2003). The Fast Track Land Reform Programme (FTLRP) began with the Land Acquisition Act in 2002 and redistributed land resulting in a decline of large, capitalist farms and foreign and domestically owned agricultural estates (Moyo, 2011). The FTLRP was designed to allocate land and natural resources to formerly landless households, diversify livelihoods and expand economic opportunities for women (Mkodzongi, 2013), but the reform was tainted by corruption and many have alleged that land allocation was actually determined by political party (Hammar et al., 2003; Sachikonye,

2003). Women were largely excluded in land allocation as were youth (Bhatasara & Chiweshe, 2017; Chipenda, 2018). This redistribution largely excluded vulnerable populations and it created problems for certain social groupings (Addison, 2019; Chiweshe & Chabata, 2019; Sachikonye, 2003). Subsequent policies such as regulation of land leasing in fast track resettlement areas and the Command Agriculture program to ensure food security further affected the country and had effects that reverberated across the landscape (Makuwerere Dube, 2021; Mudimu et al., 2020). Land in Zimbabwe is vested with a history of colonialism and is continually influenced by global capitalist forces (Makuwerere Dube, 2021). It is this historical, political, and social context of spatial resettlement and reform that has shaped the land observed and captured remotely by satellites.

2 Climate, vegetation, and land cover change

The climate in Matabeleland North is best characterized as having three seasons: a cool and rainy season starting in January and lasting through March, a cool and dry season from April until October, and a hot and dry season from October to the end of January. Occasionally seasonality is discussed in terms of precipitation only, thus the rainy season falls from Nov to March and the dry season from April through October. Eighty percent of precipitation across Zimbabwe falls between the months of November and March, with rainfall shifting earlier during dry years (Dube & Nhamo, 2019). Precipitation in Victoria Falls has recently shifted later, starting in November rather than October, with a notable decline in October monthly rainfall dating to the 1990s (Dube & Nhamo, 2019). Vegetation typically responds to precipitation by one to two months (Mberego & Gwenzi, 2014). Crop water requirements peak in December and January (Funk & Budde, 2009).

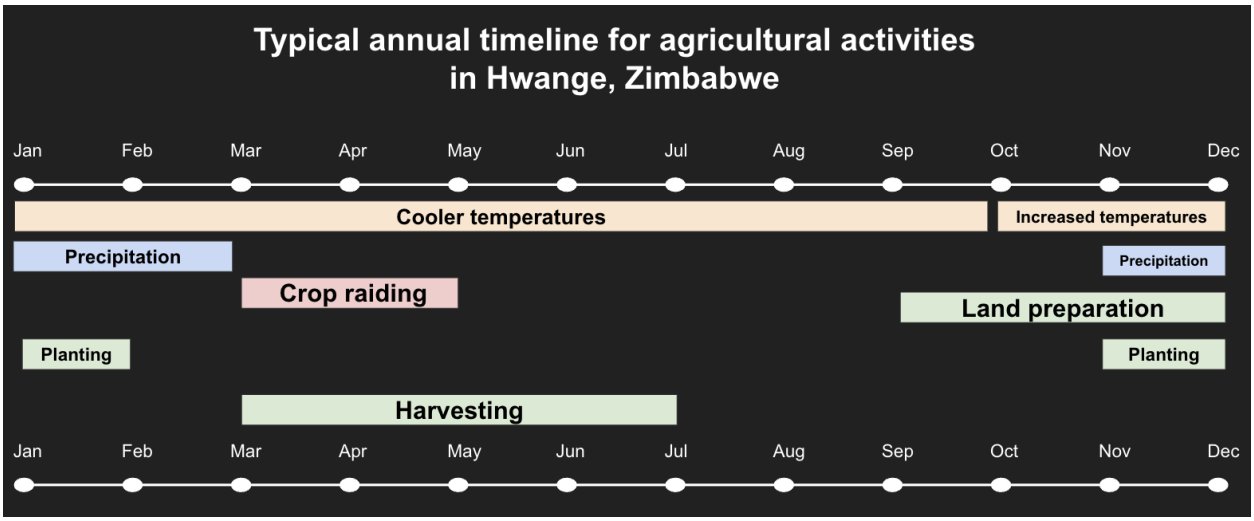

Figure 1.2. Typical annual timeline for agricultural activities in Hwange, Zimbabwe. Rainfall historically began in October but has shifted later over the past two decades. The main harvesting period typically runs from April through July. Created based on conversations with in-situ collaborators and information available on Famine Early Warning Systems Network on Zimbabwe.

Zimbabwe is also susceptible to droughts, which present a significant challenge to the country's agricultural sector (Mazvimavi, 2010). Depending on how droughts are measured (e.g. precipitation measurements alone, reservoir altimetry observations, total water storage observations, vegetation indices, etc.), the region has experienced multiple droughts. The years 2002, 2004, and 2019 are particularly notable for the region (Hulsman et al., 2021). The Matabeleland North Province experienced between five to seven years of drought from 1989 to 2019 based on remotely sensed vegetation indices (Frischen et al., 2020). Drought episodes also appear to be increasing in length recently (Dube & Nhamo, 2019). Rainfall accumulation in three out of five rainy seasons from 2015 to 2020 was the lowest since 1981 with the worst drought the 2015-2016 rainy season (Husak et al., 2020). Farmer resiliency declined, irrigation capacity was reduced, and national maize grain supplies were critically low (GEOGLAM Crop Monitors, 2020).

Except for a small strip of grassland in the east, the majority of Zimbabwe falls within the broadly-defined savanna vegetation zone (Van Wyk, 2013). Using the Köppen-Geiger System, northwestern Zimbabwe is considered a hot, semi-arid climate (type "BSh") (Beck et al., 2018). South of Victoria Falls, dominant vegetation types in the communal lands are dry forests and thickets, specifically *Baikiaea* woodland on Kalahari sand (Figure 1.3A) interspersed with Mopane woodlands, more specifically *Colophospermum* woodland (Figure 1.3B) on skeletal soils (Timberlake et al., 1993). The *Baikiaea* woodland in this region is an open woodland characterized by *Baikiaea plurijuga* 10-14m high and includes a shrub layer with *Paropsia brazzeana, Baphia massaiensis*, *Bauhinia petersiana* and others. *Colophospermum* woodland is composed of open woodland 8-12m high and vegetation approaching woodland thicket with slight variations depending on the subtype of soil (Timberlake et al., 1993). Common species found in the open woodland area include *C. mopane, Kirkia acuminata, Terminalia stuhlmannii,* and others and the shrub layer consists of *Carphalea pubescens, Dalbergia melanoxylon*, *Gardenia resiniflua*, *Dichrostachys cinera*, and others (Timberlake et al., 1993). The spatial extent of most of these vegetation types visibly changes in satellite imagery in accordance with the seasons, making the phenology, or the study of seasonal and periodic changes on biological life, particularly germane.

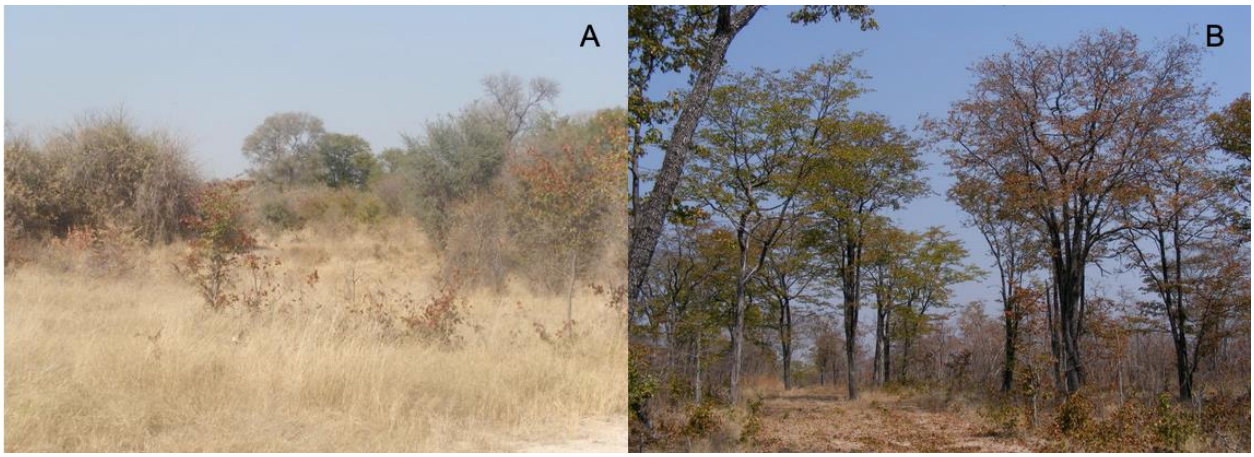

Figure 1.3. A *Baikiaea* woodland and B *Colophospermum* woodland. https://www.researchgate.net/publication/309469196_Structure_of_avian_assemblages_in_Zambezian_Baikiaea_woodlands_northern_Namibia and https://www.zambiaflora.com/speciesdata/image-display.php?species_id=126560&image_id=12

Of the five main agro-ecological regions Zimbabwe is commonly divided into, Victoria Falls is in Region IV (Figure 1.4), which receives on average between 450-650mm of rainfall annually (Manatsa et al., 2020; Moyo, 2000; Vincent & Thomas, 1960). While Matabeleland North is suitable for cattle ranching, erratic rainfall and generally poor soils significantly limit any potential for high-value crops (Manatsa et al., 2020; Moyo, 2000; Vincent & Thomas, 1960). Without irrigation systems, farmers are advised to select drought-tolerant crops, and cattle ranching and raising small livestock (poultry, goats, etc.) is also advisable, but rainwater harvesting techniques are needed (Manatsa et al., 2020).

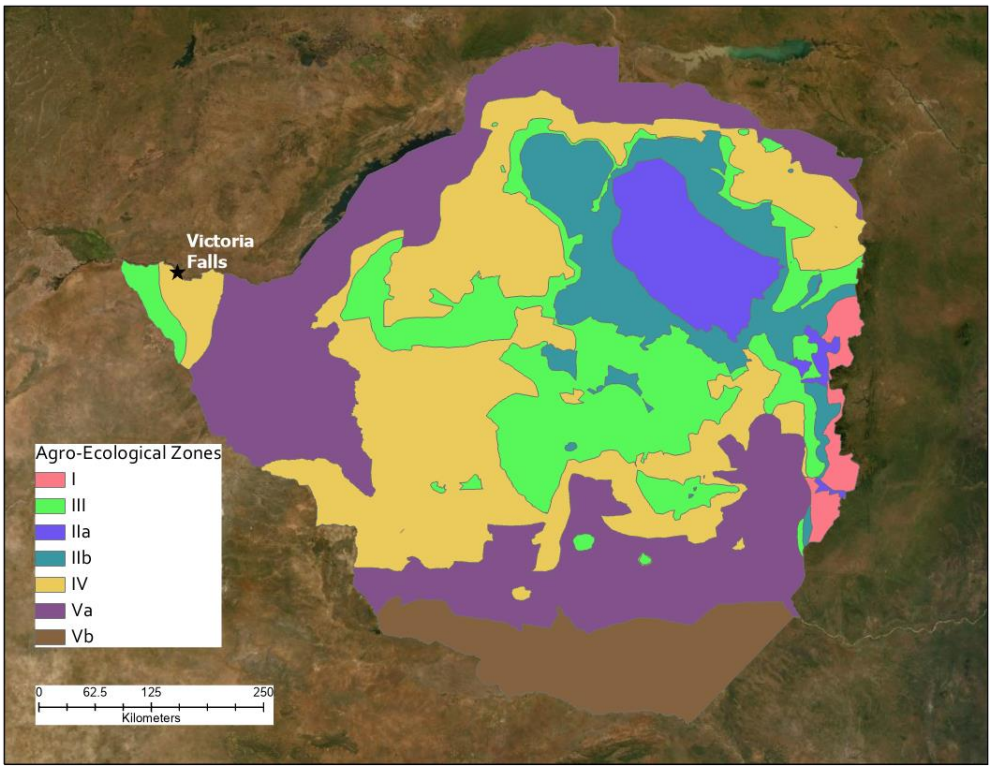

Figure 1.4. Agro-Ecological Zones for Zimbabwe. Courtesy of Dr. Desmond Manatsa. Zimbabwe National Geospatial and Space Agency (ZINGSA). The study area falls within Zone IV. Zone IV is characterized by limited rainfall and maximum temperatures between 27 and 29C. Drought-tolerant crops are recommended and extensive cattle ranching, rearing of small stock are suggested as ideal farming systems for this region. For more information about Zimbabwe's Agro-Ecological Zones, see Appendix A.

Similar to South Africa, Namibia, and Kenya, an incredible amount of land in Zimbabwe was allocated to the people of England by the English government, necessitating the restoration of land ownership and land reform. While the complexities of land use and land cover (LULC) change may preclude the establishment of direct links between land reform and LULC change, changes in land tenure and agrarian reform likely had consequences for land use. For example, the average field size as measured using Landsat imagery declined from 2001 to 2011 from 0.092 to 0.041km^2 (White & Roy, 2015); a period that covers when large, commercial farms were disaggregated as part of the FTLRP. A

study using satellite data to document changes in land cover pre- and post-FTLRP in eastern Zimbabwe found the dominant land cover type shifted from woodlands and grasslands to grasslands, cultivated lands, and bare lands in 2005 (Sibanda et al., 2016). Similarly, changes in land cover in and around Matobo National Park in southwestern Zimbabwe using Landsat imagery from 1989, 1998, and 2014 have been documented, with a decrease in agricultural area and increasingly fuzzy boundaries of communal land observed, possibly due to gradual implementation of policy reforms dating back to 1990 (Scharsich et al., 2017).

Changes in LULC can have profound effects on biodiversity and human livelihoods and are predicted to be the most important contributor to changes in biodiversity (Chapin et al., 2000). Cropland mapping is particularly important given agriculture's increasing role in sustainable resource management (Matton et al., 2015). Across Zimbabwe, changes in land cover are driven by population density, roads, and other factors (Kamwi et al., 2018). Croplands across Zimbabwe are expanding, despite recent droughts (Useya et al., 2019). Land cover change was significant from 1984-2013 in Forest Protected Areas within Zimbabwe, with settled forests predictably experiencing more degradation than unsettled forests (Mutekwa & Gambiza, 2016). Forest patches became more fragmented due to encroachment of human land cover types from 2002-2011 in the province to the south of Victoria Falls (Shoko et al., 2016).

3 Background on human-elephant conflict and interactions

Of the two species of African elephants, the endangered African savanna elephant (*Loxodonta africana)* inhabits Zimbabwe. A 2014 aerial study of Zimbabwe estimated the country's elephant population at 83,000 divided into four main populations based on geography, with the Northwest Matabeleland having the highest African savanna elephant density (*Zimbabwe National Elephant Management Plan: 2015-2020*, 2016). Zimbabwe's elephant population is second only to Botswana

which has roughly 120-130,000 elephants and where population numbers remain stable (Schlossberg et al., 2019). While elephant populations are generally rising, poaching remains a significant problem and poisonings have also been on the rise (*CITES Implementation Report*, 2021; *Zimbabwe's Fifth National Report to the Convention on Biodiversity*, 2015).

Savanna elephants are generalist herbivores. They consume grasses, woody plants, and even fruits depending on availability and environmental conditions. Their consumption of less nutritious foods, such as bark and woody vegetation, increases during the dry season (Guy, 1976; Osborn, 2004; Williamson, 1983). Their location on the landscape and their general movement patterns are influenced by water availability (Loarie et al., 2009; Tshipa et al., 2017) and forage conditions, with elephants responding to vegetation changes, moving to areas with intermediate to high levels of vegetation greenness, and tracking even short-lived vegetation greening (Bohrer et al., 2014). Their speeds and core use areas decline significantly during the dry season, presumably to conserve energy (Mlambo et al., 2021; Vogel et al., 2020). As the dry season progresses and the availability of nutritional wild grasses declines, elephants increase not only the amount of woody vegetation they consume but they are also more likely to engage in crop-raiding (Osborn, 2004).

Elephants are drivers for biodiversity changes and conflict (Guldemond & Van Aarde, 2008; Hoare, 1999; Parker & Osborn, 2001). Vegetation responds negatively to elephants in arid savanna (Guldemond & Van Aarde, 2008) and elephants have been found to inhibit forest succession in disturbed areas dominated by shrubs and grasses in Kibale National Park (Omeja et al., 2014). African elephants have also been shown to be ecosystem engineers, modifying food availability for other animal species (Valeix et al., 2011).

Human conflict with elephants has been observed in at least three ways: (1) elephant conservation efforts reduce the agency of local human populations, (2) human-elephant violence, (3) and most significantly, elephant crop-raiding. On one hand, local laws designed to protect wildlife can

harm livelihoods, but on the other, dissent about damage and losses can undermine conservation programs (Naughton-Treves & Treves, 2005). For example, adopting a militarized approach of conservation in response to elephant poaching can introduce violence to local people and diminish autonomy over daily activities and livelihoods (Mushonga & Matose, 2020). Reducing and resolving conflict with elephants is further complicated by the influence of international organizations within the Convention In the Trade of Endangered Species or CITES (O'Connell-Rodwell et al., 2000). Across protected areas in Zimbabwe, elephant management and conservation are the responsibility of the Zimbabwe Parks and Wildlife Management Authority (ZimParks), but their efforts are hindered by a small budget, low morale, and high turnover (Ncube, 2019). Lastly, elephants and humans face a myriad of pressures resulting from natural resource competition. In May of 2021, a young man was trampled to death patrolling crops (Matabeleland North Correspondent, 2021). Elephants might also attack tourists and residents of Victoria Falls, with an elephant killing a mentally ill man in 2020, and residents were concerned more conflict would arise as elephants increasingly used the streets during the pandemic ("Elephant Kills Vic Falls Mentally Ill Homeless Man," 2020).

Although crop-raiding has occurred in Africa since pre-colonial times, but it is a long-standing and ever-increasing source of conflict. Prior studies in Hwange National Park have found crop-raiding declined with decreasing distance to refuge areas along with higher household density (Guerbois et al., 2012). This finding is consistent with previous research on elephant crop-raiding, indicating that the presence of elephant refuges is a significant factor in the frequency of such incidents (M. D. Graham et al., 2010; Thant et al., 2021). Work done in the Okavango Delta in Botswana found that fields are more likely to be raided by elephants if they are far from the village and if they have a high frequency of raiding in the past, whereas fields further from waterholes, further from elephant paths, and fields not used by livestock are less likely to be raided (Songhurst & Coulson, 2014). Subsequent work conducted by the same scholars in the Okavango Delta has revealed that the relationships between elephant

density and elephant space use with crop raiding patterns are nonlinear (Pozo et al., 2018). Counterintuitively, areas with lower elephant density appear to be at higher risk for crop raiding (Pozo et al., 2018), thereby affirming the complexity of predicting and understanding crop raiding patterns in southern Africa. To effectively mitigate this type of human-wildlife conflict requires understanding the spatial and temporal patterns of crop-raiding (Linkie et al., 2007).

Multiple methods have been employed in attempts to prevent elephant crop-raiding. Across southern Africa traditional methods include burning, planting unpalatable vegetation, using drums to scare off elephants along with high-tech methods such as electrical fencing. Bees have also been tested as a potential deterrent (Karidozo & Osborn, 2005; King et al., 2007; Ndlovu et al., 2016). Unfortunately, with many of these methods, such as drums and the use of firearms to scare elephants, effectiveness declines as elephants learn when the threat is empty (Osborn, 2010). Most elephant deterrents are ineffective or prohibitively expensive, and farmers might place themselves in harm's way to defend their livelihood (Osborn, 2010). As a result, elephants that crop-raid repeatedly and endanger humans are killed.

In northwestern Zimbabwe, the use of chili powder and oil has been tested as a deterrent in multiple forms (Langbauer et al., 2021; Osborn, 2002). In comparison to traditional deterrent methods of shouting and chasing, elephants that inhale the chili powder spend less time in fields (Osborn, 2002) and burning chili bricks results in less plant damage and a reduction in the number of visits from elephants (Karidozo & Osborn, 2015). Current methods used in the study include darting, anesthetizing, and covering trunks with chili wax of problematic elephants (Langbauer et al., 2021). In the early 2000s, Connected Conservation introduced chili fences, fences that have been covered with chili oil, as an effective deterrent (L. Osborn, personal communication, July 10, 2023). They have since actively promoted a wider implementation of chili fences.

4 Habitat monitoring via satellite remote sensing, scale, and access

The potential for satellite remote sensing and GIS to aid conservation and land use change is well-documented (Buchanan et al., 2009; Rose et al., 2015; W. Turner et al., 2015). Indeed, many studies of human-elephant conflict incorporate remotely sensed data, directly or through derivatives (Branco et al., 2019; Kileo & Mbije, 2021; Sanare et al., 2022). Yet calls for greater use of high resolution satellite imagery to advance conservation and natural resource management (Boyle et al., 2014; W. Turner et al., 2015) are not answered equally across the globe. This rhetoric often ignores issues of inequity, specifically in regard to non-Western countries or the Global South.

The feasibility of these approaches may not be attainable or sustainable for nonprofit and government organizations with limited resources, especially in the long term. This might be particularly true for nonprofits based in non-Western countries. Across the African continent, lack of fast and/or reliable internet service, hardware quality, and software license fees are all potential barriers to access (de Klerk & Buchanan, 2017; Swetnam & Reyers, 2011). A global test of internet speeds ranked the US as 11th in download speed compared to Zimbabwe's rank of 162 (*Worldwide Speed League*, 2022). On average, it takes five minutes and 47 seconds to download a 5GB movie in the United States, whereas it takes one hour and 16 minutes and 22 seconds in Zimbabwe (*Worldwide Speed League*, 2022). This can make downloading large amounts of satellite imagery tedious. Even when imagery is hosted remotely and does not need to be downloaded, as with the online image processing platform Google Earth Engine (GEE), viewing and sorting through available imagery may be an arduous task stymied by slow and unreliable internet. A significant portion of the conservation monitoring studies using remote sensing in Africa have first authors external to the African continent, and just two percent had authors listed in Zimbabwe (de Klerk & Buchanan, 2017). High resolution datasets are unaffordable for African agencies or require partnerships with international institutions and cannot be relied on for continued monitoring (de Klerk & Buchanan, 2017). Inequities in research infrastructure such as journal access and reliable

internet connectivity at university libraries further disadvantage (Schipper et al., 2021). Open-source software has the ability to address some of these concerns, but training material and education is needed and interpreting remote sensing images can remain a challenge (de Klerk & Buchanan, 2017; Eilola et al., 2021). Even when university training is available, barriers such as unreliable internet and financial difficulties faced by students hinder learning (Tanyanyiwa & Madobi, 2021). A review of urban planning studies using remote sensing found Africa and South America were poorly represented in existing research and that much of the work used commercial software rather than open source (Wellmann et al., 2020).

Similar to appeals to decolonize conservation and calls for just and equitable wildlife conservation, (Armstrong, 2019; Tan, 2021) it is a matter of equity and justice that scholars and practitioners local to biodiversity hotspots, areas undergoing rapid land cover change, and high priority conservation areas are unable to use the most advanced GIS tools and access fine resolution satellite imagery. Meanwhile, their counterparts in Western countries with greater access to resources are able to access such imagery and benefit. Until such inequities are adequately addressed, it is of utmost importance that nonprofit organizations and local governments are able to address their concerns and answer their questions with the best information possible and knowing the relevant scale needed to address their concerns. For example, if a resource-strapped institution can monitor localized elephant habitat change using freely available Landsat satellite imagery (resolution of 30 meters), they can conserve resources and staff labor rather than applying for grants or nonprofit access for high resolution imagery. Nonprofit organizations and local governments operating under budgetary constraints must often exercise extreme fiscal responsibility when evaluating data needs, hence the importance of determining the appropriate scale and image resolution required.

5 Objectives

Scholars and practitioners should be able to construe how a solution in one region fits a larger pattern and how it thus may lead to an equivocal, pragmatic solution for human-wildlife coexistence in their own region. Conservation science's understanding of broad ecological patterns and theories is constructed by examining local patterns and principles. As such, we must study wildlife coexistence using a multi-scalar approach. The overarching goal of this research is to ameliorate human-elephant relations by using multi-scalar remote sensing and geospatial analysis. Through this work, I seek to ascertain: 1) methods available for scaling remotely sensed imagery; 2) how LULC and vegetation conditions are changing and the scale most suitable to monitoring these changes; and 3) where elephant conflict occurs and its underlying spatial patterns. To achieve these goals, I use geospatial analysis with scale acting as the pivotal nexus of all chapters and the conceptual framework. Findings engender greater precision in conflict mitigation efforts and bolster scientific understanding of scaling processes and human-elephant relations.

2 MARKHAM, K., FRAZIER, A. E., SINGH, K. K., & MADDEN, M. (2023). A REVIEW OF METHODS FOR SCALING REMOTELY SENSED DATA FOR SPATIAL PATTERN ANALYSIS. *LANDSCAPE ECOLOGY*, *38*(3), 619- 635[1]

[1] Markham, K., Frazier, A. E., Singh, K. K., & Madden, M. (2023). Reprinted here with permission of publisher.

Abstract

Landscape ecologists have long realized the importance of scale when studying spatial patterns and the need for a science of scaling. Remotely sensed data, a key component of a landscape ecologist's toolbox used to study spatial patterns, often requires scaling to meet study requirements. This paper reviews methods for scaling remote sensing-based data, with a specific focus on spatial pattern analysis, and distills the numerous approaches based on data type. It also discusses knowledge gaps and future directions. Key papers were identified through a systematic review of the literature. Trends, developments, and key methods for scaling remotely sensed data and spatial products derived from these data were identified and synthesized to detail the general progression of a science of scaling in landscape ecology. Upscaling both continuous and categorical data can oversimplify data, creating challenges for spatial pattern analysis. Object-based and neighborhood approaches can help, and since patch boundaries are more likely to align with objects than pixels, these may be better options for landscape ecologists. Many downscaling methods exist, but these approaches are not being widely employed for spatial pattern analysis. A diverse range of scaling methods are available to landscape ecologists, but work remains to integrate them into spatial pattern analysis. Moving forward, advances in computer science and engineering should be explored and cross-disciplinary research encouraged to further the science of scaling remotely sensed data.

1 Introduction

Spatial pattern analysis is a cornerstone of landscape ecology that has fostered unprecedented developments in both theory and practice (J. Wu et al., 2002). The wide availability of remote sensing data, particularly with the opening of the archives such as Landsat (Z. Zhu et al., 2019), has made it increasingly easy for researchers to quantify spatial patterns in landscapes (Frazier & Kedron, 2017). However, the remote sensing data that form the basis for many spatial pattern analyses are captured at

a fixed resolution, prompting researchers to change the scale (resolution) of the data in order to match observational or modeling objectives.

Ecologists have long recognized the biases associated with translating information across scales (Jelinski & Wu, 1996; Levin, 1992; Meentemeyer & Box, 1987; M. G. Turner, Dale, et al., 1989), and much work in landscape ecology has focused on how changing the scale of a dataset (grain and extent) impacts derived spatial patterns, using both categorical (Saura, 2004; M. G. Turner, O'Neill, et al., 1989; J. Wu, 2004) and continuous data (Frazier, 2016). Findings have shown that landscape pattern analysis is highly sensitive to grain, or spatial resolution (Hall et al., 2004; M. G. Turner, 1989; J. Wu, 2004; J. Wu et al., 2002), and a mismatch between the grain of the process and the pattern may produce incorrect conclusions (Galpern & Manseau, 2013). Foundational, theoretical work (e.g., (T. F. Allen & Starr, 1982; Levin, 1992; M. G. Turner, 1989; J. A. Wiens, 1989)) along with technological advances including the Landsat missions starting in 1972 and ArcGIS Desktop in the late 1990s, allowed for many different methods for scaling spatial data to emerge (Figure 2.1). These and other studies promoted scaling issues to the front of the research agenda in landscape ecology through the 1990s and early 2000s, prompting Wu and Hobbs (2002) to identify scaling as one of the top research priorities for the discipline, and it continues to be an important topic in the field (Chambers et al., 2016; Ke et al., 2017; Kedron et al., 2018; Lang, 2008; Lang et al., 2019; Z. Li et al., 2017; Y. Zhang et al., 2014).

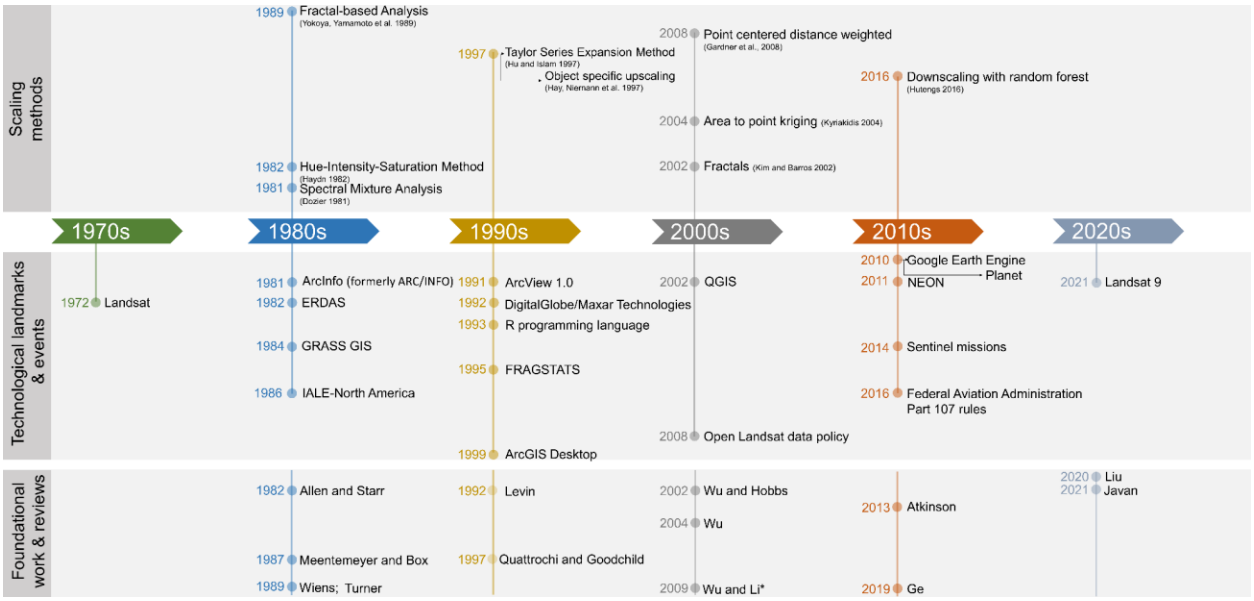

Figure. 2.1 Selected milestones contributing to the progression of the science of scaling. Milestones are grouped under foundational work and reviews, technological landmarks and events, and scaling methods. These milestones are not intended to be all-inclusive. IALE-North America - North American Regional Association of the International Association for Landscape Ecology; NEON - National Ecological Observatory Network; FAA - Federal Aviation Administration. The FAA's Part 107 rules regulate drone pilot certification and operating requirements (Frazier and Singh 2021). * Indicates a review paper.

However, despite recognition of the importance of scale and a plethora of studies testing the impacts of scale on spatial patterns, questions persist about which methods to use in different contexts (Ge et al., 2019), particularly for the remote sensing (and remote sensing-derived) data on which many spatial pattern analyses rest. When data that have been scaled are subsequently used for spatial pattern analysis, it adds an additional layer of complexity (loss of rare land cover types, sensitivity of patterns to grain size, etc.). Even with gradient surface models (McGarigal et al., 2009) and hybrid approaches to characterize landscapes, measuring landscape patterns that accurately characterize ecological processes at multiple scales continues to challenge landscape ecologists.

With the increased volume of remote sensing data being produced daily and the growing need to rescale these data for modeling in landscape ecology, it is an opportune time to review the choices for scaling and how those choices impact subsequent analyses. The objective of this review is to survey methods for scaling remotely sensed data for spatial pattern analysis with a specific focus on two broad categories of scaling: upscaling and downscaling. Within each of those categories, we detail methods for scaling the two data types most commonly used in spatial pattern analyses: continuous data and discrete/categorical data. Through a systematic review of the literature, we summarize the trends and developments used within the discipline for scaling data for spatial pattern analysis. Key papers were identified for this article through a systematic review of the literature using keywords and keyword combinations such as, “scaling” + ”technique”, “scaling” + “remote sensing,” “downscaling,” “upscaling” and others. Journal databases including *Landscape Ecology*, *Remote Sensing of Environment*, *International Journal of Remote Sensing*, the *ISPRS Journal of Photogrammetry and Remote Sensing* as well as Google Scholar were all exhaustively searched until relevant papers were no longer identified. Scaling techniques were categorized and theoretical and methodological developments, persistent issues, and gaps were identified from roughly 200 core papers. We synthesize scaling options and develop a conceptual decision tree for researchers. Finally, we propose future research directions and highlight other disciplines that landscape ecologists might consult when seeking to scale data. We begin by clarifying scale concepts and defining how we use the terms ‘scale’ and ‘scaling’ in this review. For the sake of brevity, we have chosen to use the term remote sensing to also include remote sensing-derived datasets.

2 Scale concepts and terminology

2.1. Definitions and term usage

Across the sciences, the term "scale" has been used to describe many similar but subtly different concepts. Schneider (2009) notes the Oxford English Dictionary offers 15 different definitions of scale. The term is used several different ways even within ecology and landscape ecology, and these variations complicate discussions (J. Wu, 2007). Therefore, it is important to define the terms as they are used in each situation (Schneider, 2009). Here, we use the term "scale" to refer to *the spatial scale of a measured variable*, which determines the minimum resolvable area, or resolution. The term "fine scale" is used to refer to detailed maps and "coarse scale" for maps with larger pixel sizes and/or less detail.

A distinction must also be made between the terms "scale" and "scaling". To "scale" something is the verb form and means to change the size while maintaining the same proportions. This verb form is often referred to as "scaling", which should not be confused with the term scaling as it is used in the physical sciences to describe a manifestation of the underlying dynamics and geometry relating key processes over broad ranges (Brown et al., 2004). Hereafter, we adopt the first definition and define scaling as *a change of the spatial size of the measurement unit*. We focus specifically on spatial scaling while recognizing that temporal, and organizational scaling are important concepts in landscape ecology. We are interested in the observational scale, which is the scale at which measurements are made or sampling is conducted and is distinct from intrinsic scale, which is the scale at which a pattern or process operates. We focus on scaling remotely sensed data, and do not review other geospatial data as they fall outside the scope.

2.2 General methods and data types

Methods for scaling remotely sensed data are generally classified as either “upscaling” or “downscaling” (Figure 2.2). Upscaling involves coarsening the resolution by aggregating a larger number of smaller units into a smaller number of larger units. Upscaling assumes the existence of an aggregate property. Downscaling involves disaggregating data from a larger unit into multiple smaller units to make the resolution finer. Both upscaling and downscaling are commonly performed using remote sensing-based data to change the scale for analysis. Some researchers also recognize a third category -- sidescaling-- in which the resolution is maintained (Ge et al., 2019). Sidescaling is typically employed when obtaining area-to-area predictions and is not discussed further in this review.

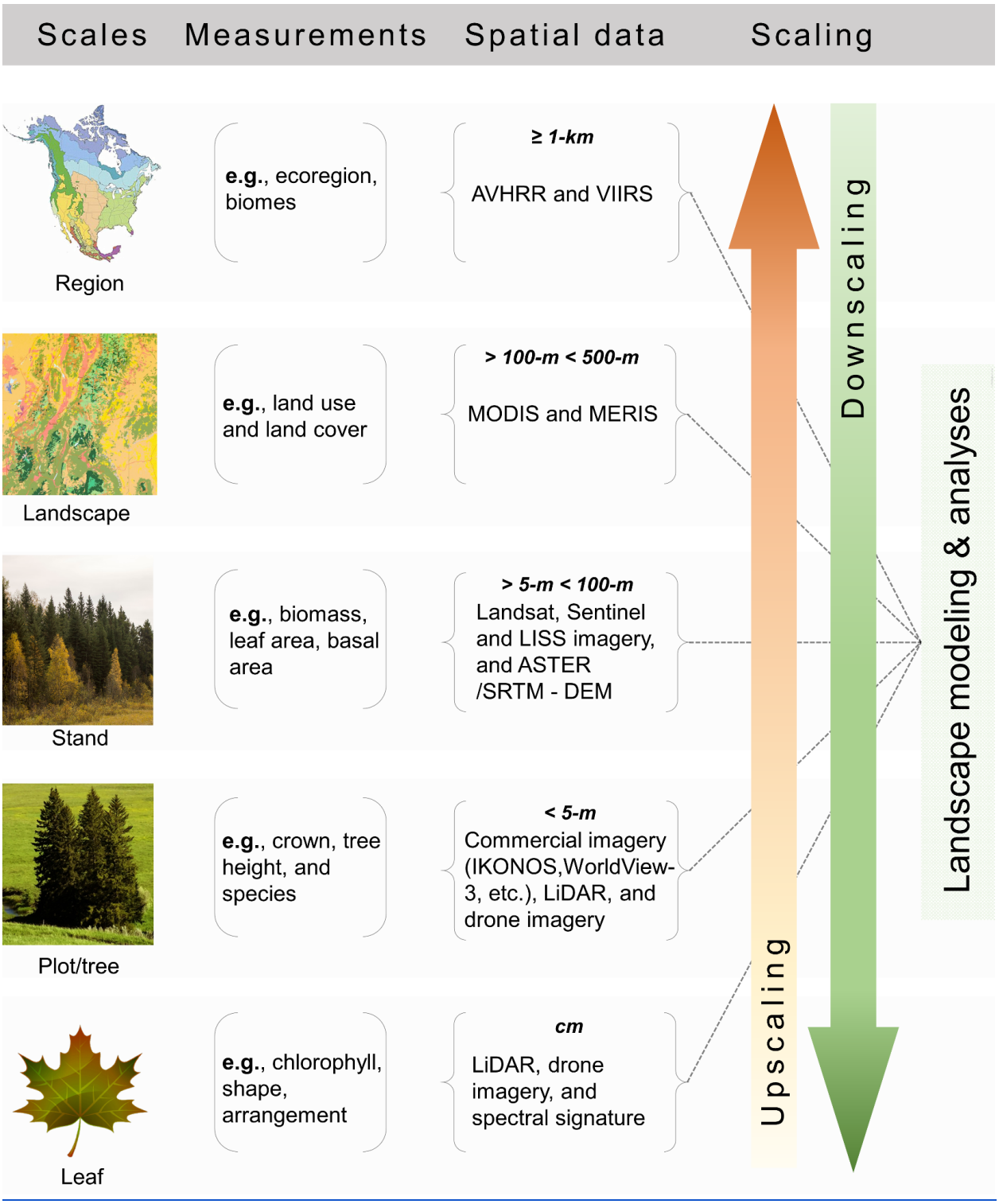

Figure 2.2 A schematic of upscaling and downscaling with examples of feature scales, typical imagery and data types for representation, and common metrics extracted from the data. ASTER - Advanced Spaceborne Thermal Emission and Reflection Radiometer; AVHRR - Advanced Very High Resolution

Radiometer; DEM - Digital Elevation Model; LiDAR - Light Detection and Ranging; LISS - Linear Imaging Self Scanning; MERIS - Medium Resolution Imaging Spectrometer**;** MODIS - Moderate Resolution Imaging Spectroradiometer; SRTM - Shuttle Radar Topography Mission; and VIRS - Visible Infrared Imaging Radiometer Suite.

For both upscaling and downscaling, the type of data being scaled determines which methods are appropriate. Two data types are commonly used for spatial pattern analysis in landscape ecology. The first type is continuous data, such as remote sensing reflectance values, vegetation indices, or digital elevation models (DEMs). These data vary continuously over the landscape and can be directly used to compute gradient surface metrics (Kedron et al., 2018; McGarigal et al., 2009) or they can be thresholded into discrete categories for patch-based analyses (Arnot et al., 2004; Frazier & Wang, 2011). While this review focuses on optical data, the same scaling principles can be applied to the products of point cloud data (LiDAR, etc.) that landscape ecologists use. The second, more common, type of data used in spatial pattern analysis are categorical data, such as land use and land cover (LULC) maps. These datasets are typically derived from remote sensing reflectance bands, but the pixels have been reassigned to thematic class codes. These datasets are used directly to compute traditional patch-based landscape metrics. The data type and scaling method can have a number of different impacts on the spatial patterns derived from them, and these impacts are the focus of the review below.

3. Upscaling

3.1. Upscaling continuous data

Upscaling continuous data can be relatively straightforward since values can be numerically summarized within the larger unit. The most basic approaches use descriptive statistics (e.g., mean, median) to re-assign the set of values within the larger aggregate pixel to a single value, which may be

categorical, (e.g., Riitters et al. 1997) (Figure 2.3), while others simply use the central pixel (Bian & Butler, 1999) or a random pixel (He et al., 2002) as the output value. A comparison of the impacts of mean and central pixel resampling on spatial pattern metrics found that, while mean aggregation filters out small patches, it produces more stable results for certain landscape metrics than other approaches (Raj et al., 2013), while central pixel resampling can substantially magnify small effects. Mean aggregation was also used in a study examining scaling effects on gradient surface metrics. Results indicated that mean aggregation led to non-linear changes in metric values with resolution, suggesting that some amount of information loss occurs during the aggregation process (Frazier, 2016). In short, while simple, numerical upscaling approaches are easy to use, they can impact spatial pattern analysis by oversimplifying the data resulting in data loss, eliminating rare or small patches, and magnifying small effects.

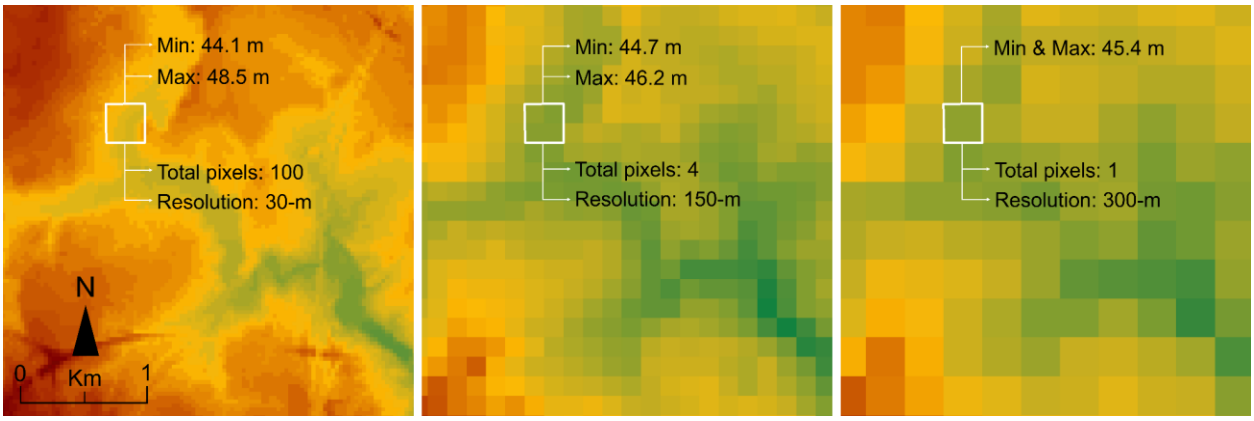

Figure 2.3 Upscaling of a digital elevation model (DEM) using the mean of the input cells to generate a coarser resolution raster. Minimum and maximum values change as input cells of the DEM are upscaled from 30-m to 150-m and 300-m.

To overcome the loss of heterogeneity that occurs with simple numerical methods, neighborhood-based (focal or moving window) approaches have been used to capture a greater amount of the surrounding information during the aggregation process. The theoretical basis for using focal

windows is that the digital value given to a pixel results not just from the ground sampling area of that pixel but also from objects in neighboring pixels (Cracknell, 1998; Jensen, 2016). Galpern and Manseau (2013) used a focal window approach to upscale continuous resistance surfaces representing movement impedances in order to match the grain of analysis to the true functional grain of the organism. The authors showed that focal windows could increase accuracy when identifying the relative importance of landscape features influencing connectivity, but that accuracy ultimately depended on the numerical operator employed (e.g., min, mean, max), as these operators performed differently depending on the spatial patterns in the landscape.

The moving window data aggregation (MWDA) method (L. J. Graham et al., 2019) is a more recent approach that uses focal windows to compute variability in continuous rasters and then use that heterogeneity as the basis for aggregation to a coarser resolution. The authors show that MWDA can capture information about the landscape spatial structure that is lost when using a direct aggregation approach, and that the method is particularly useful in landscapes where there is spatial autocorrelation in the environmental predictor variables (e.g. fragmented landscapes) and when the process scale is small relative to the aggregated resolution. The MWDA method is available as an R package (grainchanger.r).

Variance has also been incorporated into upscaling/aggregation through object-based methods. The object-specific upscaling (OSU) method was designed to reduce scaling errors by dividing a scene into homogeneous regions called objects and using those objects to guide aggregation (Hay et al., 2001). OSU defines multiscale spatial thresholds based on progressively increasing windows where the spectral variance of image objects is scale-dependent. These scale-dependent measures are then used as weighting functions to determine the upscaled values (Hay et al., 1997). A multiscale extension of OSU uses hierarchical sampling and evaluates each pixel in relation to coarse grain objects (Hay et al., 2001).

More recently, object-based segmentation coupled with Moran's I has been used to translate higher resolution training data for coarser resolution land cover classifications (Bihamta Toosi et al., 2020).

Fractals represent another approach for upscaling continuous data. Fractals are self-similar shapes that repeat their fundamental patterns at ever increasing or decreasing scales. They can be used to translate information across scales by informing a scaling transfer model that corrects for scaling effects based on the fractal relationship between approximate and exact pixel measurements (Gupta et al., 2000; L. Wu et al., 2015). Wu et al. (2015) use fractal theory to develop a relationship between image spatial resolution and leaf area index (LAI), which is a continuous vegetation index computed directly from remote sensing reflectance measurements. Their results showed that the fractal-based scaling model performed well in estimating LAI and evaluating the scaling bias.

3.2 Upscaling categorical data

When upscaling categorical data, majority rules aggregation (MRA) is a common choice, especially for LULC data. MRA assigns the LULC comprising the majority of the contributing pixels to the aggregate pixel (Benson & MacKenzie, 1995; Moody & Woodcock, 1995). The similar random rule-based (RRB) method randomly selects a class from the fine-scaled pixels and assigns it to the coarser map, maintaining cover type proportions but disaggregating categories and changing spatial patterns (He et al., 2002). Since MRA ignores proportions and assumes within-pixel values are homogenous, small effects can be substantially magnified (Holt et al., 1996). In other words, aggregating fine-scaled, mixed pixels could result in over or underrepresentation of a phenomenon, pattern, or class and rare or sparse land covers may be eliminated (Xu et al., 2020). MRA can distort land cover type proportions and frequently produces clumpy landscapes, while RRB can produce disaggregated spatial patterns (He et al., 2002; Raj et al., 2013).

Aggregation methods like MRA and RRB do not incorporate an understanding or measure of ecological processes, which some have argued makes them unsuitable for upscaling data that will ultimately be used for ecological analysis (L. J. Graham et al., 2019). Saura (2004) examined the effects of MRA on forest fragmentation indices by comparing aggregated values to actual sensor measurements and found that MRA tended to produce more fragmented patterns compared to actual sensor readings. Garcia-Gigorro and Saura (2005) also used an MRA filter to aggregate categorical data but compared it to a point-spread function (PSF), in which surrounding pixels provide a weighted contribution to the aggregate value. The authors found the PSF aggregation better mimicked the way in which the sensor captured the data and so fragmentation indices computed from PSF-scaled rasters had lower errors.

The point-centered distance-weighted moving window (PDW) method also attempts to overcome the limitation that MRA and RRB do not consider the relative proportion of each land cover type by using a weighted sampling net to maintain proportions when upscaling or downscaling (Gardner et al., 2008). First, the center point of the pixel in the map to be created is located and recorded in real dimensions. Then, the geometry of the sampling net is determined by the number of points and the distance between the points. Finally, the normalized frequency distribution of land cover types obtained from the data sampled at each point in the net is used, and the cover type of the rescaled map is randomly selected from the normalized frequency distribution of cover types (Gardner et al., 2008). Spatial autocorrelation can be included when using PDW, making it more robust compared to central pixel resampling and MRA (Raj et al., 2013).

4. Downscaling

Downscaling is usually a more difficult challenge than upscaling because it requires allocating coarser data, where there is little information about the spatial distribution of values, to finer scales, where values must be spatially distributed. Due to the lack of within-grain information, robust downscaling often requires stochastic or probabilistic approaches.

4.1 Downscaling continuous data

4.1.1. Resampling

The most basic form of downscaling continua is resampling, or downsampling, where a larger pixel is partitioned into smaller units, and the value from the larger is allocated to the smaller units (Figure 2.4). When no *a priori* information for how the values should be distributed spatially at the smaller scale is available, downsampling often assigns the value from the larger pixel to all of the smaller pixels. Downsampling in this manner does not actually change pixel values and can falsely suggest a higher level of heterogeneity is present. Scale-related findings must be cautiously interpreted in these instances (Frazier et al., 2021), and oversight can be difficult to detect and misleading in ecological modeling studies (Sillero & Barbosa, 2021). Bilinear and cubic convolution approaches can also be used in the absence of *a priori* information to interpolate pixel values at the finer resolution that fall between pixel centers in the coarser image. Depending on the method, interpolated values may contain uncertainties and biases that can propagate into spatial pattern analyses. Despite these drawbacks though, resampling continues to be widely used when researchers need to downscale data.

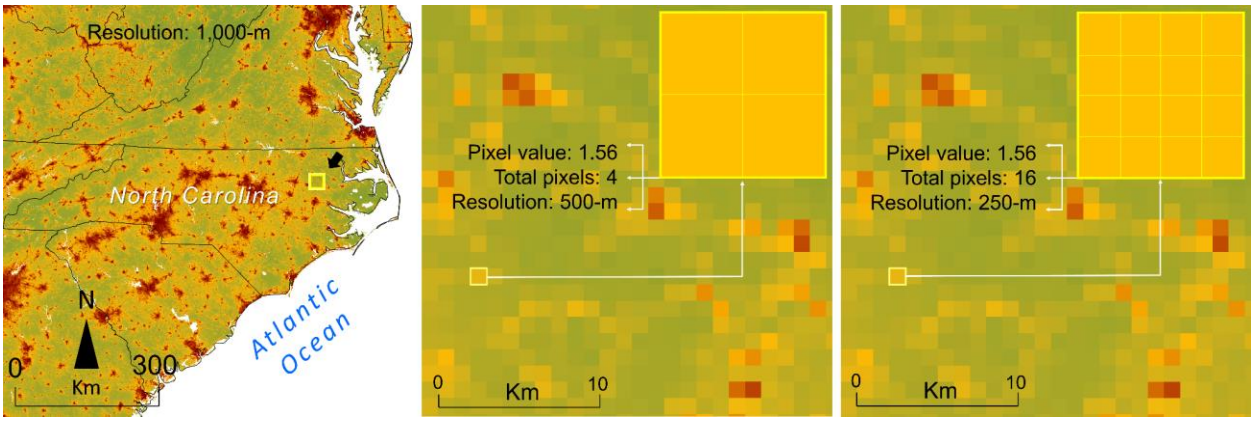

Figure 2.4 Downsampling of 1-km Visible Infrared Imaging Radiometer Suite (VIIRS) data to 500-m and 250-m via resampling. As resolution becomes increasingly fine, minimum and maximum values of pixels do not change but the number of columns and rows increases within the image, as does data volume.

4.1.2. Image Fusion

Image fusion combines images from multiple datasets to produce an output that is more informative at fine scales than any of the individual inputs. Image fusion can function for downscaling when spectral information from a finer resolution is combined with coarser-scale spatial information. Sometimes called 'pansharpening', early fusion methods recalculated the hue, intensity, and saturation of each pixel at the finer scale based on correlations between the multispectral and panchromatic bands (Gillespie et al., 1987; Haydn et al., 1982). Spectral distortions and spatial artefacts were common with pansharpening, prompting a series of improvements (Golibagh Mahyari & Yazdi, 2011; Nencini et al., 2007; Pardo-Iguzquiza et al., 2011; Ranchin et al., 2003; Shah et al., 2008). More recently, deep learning algorithms have been used (Azarang & Ghassemian, 2017; W. Huang et al., 2015; Seo et al., 2020; J. Yang et al., 2017), and in some cases the trained learning network has been shown to generalize well to images from different satellites without the need for retraining (J. Yang et al., 2017). Deep learning methods have a greater computational demand and sometimes require higher-level machine learning expertise by the user. Bayesian-based methods have also been explored, but can be limited due to the difficulty identifying an appropriate statistical model for image representation (Pandit & Bhiwani, 2021). Developing efficient pansharpening approaches remains an active research area (Kaur et al., 2021). Other types of image fusion include Kalman filtering (KF), which is a recursive algorithm for integrating disparate remotely sensed data by minimizing the mean of the squared errors (G. Welch & Bishop, 1997). KF integrates observations and their uncertainties, does not require explicit parameter tuning, and hence is well-suited for large extent applications.

Methods based on Taylor series--an expansion of a function into an infinite sum of polynomial terms-- have also been used for image fusion downscaling. The Taylor expansion assumes that most functions are smooth over the range of interest, so a polynomial can be fit to approximate it. In remote sensing, Taylor series expansion methods (TSEM) model the relationship between surface properties, such as radiance or surface fluxes and heterogeneity and variance/covariance functions, and applies these relationships to aggregate or disaggregate map features (Hu & Islam, 1997). TSEM has been refined for nonlinear functions and to correct scaling bias (Q. Gao et al., 2001; Garrigues et al., 2006). A recent iteration of TSEM is the physical scaling method (PSM), which uses contexture and radiative transfer theory (Tian et al., 2003). TSEM is conceptually straightforward, but computations can be arduous, and TSEMs can be unwieldy with many variables (Malenovský et al., 2007; Pelgrum, 2000; H. Wu & Li, 2009).

Despite the large body of research on image fusion for downscaling, these techniques have been used sparingly in landscape ecology. Townsend et al. (Townsend et al., 2009) compared 15-m pansharpened Landsat images to 30-m images in an analysis of spatial patterns in protected areas and found that the pansharpened images produced lower classification accuracies, possibly due to noise introduced by the fusion process. Chen et al. (2020) used TSEM to attribute surface temperature anomalies to different LULC spatial patterns, but the application was not directly used for pattern analysis. Beyond these, pansharpening has been used in landscape ecology for estimating aboveground biomass (Doyog et al., 2021) and counting wildlife (Duporge et al., 2020). However, an opportunity exists to use the validated fusion methods described above for downscaling in order to increase the spatial resolution of data for spatial pattern investigations.

4.1.3 Interpolation

Interpolation infers a downscaling solution through a model but does not resolve it through the production of new, fine resolution data (Atkinson, 2013). This is in contrast to the use of the term interpolation to predict between sparsely distributed points. Bilinear or bicubic interpolation samples nearby pixels to estimate the values for finer resolution pixels. Another, more advanced example is spatial area-to-point (ATP) kriging, which predicts values on a scale smaller than the original data (Goovaerts, 2006; Kyriakidis, 2004; Yoo & Kyriakidis, 2006). Since it is not possible to measure remote sensing on a strictly point scale, the punctual semivariogram required for ATP kriging must be estimated through a de-regularization or deconvolution procedure (Goovaerts, 2006; Kyriakidis, 2004; Yoo & Kyriakidis, 2006). Other kriging methods include downscaling cokriging for image sharpening (Pardo-Igúzquiza et al., 2006, 2006), geographically weighted ATP regression kriging, which considers spatial autocorrelation (Jin et al., 2018), and multiscale geographically weighted regression kriging, which is a hybrid of multiscale geographically weighted regression (MGWR) and ATP kriging (C. Yang et al., 2019). Geographically weighted ATP regression kriging has been used to downscale temperature data when studying species' range shifts (Platts et al., 2019), and bilinear interpolation has been used to downscale projected climate data to study climate change impacts on tree species (Attorre et al., 2011). Landscape metrics have been used to aid ATP residual kriging by providing supplemental information on the density of land cover patches (Liu et al., 2008), but studies using ATP kriging to downscale data prior to computing spatial pattern metrics are lacking.

4.1.4. Super-resolution mapping

Super-resolution mapping, sometimes called sub-pixel mapping (SPM), attempts to resolve the spatial distribution of land covers from a continuous raster of land cover proportions. SPM techniques are often applied to data that have been generated through spectral unmixing (i.e., spectral mixture

analysis; (Keshava & Mustard, 2002). Many SPM methods rely on fundamental theories of maximum spatial dependency to guide the placement of sub-pixels (X. Li et al., 2014), with others incorporating training models and ancillary data such as histograms, transition probabilities, and variograms into algorithm development (Boucher & Kyriakidis, 2006; Y. Wang et al., 2016). More recently, machine learning and deep learning methods have been implemented to resolve high resolution spatial information in images (Ling & Foody, 2019; Nigussie et al., 2011; Yu et al., 2013; L. Zhang et al., 2016). However, these approaches do not always outperform simpler methods (Sharifi et al., 2019), and they can be computationally intensive.

Spatial pattern metrics have been used to inform SPM algorithms, similar to ATP residual kriging (described above). Su (2019) used the scale-invariant concept of fractals to guide a Hopfield neural network for SPM. Despite much progress related to SPM in the image processing and pattern recognition communities in the past decade though, these techniques have not been widely applied in landscape ecology, perhaps due to the computational complexities and lack of a universal method (Frazier, 2015a). More research may also be needed on the upper and lower limits of scaling in SPM (Ge et al., 2019) before the techniques can be widely applied in ecological investigations. One example of their use for spatial pattern analysis is from Muad and Foody (2012), who used SPM to delineate lakes and evaluate their shape characterization (area, perimeter, compactness). SPM provided results that closely matched the ground data, but the authors found it did not outperform interpolation downscaling techniques (bilinear and bicubic).

4.2. Downscaling categorical land cover data

Landscape ecologists frequently work with remote sensing data that have already been transformed into categorical land cover classes. Land cover data such as the National Land Cover Database, Coordination of Information on the Environment, Copernicus, GlobeLand30, and others are

often produced from satellite sensors where the nominal scale is fixed. When finer scale data are needed, statistical downscaling techniques can be used to translate relationships between the coarser-grained categorical data and finer-grained covariates (e.g., climate, landforms, human activity, etc.) to produce fine-grained predictions (Atkinson, 2013). Relationships between the response variable and covariates are typically modeled using regression (Dendoncker et al., 2006), with advanced techniques using generalized additive modeling with constrained optimization (Hoskins et al., 2016) or integrating geostatistics via block-to-point kriging to include an estimation of uncertainty (Poggio et al., 2013).

An alternative approach researchers have adopted when seeking to downscale data is to downscale the landscape metric values themselves, rather than the land cover raster from which they were derived. While this approach does not technically downscale remote sensing pixels, these techniques are an important research area of landscape ecology. These techniques rest on the empirical evidence that many landscape metrics exhibit consistent and robust scaling relationships across a range of spatial grains or extent (M. G. Turner, 1989; J. Wu, 2004). These relationships between metric and scale often follow a power law relationship (Frazier et al., 2021), and this function can be extrapolated to predict the data at finer scales (Argañaraz & Entraigas, 2014; Frazier, 2014; Saura & Castro, 2007). Success has been variable though (Frazier, 2015a) because coarse-graining the land cover rasters, which is required to derive the scaling function, introduces statistical biases. Researchers are working to overcome these biases, but a universal method is not yet available.

5. Discussion and synthesis

This review highlights the plethora of upscaling and downscaling methods for remote sensing data that are available to landscape ecologists. Several summary points emerge. First, with upscaling, the oversimplification of results is a persistent challenge with both continuous and categorical data. The underlying heterogeneity and landscape structure can be lost during aggregation, and rare categorical

classes may disappear entirely, which ultimately impacts the accuracy of spatial pattern analyses performed on the data. Oversimplification is more likely to occur when using basic methods, such as mean or central pixel resampling, whereas neighborhood approaches such as MWDA are designed to better preserve the spatial structure of underlying heterogeneity. Since heterogeneity ultimately drives the spatial patterns measured across a landscape, preserving heterogeneity during upscaling or downscaling should be the primary consideration for landscape ecologists.

The review found that object-based approaches can overcome some of the challenges with precision and accuracy that result from pixel-based techniques. These object-based approaches present an interesting dilemma for landscape ecologists though. Since patch boundaries are more likely to align with spatial objects than individual pixels, these approaches may be viable options for upscaling and downscaling when the aim is ultimately to compute spatial pattern analyses. However, object-based approaches are designed to collapse inter-pixel heterogeneity based on spatial and spectral similarity, so it is important to ensure that the scale of the original image dataset being upscaled is finer than the observational scale at which the phenomenon of interest presents. Otherwise, identified objects may not represent homogenous patches, and upscaling will simply increase uncertainty.

Regarding downscaling, resampling is the most basic technique to implement, but it does not actually change pixel values and can therefore falsely suggest a higher level of heterogeneity is present. More advanced interpolation, fusion, and sub-pixel mapping methods have been developed by the remote sensing community, but landscape ecologists do not appear to be utilizing these techniques to improve the spatial resolution of datasets prior to computing spatial pattern analyses. When downscaling categorical land cover data, regression-based approaches that correlate covariates to land cover are common, however, care must be taken to ensure that the variables used in downscaling are not also used in any ancillary analyses with the downscaled data, otherwise collinearity is likely.

5.1 Considerations when scaling data for spatial pattern analyses

The many scaling methods available can quickly overwhelm researchers, particularly when considering the varying levels of complexity that characterize the different methods. Choosing the most appropriate method often requires considering the scale of any ecological patterns and processes, discrepancies between the data and the process of interest, uncertainties and biases in datasets, and limitations in computer processing, software availability, and programming familiarity. Just as there is no quintessential scale from which to study ecological phenomena, there is similarly no single method conducive for scaling remote sensing data in all ecological contexts. A visual, decision-tree guide is provided to aid researchers in selecting the most appropriate technique for their data (Fig.2.5). Below, we walk through several considerations that may be important for spatial pattern landscape analyses.

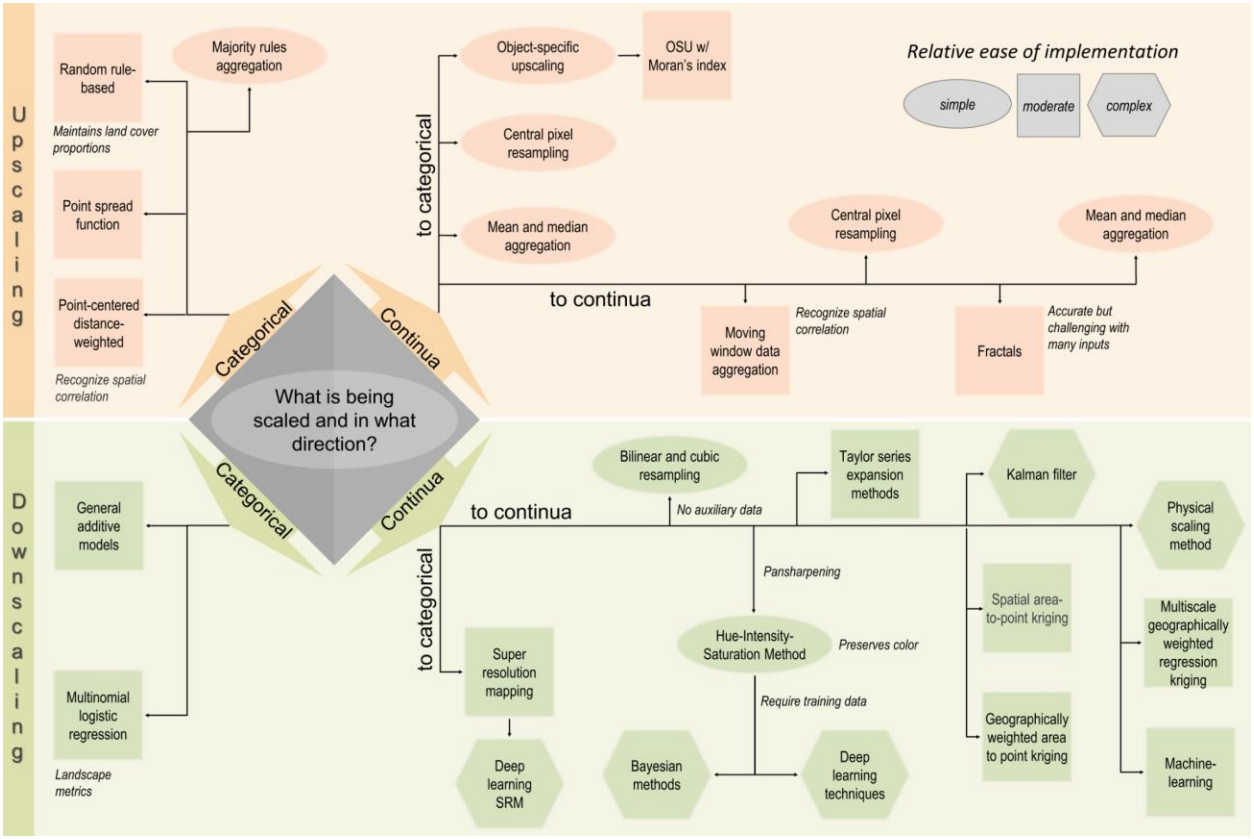

Figure 2.5 Guide for selecting methods for scaling remotely sensed data for spatial pattern analysis. Additional information about each method can be found in the text as well as in Appendix B.

Much like species richness and abundance are the central tenets of species diversity, patch richness and abundance are similarly important for landscape diversity. The elimination of small or rare patches in a dataset can drastically alter one or both of these measures, leading to biases in spatial pattern metrics, and inaccuracies in subsequent pattern-process relationships. Therefore, researchers must be particularly cognizant of how a scaling algorithm might alter patch richness and abundance. In situations where the upscaled resolution will be larger than the size of individual patches and it is important to maintain small or rare patches or values, researchers should avoid using methods that select a single value (e.g., min, max, central pixel, etc.). Instead, methods that closely maintain the original distribution of values, such as MWDA, are a better option for preserving the original heterogeneity of the landscape. An exception is when the land cover/patch type of interest is known to be characterized by the min or max value. In cases where this land cover/patch type should be prioritized, then the appropriate descriptive statistics can be used. When upscaling categorical data, majority and random rule-based methods are more likely to eliminate small or rare land covers compared to the point-centered distance-weighted method. However, if priority is placed on maintaining the largest or most dominant patches, then MRA, RRB, or central pixel resampling methods are likely sufficient. If preserving land cover type proportions and spatial information and patterns are the priority, RRB outperforms MRA (He et al., 2002).

Researchers must also consider the methodological limitations of each technique, including assumptions that underlying processes are scale independent or linear, and whether additional data are needed (F. Gao et al., 2015). The extent to which a method is robust to nonlinearity should be considered, including selecting methods that are suitable for nonlinear relationships. As advanced

computational techniques such as machine learning and deep learning are adopted for rescaling, researchers should understand how these functions operate so that they may correctly parameterize models. Platforms like Google Earth Engine (GEE) are making it easier for researchers to perform these advanced computational techniques on large datasets, but it is important to understand how these platforms handle scale. For instance, scale in GEE must be specified by the user when exporting imagery or performing analyses, and the GEE user guide explicitly notes, "understanding how Earth Engine handles scale is crucial to interpreting scientific results obtained from Earth Engine."

5.2 A way forward

5.2.1. Better incorporating heterogeneity into scaling

Scale and heterogeneity are inherently linked (T. F. H. Allen & Hoekstra, 1991; Dutilleul & Legendre, 1993; Kolasa & Pickett, 1991; H. Li & Reynolds, 1995; M. G. Turner, 1987), and it is impossible to translate data across scales without either ignoring heterogeneity or dealing with it explicitly and effectively (J. Wu, 2007). Most studies do not quantify or test the impact of heterogeneity on scaling results (Frazier, 2015b), leaving a dearth of understanding with regard to exactly how scaling impacts heterogeneity and vice versa. Certain techniques, such as MRA, will introduce different magnitudes of uncertainty into upscaled data based on the composition and configuration of the land cover classes (Frazier, 2014; Frazier et al., 2021), and these aspects should not simply be ignored when rescaling data. At a minimum, the heterogeneity of the data being rescaled can be quantified and reported. Moving forward, researchers should explore the ways in which heterogeneity impacts scaling and continue to select and develop methods that deal explicitly with heterogeneity or minimize the change in heterogeneity.

This review highlighted how advances in artificial intelligence and deep learning are being leveraged to reduce the loss of heterogeneity and improve the accuracy of scaling methods. Research applying deep learning algorithms in remote sensing has grown increasingly mature (Ma et al., 2019), and improvements continue to be made that decrease processing time and requirements and better address heterogeneous and complex data. The fields of computer vision and signal processing continue to refine methods that can be applied to scaling. Examples include new spatial filtering approaches featuring nonlinear decomposition for pansharpening (Pandit & Bhiwani, 2021), using dense blocks in deep networks to efficiently utilize shallow information for image fusion (H. Li & Wu, 2019), and employing a Generative Adversarial Network with structural similarity, gradient loss functions, and concatenating images at each layer of the deep network to retain more information when fusing images (Fu et al., 2021). Keeping abreast of methodological developments in diverse fields will allow landscape ecologists to capitalize on innovations and state-of-the-art approaches to increase the accuracy and precision of scaling while minimizing processing demands.

5.2.2. Improving spatial resolution through new technologies

Advances in very high resolution commercial and personal remote sensing systems (e.g., Planet imagery and Uncrewed Aerial Systems (UAS), or drones, respectively) are rapidly increasing the bounds of remote sensing spatial resolution and creating opportunities to better understand the impacts of scaling. As these data become more prevalent and reliable, they can be used to bridge spatial scales and calibrate scaling models (Alvarez-Vanhard et al., 2021). Fusion methods, such as those developed using neural networks and deep learning (Jia et al., 2020; Song et al., 2018; X. Zhu et al., 2018) can be used to combine UAS data with coarser, satellite-derived data streams. However, research to date has focused mainly on calibration and measurement comparison rather than image fusion (Alvarez-Vanhard et al., 2021). Nonetheless, ecologists are already adopting UAS as a key tool for bridging gaps between satellite

imagery and *in-situ* measurements (Revill et al., 2020; Thapa et al., 2021). As ecologists embrace UAS, their use may act as a catalyst for developing new downscaling methods and provide data that would otherwise be unavailable.

5.2.3. Open science frameworks to promote cross-disciplinary research

The push for reproducibility and openness in science, through platforms such as GEE and open source coding environments (Brunsdon & Comber, 2020) may serve to further the science of scaling. Platforms like GitHub host a myriad of packages, scripts, and tutorials on scaling, potentially galvanizing novel and unconventional ideas. Increased accessibility may alleviate limitations in scaling science, such as lack of sufficient training data for machine learning. These platforms and environments can also reduce computational time and processing demands. Alternatively, the progression of scaling science may be impaired if increased access leads to neglecting the nuances of remote sensing data, mischaracterizing scale effects, and improperly scaling data.

Advancing the science of scaling requires cross-disciplinary research both in regards to theory and technology (H. Wu & Li, 2009). Landscape ecologists can look to the fields of climatology, atmospheric science, computer science, and others to develop scaling approaches pertinent to their research. Questions surrounding implementing multiscale approaches, invariants of scale, and the ability to change scale may already be partially answered, but the answers are scattered across disciplines, and this lack of integration hinders knowledge production (Goodchild & Quattrochi, 1997). Cross disciplinary collaboration may lead to novel methods of incorporating heterogeneity into scaling techniques, a universal method for developing scaling functions, and closing or shrinking additional knowledge gaps. A number of recent reviews in adjacent and germane fields have discussed scale and scaling remotely sensed data (e.g., in earth science (Ge et al., 2019), irrigation science (Ha et al., 2013), agronomy

(Grunwald et al., 2015), geophysics/soil moisture (Peng et al., 2017), providing ample opportunity to compare perspectives.

6. Conclusion

Remotely sensed data and derived products are key components of landscape analysis, but often need to be scaled to meet modeling or analysis assumptions. A plethora of scaling methods are available ranging from simple techniques with limited computational demands to more advanced methods that use deep learning algorithms. However, recognizing the advantages and limitations of different scaling methods as well as the differences between techniques is obligatory for landscape ecologists studying spatial patterns. Scale biases can add significant uncertainty and inaccuracies to an analysis. Neglecting these potential effects can complicate spatial pattern analysis and obfuscate results. We reviewed the methods available for upscaling and downscaling remote sensing data and identified the following key findings.

First, with both upscaling and downscaling, there is no single appropriate scaling method, and so there are always tradeoffs that must be considered. While a diversity of scaling methods are available to landscape ecologists, work remains to integrate these into spatial pattern analyses. Second, landscape ecologists must be particularly aware of how scaling impacts patch richness and abundance, as these pillars of landscape diversity will be impacted differently by different scaling methods (e.g., through the elimination of patches, promoting dominance of one class. etc.). Third, methods that preserve heterogeneity, such as moving window or object-based approaches, may ultimately be better suited for spatial pattern analysis, but more work is needed to understand how heterogeneity is impacted by scaling and vice versa. Fourth, the field can focus on leveraging technological advances in machine learning and deep learning and methodological innovations in computer vision and signal processing. Lastly, plenty of scaling techniques exist, but it appears many are not widely applied in landscape ecology. We can suggest more collaborations with remote sensing and signal processing scientists, but

ultimately, the path forward is to ensure landscape ecologists know about the different options, understand the potential benefits of scaling data (particularly for downscaling), and feel comfortable determining an appropriate method.

3 SPATIAL-TEMPORAL SCALE EFFECTS QUANTIFYING LAND USE LAND COVER CHANGE AND VEGETATION CONDITION RELATED TO ELEPHANT RESOURCES AND HABITAT[2]

[2] Markham, K. To be submitted to *Pachyderm*.

Abstract

Land use and land cover maps form the basis of many wildlife conservation studies. They are often formed from remotely sensed satellite imagery, but there is a variety of imagery available at different spatial, temporal, and spectral resolutions and not all options are free of cost. Selecting the imagery most suitable to the study is a matter of great importance, as differences in the scale of measurement can impact land cover classifications and ensuing analysis. This study modeled land cover around Victoria Falls, Zimbabwe using Landsat 8 OLI, Sentinel-2 MSI, and Planet Quarterly Basemaps in 2019 and 2021. As this region is highly seasonal, maps were created in the wet and dry season. The purpose of this study was to identify the spatial resolution necessary for studying land cover and vegetation in relation to elephant habitat and human-elephant conflict. The random forest machine learning algorithm was used to classify land cover and generate 12 digital maps in total. Landscape metrics were calculated from top-performing land cover models and vegetation health was examined. While maps created using Landsat imagery were consistent in their high accuracy, they might not be best suited for this analysis. The higher spatial resolution provided by Sentinel imagery identifies small patches of forest that might be crucial to modeling conflict.

1 Introduction

Mapping land use/land cover (LULC) is a key component of studying biodiversity loss, monitoring protected areas, and detecting changes in ecosystem services (Jones et al., 2009; Powers & Jetz, 2019; J. Wiens et al., 2009). Remote sensing allows for consistent monitoring of large areas without the costs and effort associated with field-based land cover mapping (Cihlar, 2000; Green et al., 1994; Z. Zhu et al., 2019; Z. Zhu & Woodcock, 2014). For wildlife conservation studies, land cover maps provide the basis of habitat suitability studies, corridor mapping, and other geospatial analysis (Dejene et al., 2021; Kileo & Mbije, 2021).

Results of LULC and vegetation mapping can be impacted by the scale of measurement (Moody & Woodcock, 1995; Townsend et al., 2009; R. Welch et al., 1999) and are also subject to constraints based on local phenology (Dymond et al., 2002). Maps created during the dry season may inaccurately represent vegetation health and agricultural land usage, affecting predictions of wildlife land use. Imagery with higher spatial resolution may contain more detailed information on spatial patterns required at times to precisely capture nuances in resource availability for wildlife.

The importance of accurate and timely land cover maps is particularly needed in Zimbabwe, which experiences variable annual precipitation that is hard to predict (Mamombe et al., 2017), human population largely reliant on agriculture (*Zimbabwe Livelihoods Zone Profiles*, 2010), and high elephant density that exceeds carrying capacity in some regions (*ZIMBABWE NATIONAL ELEPHANT MANAGEMENT PLAN (2021 – 2025)*, 2021).

1.1 Local climate and phenology

The climate in Matabeleland North is frequently divided into two seasons: a rainy season starting in October and lasting through March and a dry season from April until October. Eighty percent of precipitation across Zimbabwe falls between the months of November and March, with rainfall shifting earlier during dry years (Mberego & Gwenzi, 2014). The rainy season in Victoria Falls recently shortened by a month, starting in November now rather than October, with a notable decline in October monthly rainfall dating to the 1990s (Dube & Nhamo, 2019). Vegetation typically responds to precipitation by one to two months (Mberego & Gwenzi, 2014). Green up starts in November and declines starting in April (Mberego & Gwenzi, 2014). Crop water requirements peak in December and January (Funk & Budde, 2009). Interannual rainfall is highly variable in Zimbabwe (Mamombe et al., 2017). Average monthly rainfall for the Hwange region over the course of this study period is shown in

Figure 3.1. Interannual precipitation is highly variable and precipitation in 2019 was less than normal.

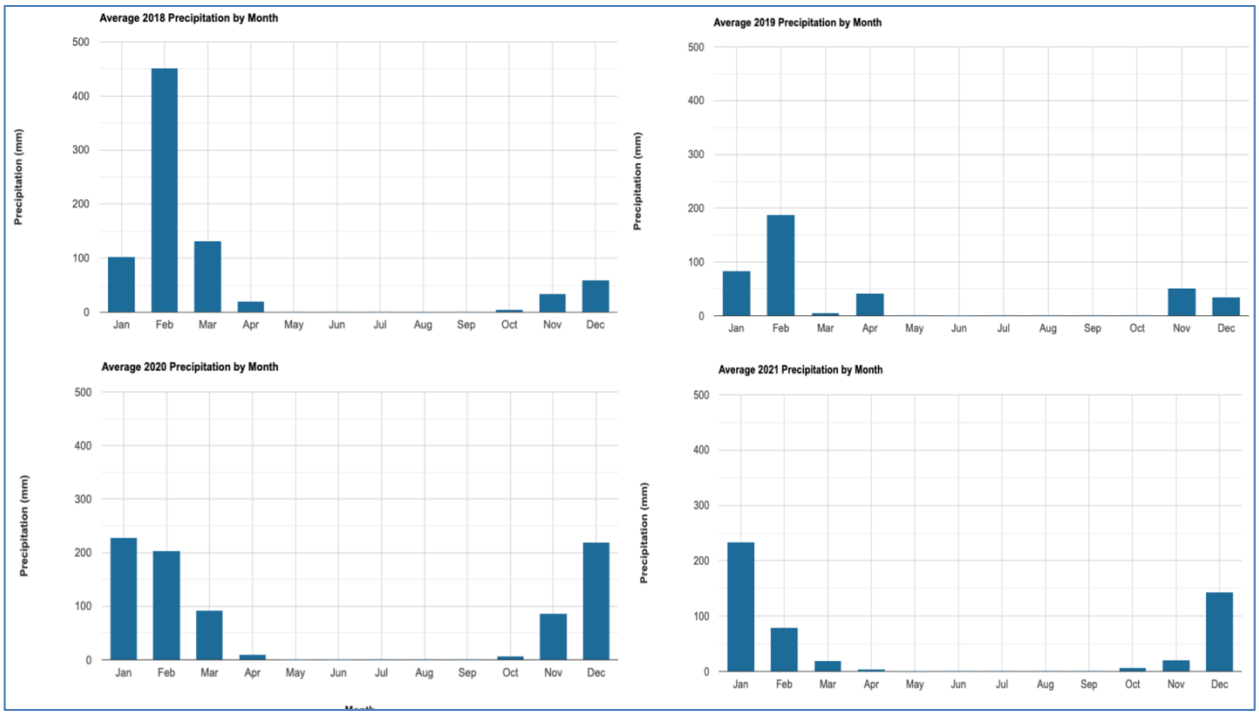

Figure 3.1. Clockwise from left to right, average monthly precipitation in Hwange from 2018-2021. Precipitation is in mm. Data from Climate Hazards Group InfraRed Precipitation with Station data through Google Earth Engine (Funk et al., 2015).

Zimbabwe experiences droughts that are occasionally followed by periods of higher than average rainfall. The Zambezi Basin experienced its lowest annual precipitation levels in 2019 along with decreased water storage due to higher water release from the soil (Hulsman et al., 2021).

Except for a small strip of grassland in the east, the majority of Zimbabwe falls within the broadly-defined savanna vegetation zone (Van Wyk, 2013). Using Köppen-Geiger System, northwestern Zimbabwe is considered a hot, semi-arid climate (type "BSh"). African drylands can present a particular challenge for land cover classification; trees found outside of areas classified as forest account for 30-40% of woody vegetation in Zimbabwe (Reiner et al., 2023). South of Victoria Falls, dominant vegetation

types in the communal lands are dry forests and thickets, specifically *Baikiaea* woodland on Kalahari sand interspersed with Mopane woodlands, more specifically *Colophospermum* woodland) on skeletal soils (Timberlake et al., 1993). The *Baikiaea* woodland in this region is an open woodland characterized by *Baikiaea plurijuga* 10-14 m high and includes a shrub layer with *Paropsia brazzeana, Baphia massaiensis*, *Bauhinia petersiana* and others. *Colophospermum* woodland is composed of open woodland 8-12m high and vegetation approaching woodland thicket with slight variations depending on the subtype of soil (Timberlake et al., 1993). Common species found in the open woodland area include *C. mopane, Kirkia acuminata, Terminalia stuhlmannii,* and others and the shrub layer consists of *Carphalea pubescens, Dalbergia melanoxylon*, *Gardenia resiniflua*, *Dichrostachys cinera*, and others (Timberlake et al., 1993). The greenness of most of these vegetation types drastically changes in satellite imagery in accordance with the seasons, making the phenology, or the study of seasonal and periodic changes on biological life, particularly germane.

1.2 Land use and land cover change

Changes in LULC can have profound effects on biodiversity and human livelihoods and are predicted to be the most important contributor to changes in biodiversity (Sala et al., 2000). Cropland mapping is particularly important given agriculture's increasing role in sustainable resource management (Matton et al., 2015). Across Zimbabwe, changes in land cover are driven by population density, roads, and other factors (Kamwi et al., 2018). Croplands across Zimbabwe are expanding, despite recent droughts (Useya et al., 2019). Land cover change was significant from 1984-2013 in Forest Protected Areas within Zimbabwe with settled forests predictably experiencing more degradation than unsettled forests (Mutekwa & Gambiza, 2016). Forest patches became more fragmented due to encroachment of human land cover types from 2002-2011 in the province to the south of Victoria Falls.

(Shoko et al., 2016) This increase in fragmentation can lead to lower habitat suitability for large herbivores, such as African elephants (Ntukey et al., 2022).

The study area for this research is just over 2,000 km^2 and encompasses Victoria Falls National Park and the communal lands situated south of the city of Victoria Falls (Figure 3.2). The areas known as communal lands in Zimbabwe were established following the country's independence and, while grazing lands are communal, households manage their land through agreements (Matondi, 2012). Technically state land, communal lands are governed by Rural District Councils (Matondi, 2012). Multiple ecosystem types cover the region, including tropical forests near the Zambezi River and the drier Miombo woodlands. Dry forests and woodlands are the least protected and most threatened ecosystem across Africa (Mertz et al., 2007), making their monitoring particularly important. In northwestern Zimbabwe, there is a dearth of consistent and up-to-date data on vegetation productivity in the semi-arid savanna woodlands of southern Africa (Murwendo et al., 2021). Projections of future land cover change for croplands vary considerably in Zimbabwe (Prestele et al., 2016), underscoring the importance of accurately quantifying growth and distribution. The city of Victoria Falls is also growing; the population in the Matabeleland North Province in 2012 was 749,017 growing to 827,626 in 2022 (ZimStats, 2022). The area is also a popular tourist destination; Mosi-oa-Tunya, also known as Victoria Falls, is the largest waterfall on earth and one of the seven natural wonders of the world. Fifty billion US dollars in proposed development are currently planned across such an extent that plans are not without controversy (Keep Victoria Falls Wild, 2023). Further research on landscape changes in Southern Africa is particularly needed, given growing urban populations and the resulting intensification of agricultural production leading to increased human-elephant conflict (Musakwa & Wang, 2018).

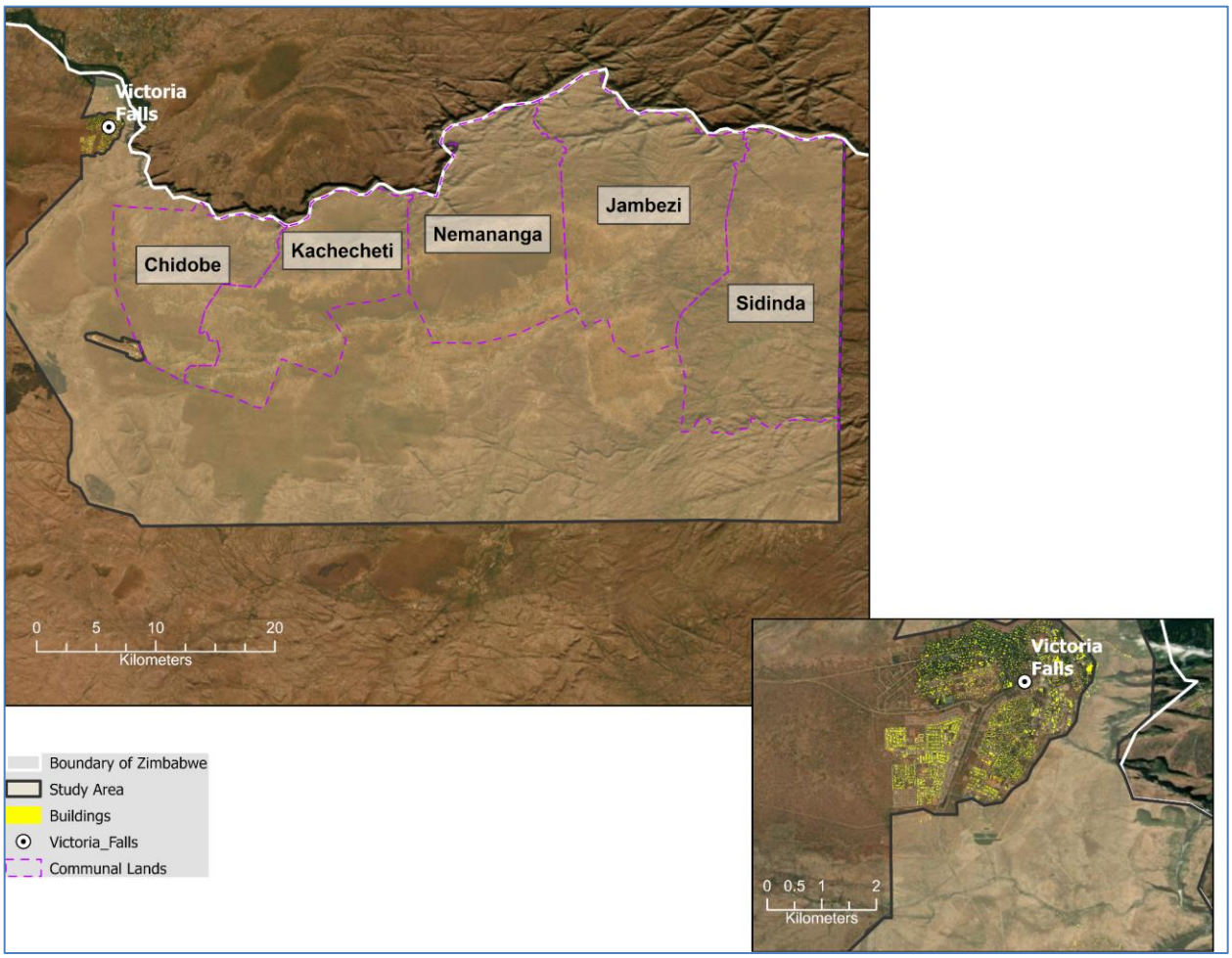

Figure 3.2. Study area for land cover classification. Study area outlined in black with beige transparency. Communal lands are identified by number and outlined in bright pink, dashed lines. Buildings from Open Street Map are in yellow. The city of Victoria Falls is indicated by a black dot encircled in a white dot. The country border of Zimbabwe is in white.

1.3 Objectives

To characterize land cover change and determine the appropriate spatial resolution needed to understand elephant resources, we map land cover around the communal agricultural area south of Victoria Falls, Zimbabwe in 2019 and 2021. Our main objectives are to 1) understand how spatial scale

and seasonality affect LULC monitoring and 2) understand how vegetation greenness, related to the health and biomass of the vegetation, changes seasonally in this region.

2 Methods

To identify how spatial scale and seasonality affect LULC monitoring and understand how vegetation biomass changes seasonally, land cover was mapped for two distinct phenological periods in 2019 and 2021 corresponding roughly with the wet and dry season. Landcover during these periods was classified using imagery from three satellite sensors with varying spatial resolution, thus, 12 land cover maps were created in total. An overview of methods can be found in Figure 3.3.

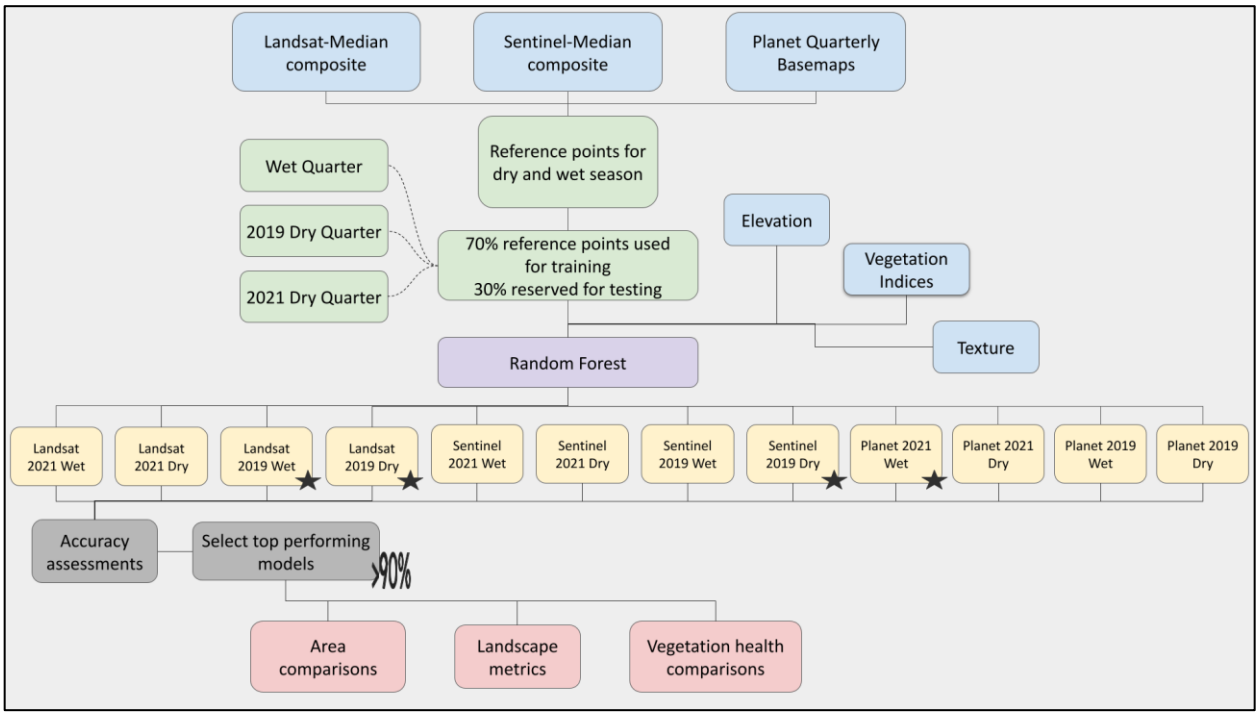

Figure 3.3. Methods flowchart for land cover classification. Blue boxes indicate model inputs and include elevation, and vegetation indices and texture generated from Landsat median composites, Sentinel median composites, and Planet Quarterly Basemaps. Processes related to generating reference points are in green, the machine learning model used for classification, random forest, is in purple. Land cover

maps generated are in yellow. Stars indicate top-performing models. Model evaluation steps are in grey and further analyses are in red. For more information on methods, refer to the text.

2.1 Imagery collection and preprocessing

Landsat 8 OLI, Sentinel-2A/2B MSI, and PlanetScope imagery were used to create LULC maps. PlanetScope imagery was obtained through an educational account granting access to a limited amount of data that can be downloaded per month free of charge. Landsat and Sentinel imagery, on the other hand, are both freely available and open to the public. Each satellite sensor differs in imagery collection dates and spectral resolution (Table 3.1). Images were selected to minimize cloud coverage in the area of interest.

The organizations producing such imagery (US Geological Survey, European Space Agency, and Planet Labs, respectively,) vary in the level of image processing they provide, the ease in accessing and viewing their data, the products they create and for which dates those products are available. At the time of writing, Planet Quarterly Basemaps did not include a near infrared (NIR) band.

Table 3.1. Imagery for land use land cover classification

Satellite product	**Spatial resolution**	**Spectral resolution**	**Temporal resolution**
Planet Quarterly Basemaps	3.7m	Red, green, and blue (RGB) only	Daily but mosaic grabs a cloud-free pixel from the earliest available date
Harmonized Sentinel-2 MSI: MultiSpectral Instrument, Level-2A	10m-RGB and near infrared (NIR) 20m-Vegetation red edge, narrow NIR, shortwave infrared (SWIR)	RGB and NIR 4 narrow bands in the narrow NIR 2 wider SWIR bands	Every 5 days

Landsat 8 OLI Level 1, Surface Reflectance	30m (15m panchromatic)	RGB, 1 NIR band, 2 SWIR bands	16 days

The wet season in Zimbabwe typically spans November through March and the dry season April through October (Dube & Nhamo, 2019). Maps were created to reflect the approximate midpoint of these respective seasons for both 2019 and 2021. These years were chosen based on the availability of imagery across all satellite sensors/products. To correspond with local weather patterns and Planet Quarterly Basemaps, the wet quarter is defined as January, February, and March and the dry quarter as July, August, and September. Using Google Earth Engine (GEE), atmospherically corrected Sentinel and Landsat imagery were collected for the corresponding months, clouds were masked, and wet and dry quarter median composites were created to accurately represent the land conditions during these times (Phan et al., 2020). Figure 3.4 shows imagery used for 2019 classifications.

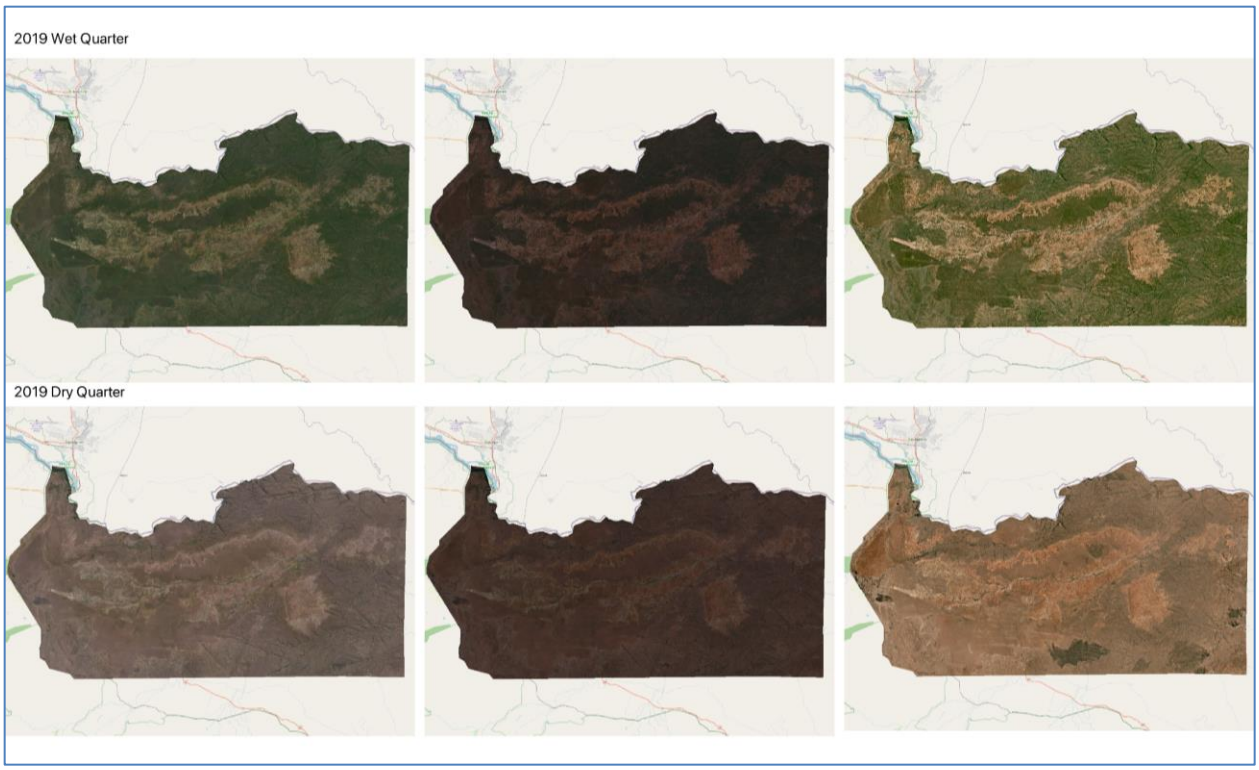

Figure 3.4. True color composites of 2019 imagery used for land cover classification. Dry quarter shown on top and wet quarter on bottom. From left to right, Landsat, Sentinel, and Planet.

2.2 Land cover classification

Land cover was classified using random forest, an ensemble machine learning classification method using decision trees that can learn complex non-linear relationships (Breiman, 2001). The algorithm is optimized based on the number of trees grown and the number of predictors used at each branch as new nodes are created (Breiman, 2001). Compared with other machine learning classifiers, random forest handles noise well, is insensitive to outliers, and is highly accurate (Na et al., 2010; Rodriguez-Galiano & Chica-Rivas, 2014). Other machine learning algorithms were tested, including classification and regression trees and naive Bayes, but random forest was the most consistent across satellites in its high accuracy (accuracy percentages 80 to >90 using random forest compared to accuracy percentages 70-90% for classification and regression trees and <50% for naïve Bayes).

Classification was completed in Google Earth Engine using the Smile.RandomForest classifier. Seventy percent of the reference points per class were used for training and the remaining 30% were reserved for testing. A total of 500 trees were used with no maximum number of leaf nodes per tree.

Reference points used to train and test the random forest classifier were taken for each class and verified using a combination of high resolution imagery from Google Earth Pro and in consultation with partners *in-situ*. All reference points were visually checked for each satellite sensor, year, and quarter. Any points requiring adjustment due to ephemeral differences in use or condition (bare soil versus agriculture) or due to pixel alignment issues caused by differing pixel size were corrected. A minimum of 100 reference points per class were created. For dry quarter classifications, 822 reference points were used and, for the wet quarter, 719 reference points.

The land cover classes deemed most applicable to this region were: lowland vegetation, closed canopy forest, open canopy forest, shrubland/thicket, grassland, agriculture, bare soil, and water (Table 3.2). A dry quarter only class, burn, was also included, as burned agricultural/natural areas show a distinct pattern on the landscape. The aforementioned classes were chosen based on a review of the region's ecology, existing land cover classifications, and after consultation with collaborators *in-situ*. Given the relatively small area of developed land and the lack of surface distinguishable from bare soil, developed area was not a chosen class. Attention was also paid to the likelihood that class would be detectable at all spatial resolutions.

Table 3.2. Land cover classes used along with ecological and visual description and the equivalent classes from the European Space Agency's (ESA) Global Land Cover.

Name	**Description**	**ESA Global Land Cover**
Lowland vegetation	Land with soil and vegetation periodically or regularly saturated with water. Water saturated areas may make up over 50% of the coverage at times.	Herbaceous wetland

Closed canopy forest	Tree coverage is greater than 75%	Tree cover
Open canopy forest	Tree coverage is between 25-75%.	Tree cover
Thicket/shrubland	Land dominated by *Baikiaea* woodland and Mopane woodland interspersed with herbaceous grasses and shrubs. Dry forest.	Shrubland
Agriculture	Agricultural land that is being used for crops or as pasture. Agricultural land is geometric and has an obvious shape.	Cropland
Bare soil	Exposed soil or rock that has less than 10% vegetation.	Bare/sparse vegetation
Water	Includes rivers, lakes, streams, water contained in pools, etc.	Permanent water bodies
Burn	Class only relevant to the dry quarter. Area that showed visible fire damage. May have been forest, lowland vegetation, thicket, agricultural area, or bare soil prior to burn scar.	No equivalent class

In addition to individual spectral bands (refer to Table 3. 8 in Appendix C for further information on imagery), select vegetation indices and elevation data from ASTER Global Digital Elevation Model V003, and texture calculations were included as additional explanatory variables (Table 3.3) (Theobald et al., 2015). The Normalized Vegetation Index (NDVI) is widely used for its sensitivity to ecosystem conditions (Goward et al., 1985; S. Huang et al., 2021; Myneni et al., 1995; Ollinger, 2011). It uses the green band and the near infrared band and can be thought of as a measure of greenness in a pixel (Rouse et al., 1974). The Normalized Difference in Green/Red Index (NGRDI) was also used as an indicator of vegetation (Tucker, 1979). This index is calculated from the red and green bands only, thus it could be used to classify regardless of the satellite sensor chosen. It is more commonly used with uncrewed aerial vehicles or drones which often capture a limited number of bands (Hunt et al., 2005; Jannoura et al., 2015; Motohka et al., 2010). Finally, the Normalized Difference Red Edge Index (NDRE) has shown considerable promise for mapping vegetation. This index is similar to NDVI but it uses the red

edge band, ranging from approximately 680 to 730 nm (E. M. Barnes et al., 2000). NDRE is often used when studying crops and is potentially more informative for vegetation health, particularly in regards to identifying stress, measuring chlorophyll content, etc. (Adelabu et al., 2014; Delegido et al., 2011; Eitel et al., 2011; Marx & Kleinschmit, 2017). For index formulas, see Table 3.9 in Appendix C. Measures of image texture offer a quantitative depiction of the visual attributes within an image, encompassing factors like smoothness, roughness, and other relevant characteristics (Baraldi & Panniggiani, 1995). Texture measurements are extracted from the image itself and have the potential to improve land cover classification (Hurni et al., 2013; Shaban & Dikshit, 2001; Soares et al., 1997). Texture calculations were done by measuring entropy in Google Earth Engine using a kernel with a radius of four (Haralick et al., 1973). Calculations were done for individual bands as well as vegetation indices and tested in the classification models. If including the texture measurement improved the classification, it was retained as an additional explanatory variable in the model.

Table 3.3. Data used to train random forest classifiers. *Formulas for indices are included in Appendix C.

	Bands	**Indices***	**Auxiliary variables**
Planet Quarterly Basemaps	RGB	Normalized difference in green/red index NGRDI (Tucker, 1979)	Aspect, elevation, slope green texture (entropy), and red texture
Harmonized Sentinel-2 MSI: MultiSpectral Instrument, Level-2A	RGB, Red Edge 1, 2, & 3, NIR, Red Edge 4, SWIR 1 and 2	NDVI, normalized difference red edge index (NDRE)	NIR texture, SWIR texture, NDVI texture, elevation, slope
Landsat 8 OLI Level 2, Surface Reflectance	RGB, NIR, SWIR 1, and SWIR 2	NDVI and NGRDI	Elevation, slope, NIR texture, NDVI texture, SWIR texture

ASTER Global Digital Elevation Model V003	Elevation. Slope and aspect calculated from elevation.	N/A	N/A

Classification was completed for each year, quarter, and with imagery from each satellite sensor. Accuracy was assessed using total accuracy, user's and producer's accuracy, and kappa coefficients; all of which are commonly used to assess how well a classification distinguishes classes (Congalton & Green, 1999). Total accuracy, user's accuracy, and producer's accuracy all range from 0-1 with 1 meaning 100% of the reference points were classified accurately. Producer's accuracy is the accuracy from the view of the map maker and the user's accuracy the accuracy from the map user, with accuracy indicating how often the land cover class on the map will be found *in-situ*. The kappa coefficient was also calculated. Kappa scores falling between 0.61 and 0.8 indicate a "substantial" level of agreement and scores 0.81 and higher are considered "almost perfect" (Landis & Koch, 1977a, 1977b). Thirty percent of reference points were reserved for testing and these were used to tabulate a confusion or error matrix (Congalton, 1991). Variable importance factors were examined for all models with a total accuracy that exceeded 0.9.

2.3 Landscape metrics

Landscape metrics were calculated for models with an overall accuracy that exceeded 0.9 (accuracy range of 0-1.0) in Fragstats 4.2 (McGarigal et al., 2023). Landscape metrics are one method of efficiently quantifying spatial patterns for ecological analyses. They can be useful for linking patterns to ecological processes, provided one is not capturing the scale-dependency of the metrics themselves (Frazier & Kedron, 2017; Kupfer, 2012). Prior to calculations, the categories of open and closed canopy forest were consolidated into a single forest class. Metrics chosen were based on their informative value and ability to detect habitat fragmentation rather than habitat abundance (X. Wang et al., 2014). Class

metrics calculated include Clumpiness Index (CLUMPY), percent of landscape, and mean patch area. Landscape metrics calculated include Perimeter-Area Fractal Dimension (PAFRAC), Core Area Index Mean (CAI_MN), and Total Edge Contrast Index (TECI). The description of each of these metrics along with the units of measurement and abbreviation can be found in Table 3.4.

Table 3.4. Landscape metrics assessed.

Metric: Landscape (L) and Class (C)	Abbreviation	Unit	Description
Core Area Index Mean (L)	CAI_MN	Percent	The percentage of a patch that is core area.
Total Edge Contrast Index (L)	TECI	Percent	Quantifies edge contrast for the landscape as a whole as a percentage of maximum possible.
Perimeter-Area Fractal Dimension (L)	PAFRAC	N/A	Indicates shape complexity. PAFRAC approaches 1 for shapes with very simple perimeters, such as squares, and approaches 2 for shapes with highly convoluted, plane-filling perimeters.
Clumpiness (C)	CLUMPY	Percent	Measure of habitat subdivision. Calculated from the adjacency matrix, which shows the frequency with which different pairs of patch types appear side-by-side. Score is -1 when patch type is maximally disaggregated and 1 when maximally aggregated.
Percentage of Landscape (C)	PL	Percent	Proportion of each patch type.
Mean Patch Area (C)	AREA_MN	Hectares	Area-weighted mean patch size of patches of the corresponding class, where the proportional area of each patch is based on total class area. AREA_MN at the class level is a function of the number of patches in the class and total class area and does not detail how many patches exist.

2.4 Vegetation condition

Vegetation conditions were examined using the NGRDI, as Planet imagery obtained for this work did not include an infrared band. Index values were compared per land cover class for top performing land cover models.

2.5 Scale effects

Scale effects for select vegetation land classes were identified by comparing the accuracy estimates, area calculations, as well as select landscape metrics for particular dates. Following normality tests, including examining QQ plots and the Shapiro-Wilk normality test, multivariate regression was used to identify any significant effects of seasonality or satellite sensor resolution on land cover area. User's and producer's accuracy were also compared.

3 Results

3.1 Land classification accuracy, variable importance, and classification results

It is important to note that the land cover classification maps referred to in the forthcoming sections are the result of classifications completed using specific bands, indices, and textural calculations that are not consistent across all satellite sensors and products. These classifications are the result of the exact methods and predictors modeled. While the forthcoming text may refer to these maps as "Landsat-based 2019 wet season map" for the sake of brevity, it should always be understood that the comparisons between land cover maps, their accuracies, etc. do not generalize to the satellite sensors and products themselves but instead refer maps created by the specific processing described earlier.

3.1.1 Land classification accuracy

All models performed well, with kappa scores between 0.82 to 0.95 and total accuracies between 0.84 and 0.96. The top two performing models in regards to overall accuracy used Landsat

imagery and reached accuracies of 0.95 or higher (Table 3.5). Models using Landsat outperformed those using Sentinel and Planet across season and year, with the exception of the 2021 wet quarter, in which the random forest models for Landsat and Planet performed similarly (Table 3.5). Across satellites and years, the overall accuracy was slightly higher on average for the wet (0.91) than the dry quarter (0.89) and kappa coefficients on average were similar by season (0.89 wet vs 0.88 dry). Overall accuracy exceeded 0.9 for the 2019 wet quarter using Planet and Landsat, the 2019 dry quarter using Sentinel and Landsat. None of the 2021 models exceeded 0.9 overall accuracy.

Table 3.5. Overall accuracy and kappa coefficients for each year and season by satellite. Models with overall accuracy higher than 0.9 are in bold.

Year	Season	Planet	Sentinel	Landsat
2019	Wet	**Accuracy: 0.91** **Kappa coefficient: 0.90**	Accuracy: 0.89 Kappa coefficient: 0.87	**Accuracy: 0.96** **Kappa coefficient: 0.95**
	Dry	Accuracy: 0.84 Kappa coefficient: 0.82	**Accuracy: 0.94** **Kappa coefficient: 0.93**	**Accuracy: 0.95** **Kappa coefficient: 0.94**
2021	Wet	Accuracy: 0.9 Kappa coefficient: 0.88	Accuracy: 0.88 Kappa coefficient: 0.86	Accuracy: 0.90 Kappa coefficient: 0.88
	Dry	Accuracy: 0.84 Kappa coefficient: 0.82	Accuracy: 0.89 Kappa coefficient: 0.87	Accuracy: 0.90 Kappa coefficient: 0.89

The range of user's accuracy by class was smaller with Landsat imagery compared to Planet and Sentinel (Figure 3.5.A). Models using Planet imagery had user's accuracy scores consistently below 0.9 for agriculture whereas models using Landsat and Sentinel consistently performed better (Figure 3. 5.A). User's accuracy for closed and open forest ranged from perfect to less than 0.8 for closed forest in some models (Figure 3.5.A). User's accuracy for models of open forest were generally higher across satellites.

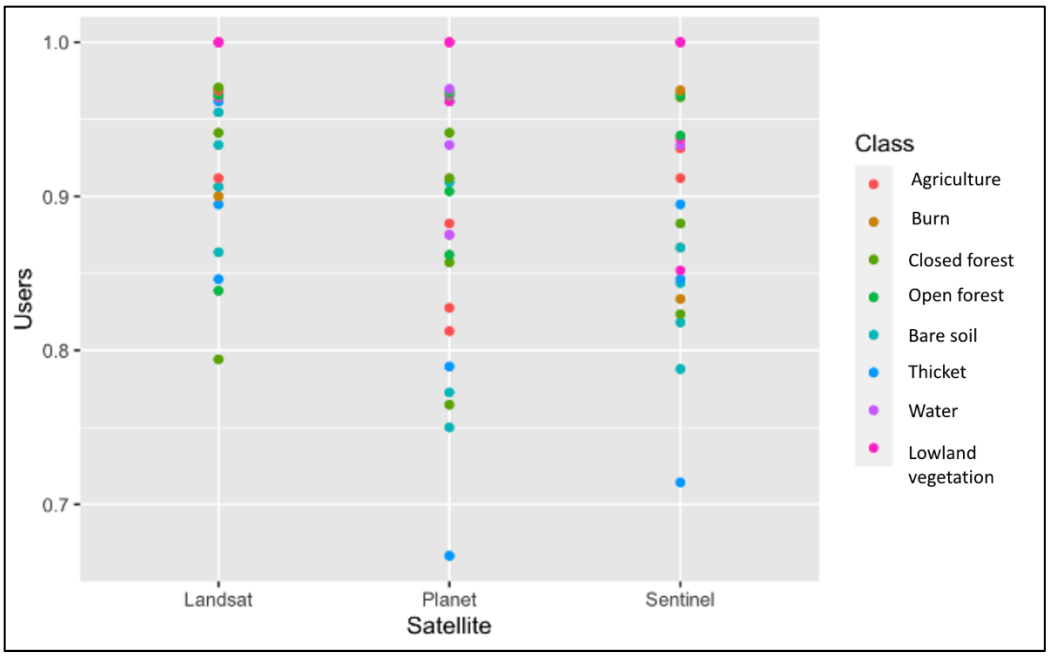

A

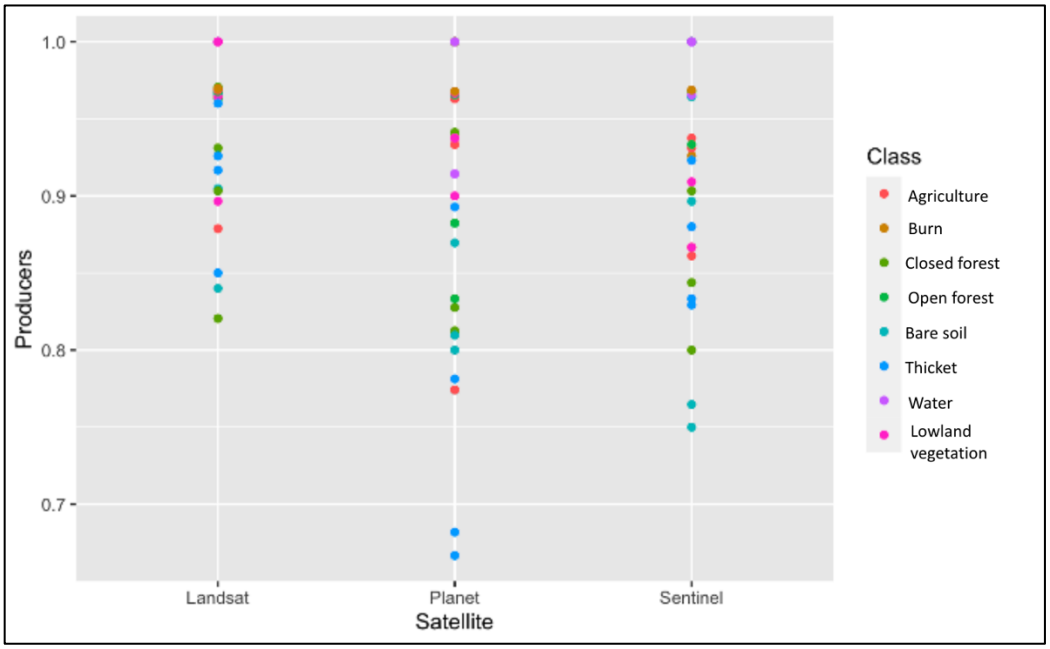

B

Figure 3.5 User's (A) and Producer's (B) accuracy by class: all years, seasons, and satellites. Each dot represents a distinct year, quarter (wet or dry), and class (as indicated by color).

Producer's accuracy also ranged less widely when using Landsat compared to Planet and Sentinel (Figure 3.5.B). Producer's accuracy for agriculture dropped below 0.9 twice using Sentinel

imagery and once using Landsat and Planet imagery. Models using Landsat were generally more successful at classifying both forest types, with producer's accuracy never dropping below 0.95 for open forest. Closed forest was more variable, with perfect accuracy in one model using Planet imagery but with five out of the twelve models scoring below 0.85 (Figure 3.5.B).

Results from linear regression show no significant effect of year or season on model user's accuracy, but using Planet imagery lowered accuracy by 0.05% ($p<0.01$). In reference to the producer's accuracy of land classification models, again Planet imagery lowered accuracy by 0.05% ($p<0.001$). Models using Sentinel imagery lowered accuracy by 0.03% ($p<0.05$). No significant effect of year or season was found for producer's accuracy.

The top performing models generally were quite similar in their user's accuracy between satellites, often scoring within a few percentage points. Exceptions include the class of agriculture during the wet quarter, with user's accuracy of 87.5% using Planet compared to 96.9% using Landsat, soil, with accuracy of 90.1% compared to 86.4%, and closed forest, 91.2% compared to 97.1%. User's accuracy for classifications done in the dry quarter using Landsat and Sentinel differed in the classes of soil, Sentinel having 84.4% accuracy and Landsat 90.6%, and lowland vegetation, Sentinel reaching 85.2% accuracy compared to 96.4% accuracy using Landsat imagery.

3.1.2 Variable importance-top performing models

Of the top performing models, the NGRDI was an important contributing variable in most models (Figure 3.6). The variables with the highest importance in the 2019 wet quarter model using Landsat were NIR, followed by the NGRDI and NDVI. Classification in 2019 using Landsat during the dry quarter shows similar trends, with the NGRDI acting as the most important variable, followed by NDVI, NIR, and then elevation and short wave infrared (SWIR) 2. In the 2019 wet quarter model using Planet imagery, the NGRDI was the most important variable, followed by the blue wavelength and then

elevation. The variables with the greatest importance in the 2019 dry quarter model using Sentinel imagery were elevation followed by SWIR 2, NDVI, and the blue wavelength.

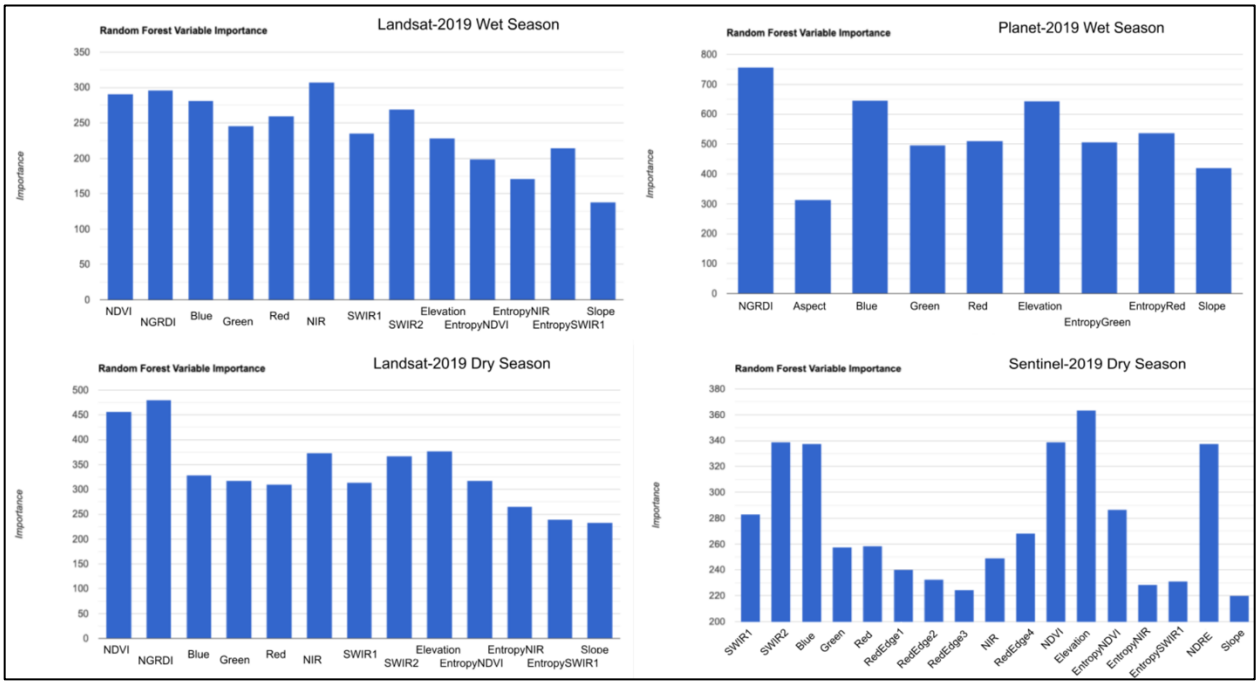

Figure 3.6. Random forest predictor variable importance for top performing land cover classification models. NGRDI= Normalized difference in green/red index, NDRE=Normalized red edge index.

3.1.3 Land cover differences-top performing models

Wet quarter differences between land cover classifications from Landsat and Planet include differences in area classified as thicket with 541.77 km^2 using Landsat compared to 461.39 km^2 using Planet. While the square kilometers classified as bare soil and agriculture between the two satellite sensors were similar, the maps show differences concentrated in particular areas: area in the northeast of the study site classified as agricultural land using Landsat was classified as bare soil when Planet imagery was used (Figure 3.7). There was also a difference in the area classified as thicket during the dry quarter using Landsat and Sentinel, with 416.35 km^2 using Landsat and 541.77 km^2 with Sentinel. Dry

quarter classifications using Sentinel and Landsat both resulted in more area classified as forest when compared to the wet quarter.

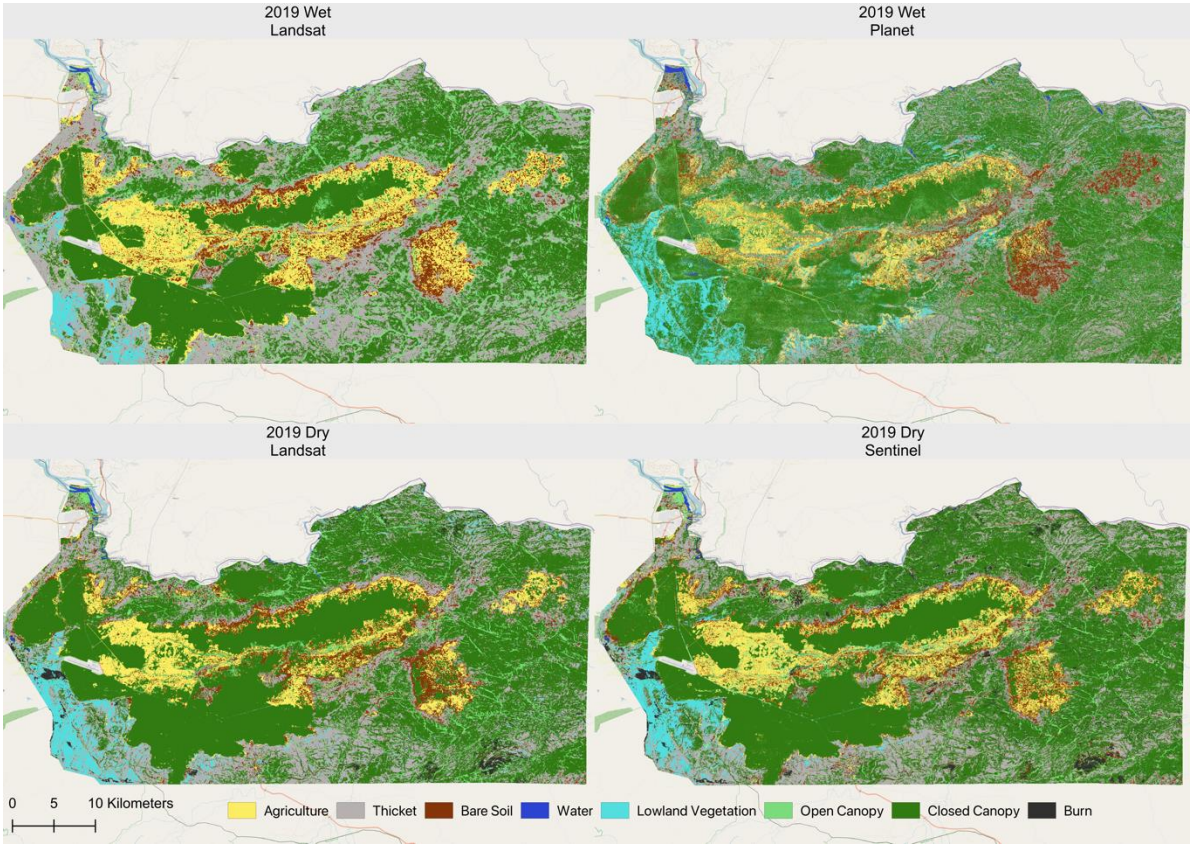

Figure 3.7. Land cover classification maps for the 2019 wet and dry quarter.

In regards specifically to classification of forest, total forest area was slightly greater during the dry quarter than the wet quarter. Total area classified as forest during the dry quarter were similar between Landsat and Sentinel; differing by less than 10 km^2 for open canopy forest and less than 30 km^2 for closed canopy forest. During the wet quarter, the classification using Planet imagery included slightly more closed canopy forest (903.99 km^2) compared to Landsat (1,120.66 km^2) but less open canopy forest (153.47 km^2 versus 203.77 km^2). When consolidating open and closed canopy forest, the extent of

agreement between Landsat and Planet covers most large extents of forest, but Planet, with its greater spatial resolution, classifies more small patches of land as forest (Figures 3.8 & 3.9).

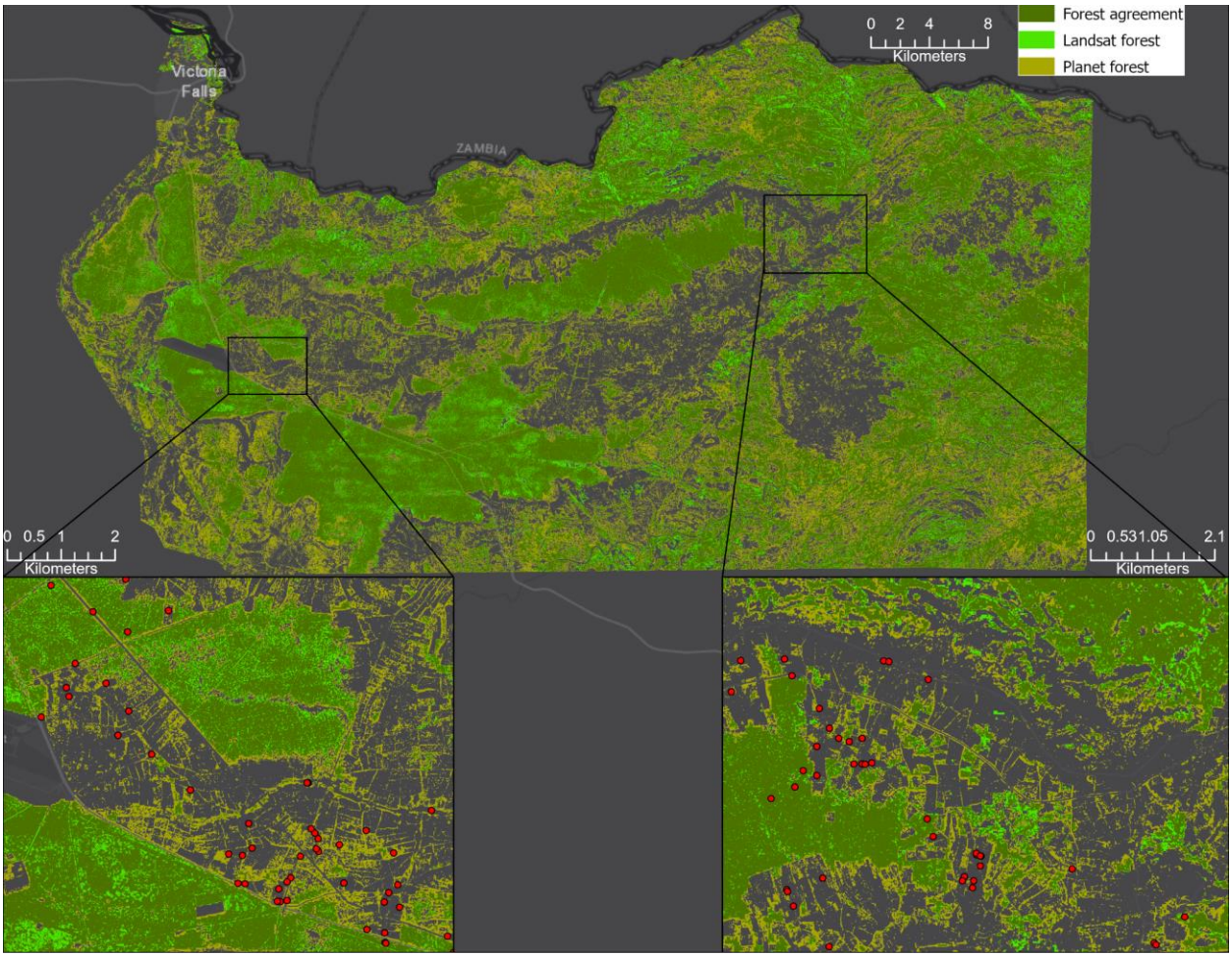

Figure 3.8. Comparison of forest classifications during the 2019 wet quarter using Landsat and Planet imagery. Areas classified as forest (either closed or open canopy) when using Landsat imagery but not when using Planet imagery are shown in bright green. Areas classified as forest when using Planet imagery but not Landsat are shown in olive green. Two insert maps in the bottom also show elephant-human conflict locations from 2015-2021. Note that forest cover at the date of these conflict points may or may not differ from what is shown.

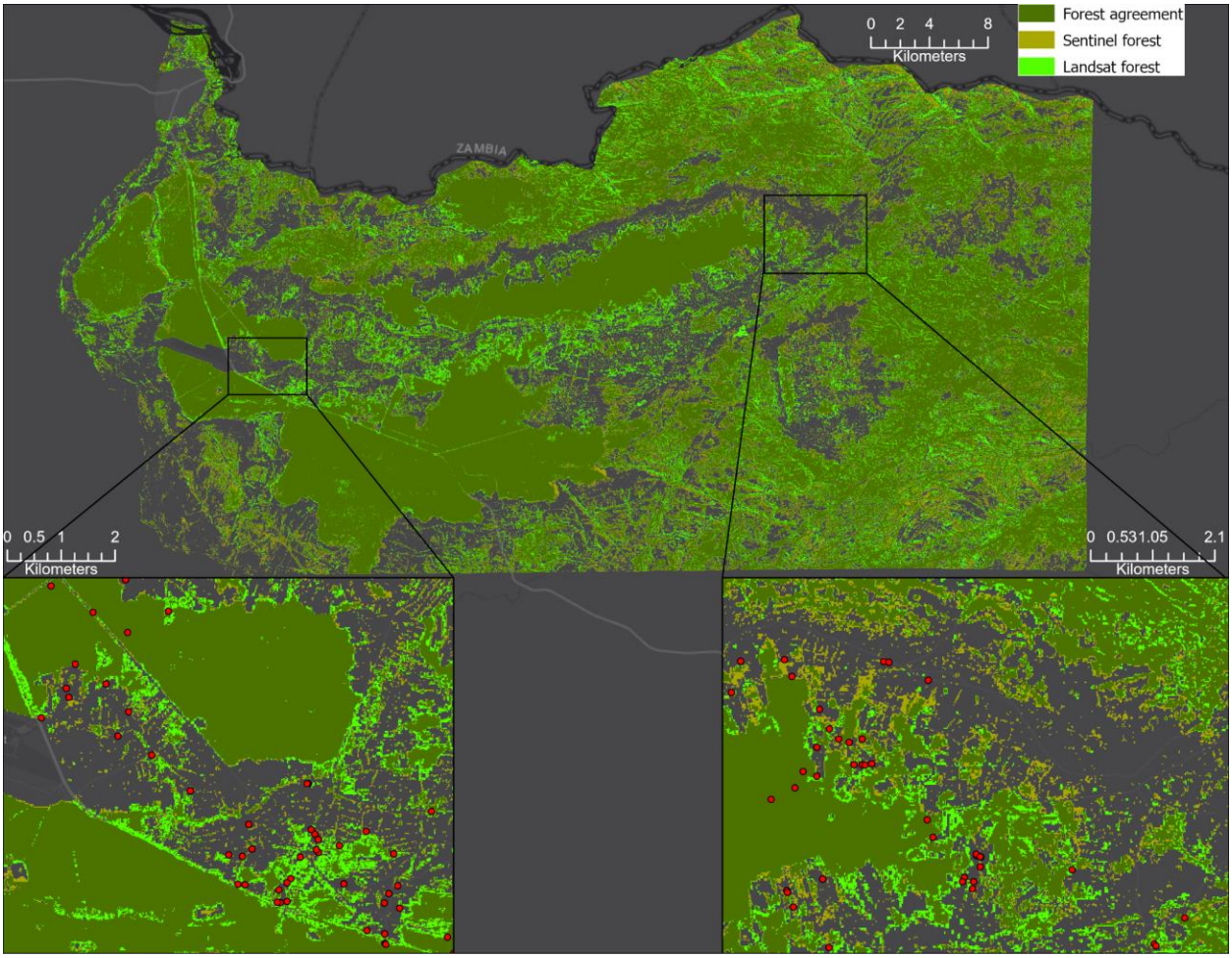

Figure 3.9. Comparison of forest classifications during the 2019 dry quarter using Landsat and Planet imagery. Areas classified as forest (either closed or open canopy) when using Landsat imagery but not when using Planet imagery are shown in bright green. Areas classified as forest when using Planet imagery but not Landsat are shown in olive green. Two insert maps in the bottom also show elephant-human conflict locations from 2015-2021. Note that forest cover at the date of these conflict points may or may not differ from what is shown.

Results from linear regression indicate the total square kilometers of agricultural land is 49.83 higher in the wet quarter ($P < 0.01$). Using Planet imagery results in 77.81 fewer square kilometers of agricultural land ($P<0.01$). No significant effects of imagery, season, or year were found when examining areas of forest or thicket.

3.2 Land cover metrics-top performing models

Across metrics made at the landscape level, Planet generally scored lower than Landsat (Table 3.6). There was considerable variation in CAI_MN scores between satellite and season, with the land cover classification using Planet during the wet quarter having a score close to zero and the classification using Sentinel during the dry quarter having a score over 0.8. Whereas PAFRAC and TECI scores of dry quarter land cover were comparable between Landsat and Sentinel, CAI_MN scores were distinct. TECI scores across models and seasons suggest a moderate level of edge is present in this landscape across wet and dry quarters. PAFRAC scores greater than one but less than two indicate patch shapes in this landscape are neither complex nor simple but fall somewhere in the middle. Scores were in top performing dry quarter models but differed for wet quarter models slightly.

Table 3.6. Landscape scale metrics of the top performing land cover classification models.

	CAI_MN	PAFRAC	TECI
Landsat Wet	0.2813	1.58	61.7515
Planet Wet	0.0007	1.40	51.2318
Landsat Dry	0.3913	1.42	57.5099
Sentinel Dry	0.817	1.49	60.1216

Across all seasons and models, the land cover making up the greatest portion of the landscape was forest (approximately 45-35%) followed by thicket (roughly 14-16%) (Table 3.7). As expected, water availability in terms of total area and percentage of landscape was higher in the wet quarter than the dry quarter, although there was a considerable intraseasonal difference between Landsat and Planet measurements during the wet quarter. The percentage of landscape classified as forest was higher in

the dry quarter than the wet, but the mean patch area between the wet and dry quarter Landsat maps remained around ~10

Table 3.7. Landscape metrics of the top performing land cover classification models. Metrics computed at the class level.

	Percentage of Landscape	AREA_MN	CLUMPY
Landsat-Wet			
Water	3.7826	0.2228	0.1998
Forest	35.1354	10.8619	0.8448
Lowland vegetation	4.7439	0.2754	0.2895
Thicket	16.5994	1.5352	0.6703
Bare soil	7.3881	0.3899	0.4006
Agriculture	6.9357	3.2888	0.7615
Planet-Wet			
Water	0.8998	0.0135	0.614
Forest	42.5581	0.6005	0.8671
Lowland vegetation	4.9309	0.041	0.7715
Thicket	16.843	0.1007	0.7674
Bare soil	5.2324	0.0676	0.794
Agriculture	5.2332	0.083	0.7898
Landsat-Dry			
Water	0.1668	1.7805	0.8396
Forest	45.206	10.1966	0.8789
Lowland vegetation	2.7991	1.1275	0.8107
Thicket	15.3497	2.3742	0.7867
Bare soil	4.557	1.0135	0.7483
Agriculture	6.6512	1.6512	0.8128
Burn	1.7421	0.5347	0.6972

Sentinel-Dry			
Water	0.1194	2.5472	0.855
Forest	43.7904	3.2797	0.793
Lowland vegetation	2.9449	0.3722	0.6945
Thicket	14.1427	0.9453	0.6847
Bare soil	5.3626	0.3712	0.5706
Agriculture	7.3807	0.8091	0.6834
Burn	2.7767	0.329	0.6022

The CLUMPY index is affected by cell size, with smaller cell sizes resulting in higher scores and a more clumpy landscape. Thus, as expected, all scores using Planet imagery were higher than Landsat, and while the classes of thicket, lowland vegetation, bare soil, and agriculture all scored similarly using Planet imagery, there was considerably more variation between classes with the Landsat-based map (Table 3.7). In comparison to the Landsat-based equivalent map, CLUMPY scores were not noticeably smaller for measurements made using the Sentinel-based map. The Sentinel-based land cover maps were exported at 20m resolution.

3.3 Vegetation condition-top performing models

In the dry quarter, maximum NGRDI values were slightly higher in agricultural lands (0.52) than in forest (0.42) when classification was completed using Landsat but not when using Sentinel imagery (0.49 vs 0.59). Areas classified as agriculture had similar ranges (0.42 for Landsat versus 0.45 for Sentinel), maximum (0.49 versus 0.52), and median values (0.26 versus 0.27). The median NGRDI value for forest classified using Sentinel was 0.19 compared to 0.16 with area classified as forest using Landsat imagery. The maximum recorded NGRDI value was slightly higher for Sentinel forest than Landsat and the range of values was slightly greater (Table 3.12 in Appendix C). Minimum NGRDI values were also comparable between satellite sensors during the dry quarter (Table 3.12 in Appendix C).

In the wet quarter, areas classified as agriculture using Planet had a much larger range of NGRDI values compared to agriculture classified using Landsat (0.72 vs 0.34). There were also differences in median and minimum values between agricultural land but maximum values were comparable (Table 3.12 in Appendix C). Areas classified as forest had similar median values (0.09 versus 0.02). Maximum values differed (0.22 for Landsat and 1.0 for Planet) as did minimum values (0.02 and -1.0) and the range of NGRDI values (0.19 vs 2.0).

4 Discussion

Studies of wildlife conservation frequently rely on land cover maps created from remotely sensed imagery, as they provide the basis of habitat suitability models, corridor mapping, and other geospatial analysis (Dejene et al., 2021; Kileo & Mbije, 2021). Land cover maps based on remotely sensed imagery can be affected by the grain size of the image (or the spatial resolution), affecting analysis (Ju et al., 2005; Moody & Woodcock, 1995; J. Wu, 2004). Satellite imagery and products range in their affordability and accessibility, and conservation nonprofits and local governments may not have use of imagery of all spatial, spectral, and temporal resolutions. Therefore, it is crucial to determine the optimal scale required for classifying land cover. We characterized land cover change and determined the appropriate spatial resolution needed to understand elephant resources by mapping land cover around the communal agricultural area south of Victoria Falls, Zimbabwe in 2019 and 2021. We also identified how vegetation greenness, an indicator of vegetation health and biomass, changes seasonally.

In general, land cover maps produced using Landsat, Sentinel, and Planet imagery had high accuracy regardless of season. Planet was not quite as accurate as classifications using Sentinel and Landsat imagery for agriculture; all models using Planet imagery had user's accuracy scores consistently below 0.9 for agriculture whereas models using Landsat and Sentinel performed better. The lack of infrared bands is a probable contributor to the lower accuracy, as vegetation is highly reflective in infrared wavelengths, but such information would not have been present in maps created using Planet.

Accuracy was generally more consistent using Landsat compared to Sentinel or Planet. When implementing a cutoff of accuracy greater than 0.9, two maps created from Landsat applied compared to one map created using Sentinel and one using Planet. In regards to top performing models, NGRDI was of high importance when modeling land cover, as was NDVI. Top performing land cover maps created from Landsat and Sentinel imagery were improved with a short wave infrared band (absent in the Planet imagery employed in this study). Overall, these findings suggest that freely available Landsat and Sentinel imagery are suitable for land cover mapping in the Hwange region of Zimbabwe. Landsat imagery extends as far back as the 1970s and Sentinel imagery is available starting in 2014. Landsat and Sentinel sensors also have more spectral information available in comparison to Planet (see Table 3.8 in Appendix C), providing additional benefits. However, the section, "In relation to elephants and human-elephant conflict" explains why further investigative work may need to be done and why Landsat may not be the most suitable for studying areas of human-elephant conflict.

As expected, water availability was lower during the dry season compared to the wet with higher mean patch area during the dry quarter, indicating that, of the water available, it is concentrated into larger patches during the dry season. Visual inspection of land cover maps appears to confirm this (see Figures 3.11-3.14 in Appendix C for top performing land cover maps in larger size). While the total area of forest was similar during the wet and dry quarters, it was slightly higher during the dry quarter when examining land cover maps from Landsat. This is likely due to misclassifications of thicket as forest. Reference points may need to be refined during the dry period or classifications done during the dry quarter may overestimate the extent of forest.

Vegetation health, as indicated by NGRDI values for forest, is higher during the dry season compared to the wet, which is highly unlikely. In this area, green up is known to generally start in November, declining starting in April (Mberego & Gwenzi, 2014). Using the more preferable NDVI to examine seasonal differences in vegetation led to disparate but expected results. When examining NDVI

values for 2019, vegetation health follows expected patterns, with average NDVI in forested areas (using Landsat) 0.71 in the wet quarter and 0.34 in the dry quarter. For agricultural areas, average NDVI was 0.57 during the wet quarter and 0.30 during the dry quarter. The 2019 land cover map created using Sentinel for the dry quarter had similar values compared to the Landsat land cover map. Based on these findings and the well-established seasonal phenology of the region, NGRDI is not a suitable indicator of vegetation health for monitoring the communal lands south of Victoria Falls.

4.1 Scale effects

In general, land cover classifications in both the wet and the dry quarter using all satellite sensors performed well, suggesting freely available Landsat imagery is suitable for monitoring land cover changes and vegetation health in this region. Area classified as forest was comparable between land cover maps for the dry season. During the wet season, Planet classified more land as closed canopy forest but less as open canopy forest compared to Landsat. Accuracy and area measures were generally comparable across all top performing models.

Our understanding of any landscape patterns and subsequent ecological processes is limited by the extent of the landscape or study area and by the size of the pixel or the grain (J. A. Wiens, 1989). Thus, using land cover maps based on imagery with differing spatial resolution might expectedly produce differing results. Some metrics are not correlated with the abundance of a class present on the landscape, making for more informative measures of landscape fragmentation (X. Wang et al., 2014). CAI_MN scores differed between Landsat and Planet during the wet quarter and between Landsat and Sentinel in the dry quarter. The percentage of patches that are considered core area is thus higher in the wet quarter when using maps created from Landsat (compared to Planet) and lower using maps created from Landsat (compared to Sentinel) during the dry quarter. The resolution at which the land cover maps were created had little impact on PAFRAC and TECI scores. PAFRAC scores were slightly higher

using Landsat compared to Planet during the wet quarter, but scores from all models show moderate complexity in patch shapes. The amount of edge present in the landscape did not differ by season between the two land cover maps created using Landsat, and TECI scores ranged from ~51 to ~61 across all models, indicating a moderate amount of edge present in the landscape.

In regards to vegetation health, NGRDI median values differed for dry quarter classifications of forest. Wet quarter classifications of forest had similar median values despite variation in terms of maximum and minimum values. Wet quarter NGRDI measures for agriculture also displayed variability whereas dry quarter agricultural NGRDI values were largely similar (Table 3.12in Appendix C). Planet may not have been effective in identifying agriculture during the wet quarter, as NGRDI measures of agriculture using Planet-based classification had a negative median value (Table 3.12 in Appendix C), indicating water may have been misclassified as agriculture. Negative median NGRDI values were also reported for thicket and bare soil, suggesting a closer look at this image's accuracy may be needed.

4.2 In relation to elephants and human-elephant conflict

Human-elephant conflict can occur in multiple forms, but one of the most common is through crop-raiding. As forage availability declines in naturalized areas, African savanna elephants (*Loxodonta africana*) increase the amount of woody vegetation they consume and are more likely to engage in crop-raiding (Osborn, 2004). Crop-raiding can cause serious damage to a farmer's livelihood and attempts to protect and patrol crops can lead to injury or fatalities. Furthermore, these repeated incidents understandably contribute to less than tolerant views of elephant conservation (Hariohay et al., 2018).

Accurate measures of vegetation health in forested areas and croplands are particularly germane to understanding and mitigating human-elephant conflict. Responding to vegetation changes, elephants move to areas with intermediate to high levels of vegetation greenness and track even short-lived vegetation greening (Bohrer et al., 2014). Their resource preference tracks scarcity, with

preference for crucial resources increasing as scarcity increases (Tsalyuk et al., 2019). The relatively high levels of forest connectivity reported across all scales in this study may suggest that elephants in this region can navigate this landscape easily, particularly if seeking areas of refuge as has been suggested (M. D. Graham et al., 2010; Oppong et al., 2008; Thant et al., 2021). Upon examining Figures 3.8 and 3.9, two areas with visible discrepancies in area classified as forest, when human-elephant conflict is overlaid, questions arise as to whether or not classifications of forest created from Landsat imagery are of high enough spatial resolution. Many of the points are located adjacent to forest that has been missed by Landsat classifications. Figure 3.10 shows the point locations of human-elephant conflict (HEC) provided by Connected Conservation (www.connectedconservation.com) in collaboration with Zimbabwe Parks and Wildlife and the Rural District Council and forest classifications for Planet, Landsat, and their agreement for the 2019 wet season. The two insert maps show hotspots identified for HEC. Forest classified using Planet imagery identifies smaller patches missed when classifying land cover using Landsat, and these patches are often adjacent to conflict points. Figure 3.11 is identical except forest classified using Sentinel imagery is shown. Again, Sentinel identifies smaller patches of forest that classifications using Landsat failed to detect with small patches adjacent to conflict. This may highlight that land cover classifications for use in human-elephant conflict studies would be better served using Sentinel or Planet imagery. A quick visual comparison suggests the forest identified using Sentinel is similar to that identified using Planet.

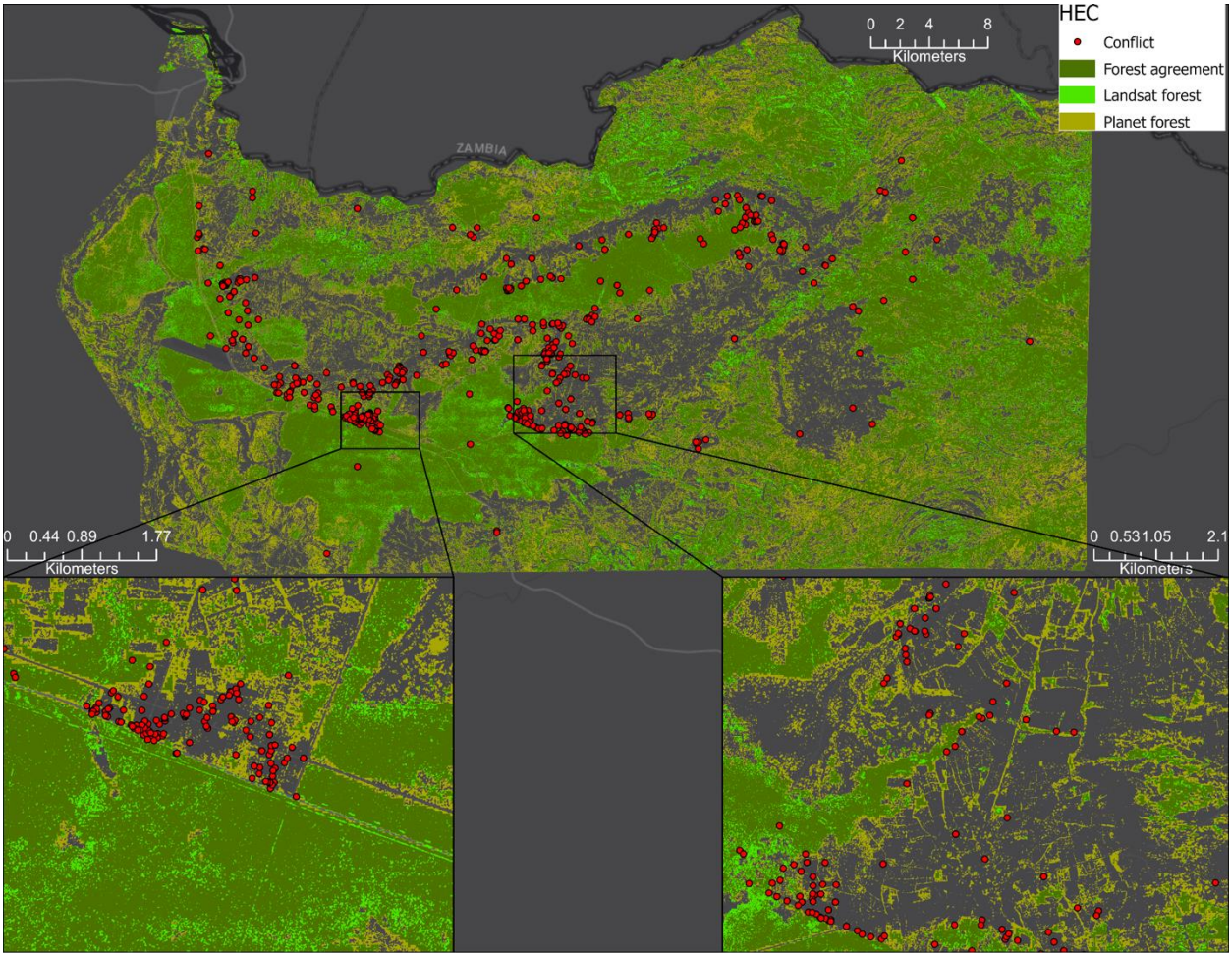

Figure 3.10. Comparison of forest classifications during the 2019 wet quarter using Landsat and Planet imagery. Areas classified as forest (either closed or open canopy) when using Landsat imagery but not when using Planet imagery are shown in bright green. Areas classified as forest when using Planet imagery but not Landsat are shown in olive green. Human-elephant conflict (HEC) points shown in red. The two insert maps show hotspots identified for HEC.

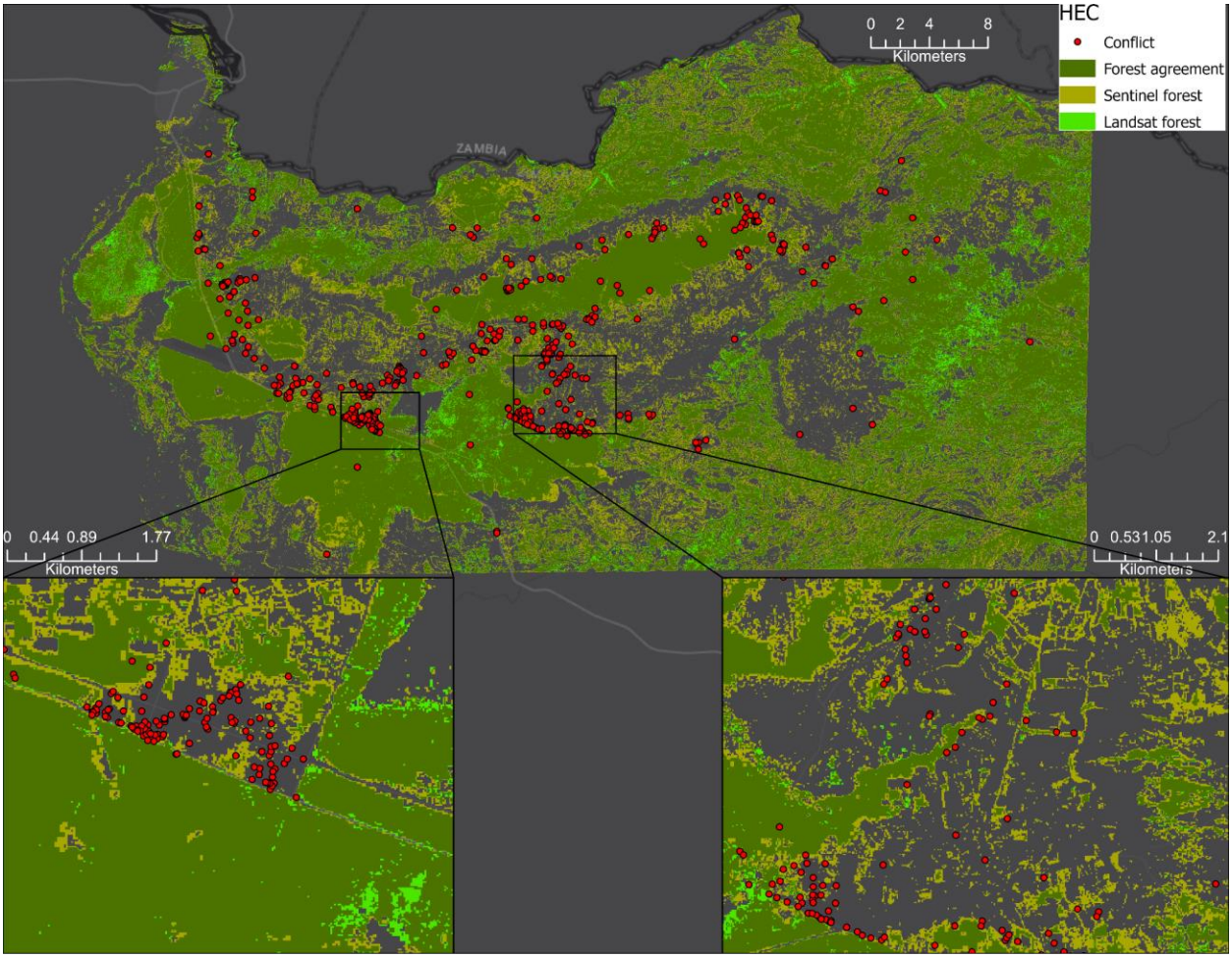

Figure 3.11. Comparison of forest classifications during the 2019 wet quarter using Landsat and Sentinel imagery. Areas classified as forest (either closed or open canopy) when using Landsat imagery but not when using Sentinel imagery are shown in bright green. Areas classified as forest when using Sentinel imagery but not Landsat are shown in olive green. Human-elephant conflict (HEC) points shown in red. The two insert maps show hotspots identified for HEC.

4.3 Limitations and future work

Finding suitable imagery overlap during the wet quarter across three satellite sensors is challenging. Multiple attempts were made to use Planet imagery but difficulties with cloud coverage, the temporal resolution of the products available, the processing needed to generate suitable mosaics,

and temporal overlap with Sentinel and Landsat imagery available in Google Earth Engine, leading to few actual choices in Planet imagery and ultimately the use of Planet Quarterly Basemaps. This was less-than-ideal due to their lack of a near infrared band. The processing that goes into Planet basemaps is also not transparent at present, thus we cannot estimate the impact that differences in image preprocessing may have had on classification results using Planet Quarterly Basemaps.

Future work should further explore the land cover classifications of Sentinel and Landsat to determine if Sentinel imagery is the most appropriate. The two hotspots of conflict examined here appear to show that the higher resolution offered by Sentinel may be more suitable for land cover mapping in relation to human-elephant conflict. While the overall accuracy did not differ substantially between all satellite sensors, a more thorough exploration of Landsat- and Sentinel-identified forest combined with conflict across the region should be completed. Further refinements to wet and dry season reference points for forest might also be necessary, as more land was classified as forest during the dry quarter when compared to the wet using Landsat imagery, although wet quarter classifications appear more reliable in regards to the main classes of interest for this study. Classifying imagery during the wet season is challenging due to cloud coverage and cloud-free images are not always available, thus imagery recorded during the dry season might be relied upon, in which cases reference points should be improved.

5 Conclusion

In general, land cover maps produced using Landsat, Sentinel, and Planet imagery had high accuracy regardless of season. Accuracy was generally more consistent using Landsat compared to Sentinel or Planet. In regards to top performing models, NGRDI was of high importance when modeling land cover as was NDVI. Top performing land cover maps created from Landsat and Sentinel imagery were improved with a short wave infrared band. Vegetation health follows well-established seasonal

patterns when measured using NDVI, with forest and agricultural land much greener in the wet quarter compared to the dry quarter. The opposite pattern was found using NGRDI, suggesting NGRDI is not a suitable indicator of vegetation health for monitoring the communal lands south of Victoria Falls. The amount of edge and the complexity of patch shapes was not greatly influenced by the resolution of the land cover maps. When specifically examining hotspots of human-elephant conflict for differences in land cover between maps produced using Landsat, Sentinel, and Planet imagery, forest classified using the higher resolution of Sentinel and Planet imagery becomes apparent adjacent to many conflict points. Sentinel and Planet appear to be alike in land classified as forest. On these grounds, Sentinel, with its higher spectral resolution and lack of cost, may produce land cover maps best suited to monitoring human-elephant conflict rather than maps modeled from Landsat or Planet imagery.

4 UNDERSTANDING SPATIAL PARAMETERS IMPLICATED IN ELEPHANT CROP-RAIDING: MACHINE LEARNING APPROACHES FOR ELEPHANT CONSERVATION AND SOLUTIONS TO HUMAN-ELEPHANT CONFLICT[3]

[3] Markham, K. To be submitted to *Remote Sensing in Ecology and Conservation*.

Abstract

Humans and elephants come into conflict when space and resources overlap. Patterns of human-elephant conflict are complex, often dependent on scale, and the drivers not always known. Most studies of conflict with African savanna elephants have been conducted in Kenya, Botswana, and South Africa, with little known about the trends south of Victoria Falls, Zimbabwe. To the southeast of one of the seven natural wonders of the world, conflict in communal lands occurs when resource availability declines in natural areas, as crops mature. We tested multiple machine learning techniques to model crop raiding, using over 700 data points collected from 2015 through 2021. Of the machine learning methods tested, random forest was the most accurate. The likelihood of conflict increases as proximity to protected areas and to agricultural land declines, as distance from buildings increases and building density declines. Results broaden our understanding of human-elephant conflict by presenting findings in a largely understudied region of Zimbabwe and make way for future mitigation and planning to reduce conflict.

1 Introduction

1.1 African elephants and human-environment interactions

Elephants are drivers for biodiversity changes and conflict (Guldemond & Van Aarde, 2008; Hoare, 1999; Parker & Osborn, 2001). Vegetation responds negatively to elephants in arid savanna (Guldemond & Van Aarde, 2008) and elephants have been found to inhibit forest succession in disturbed areas dominated by shrubs and grasses in Kibale National Park (Omeja et al., 2014). Elephants consume grasses and browse (green shoots and leaves as well as twigs and branches), strip bark off trees, and push over and break smaller, younger trees (R. F. W. Barnes, 1982; Dublin et al., 1990; Mapaure & Campbell, 2002; Plumptre, 1994). They spend around 75% of the day foraging (Ruggiero, 1992; Wyatt &

Eltringham, 1974). African elephants have also been shown to be ecosystem engineers, modifying food availability for other animal species (Valeix et al., 2011). Their foraging preferences attract them to dense vegetation which increases the openness of the landscape with time (Gordon et al., 2023) and they can negatively impact local biodiversity (Cook et al., 2017; Kerley & Landman, 2006; Midgley et al., 2020) as well as resilience to extreme events (Western & Mose, 2023).

Savanna elephants are generalist herbivores. They consume grasses, woody plants, and even fruits depending on availability and environmental conditions. Their consumption of less nutritious foods, such as bark and woody vegetation, increases during the dry season (Guy, 1976; Osborn, 2004; Williamson, 1983). Their location on the landscape and their general movement patterns are influenced by water availability and forage conditions (Bohrer et al., 2014; Chamaillé-Jammes et al., 2013; Loarie et al., 2009; Tshipa et al., 2017); elephants respond to vegetation changes, moving to areas with intermediate to high levels of vegetation greenness, and tracking even short-lived vegetation greening (Bohrer et al., 2014). Their resource preference tracks scarcity, with preference for crucial resources increasing as scarcity increases (Tsalyuk et al., 2019). The same is true for permanent water resources, with preference increasing as precipitation decreases (Tsalyuk et al., 2019). Elephant speed and core use areas decline significantly during the dry season, presumably to conserve energy (Mlambo et al., 2021). As the dry season progresses and the availability of nutritional wild grasses declines, elephants increase not only the amount of woody vegetation they consume but they are also more likely to engage in crop-raiding (Osborn, 2004).

The endangered African savanna elephant (*Loxodonta africana*) inhabits Zimbabwe. A 2014 aerial study of Zimbabwe estimated the country's elephant population at 83,000 divided into four main populations based on geography, with the Northwest Matabeleland having the highest African savanna elephant density (*Zimbabwe National Elephant Management Plan: 2015-2020*, 2016). Zimbabwe's elephant population is second only to Botswana which has roughly 120-130,000 elephants and where

population numbers remain stable (Schlossberg et al., 2019). While elephant population numbers are generally rising in Zimbabwe, poaching remains a significant problem and poisonings have also been on the rise (*CITES Implementation Report*, 2021; *Zimbabwe's Fifth National Report to the Convention on Biodiversity*, 2015). As their numbers continue to rise, so does the likelihood they will be forced to encounter humans more regularly. Zimbabwe is currently over its carrying capacity for elephants and contact with humans is increasingly concerning (*ZIMBABWE NATIONAL ELEPHANT MANAGEMENT PLAN (2021 – 2025)*, 2021).

Conflict with elephants can occur when elephants crop-raid, if elephant conservation efforts reduce the agency of locals, and if elephants feel threatened and become violent. As recently as May of 2021, a young man was trampled to death patrolling crops in Zimbabwe (Matabeleland North Correspondent, 2021). Elephants might also attack tourists and residents of Victoria Falls, with an elephant killing a mentally ill man in 2020 and residents concerned more conflict would arise as elephants increasingly used the streets during the pandemic ("Elephant Kills Vic Falls Mentally Ill Homeless Man," 2020). Crop-raiding has occurred in Africa since pre-colonial times, but the effects are now magnified; local laws designed to protect wildlife can harm livelihoods and dissent about damage and losses can undermine conservation programs (Naughton-Treves & Treves, 2005). Adopting a militarized approach of conservation in response to elephant poaching can introduce violence to local people and diminish autonomy over daily activities and livelihoods (Mushonga & Matose, 2020). Reducing and resolving conflict with elephants is further complicated by the influence of international organizations within the Convention In the Trade of Endangered Species or CITES (O'Connell-Rodwell et al., 2000). In protected areas within Zimbabwe, elephant management and conservation are largely the responsibility of the Zimbabwe Parks and Wildlife Management Authority (ZimParks), but their efforts are hindered by a small budget, low morale, and high turnover (Ncube, 2019). In communal lands, problem wildlife is the responsibility of the Rural District Councils, where similar issues of limited

resources may also occur. Elephants and humans face a myriad of multifarious pressures complicating their relations of space and natural resource use.

1.2 Patterns in conflict and mitigation attempts

Previous work in Hwange National Park found crop-raiding declined with increasing distance to refuge areas along with higher household density (Guerbois et al., 2012). This aligns with other work on elephant crop-raiding suggesting that elephant refuge is a significant predictor in crop-raiding occurrence (M. D. Graham et al., 2010; Oppong et al., 2008; Thant et al., 2021). Work done in the Okavango Delta in Botswana found fields are more likely to be raided by elephants if they are far from the village and have been raided considerably in the past, whereas fields further from waterholes, further from elephant paths, and fields not used by livestock are less likely to be raided (Songhurst & Coulson, 2014). More recent work in the Okavango Delta by these same researchers found that the relationships between elephant density and elephant space use with crop raiding patterns were nonlinear, and that the probability of crop raiding is actually higher in low elephant density areas (Pozo et al., 2018), affirming the complexity of predicting and understanding crop raiding patterns in southern Africa. To effectively mitigate this type of human-wildlife conflict requires understanding the spatial and temporal patterns of crop-raiding (Linkie et al., 2007).

Multiple methods have been employed in attempts to prevent elephant crop-raiding. Across southern Africa traditional methods include burning, planting unpalatable vegetation, using drums to scare off elephants along with high-tech methods such as electrical fencing, but with many of these methods demonstrating declining effectiveness as elephants learn when the threat is empty (Osborn, 2010; Parker & Osborn, 2001). Bees have also been tested as a potential deterrent (Karidozo & Osborn, 2005; King et al., 2007; Ndlovu et al., 2016). The majority of elephant deterrents are ineffective or impossibly expensive, and farmers might place themselves in harm's way to defend their livelihood

(Osborn, 2010). Even patrolling fields in groups does not guarantee safety (Matabeleland North Correspondent, 2021). Elephants that crop-raid repeatedly and endanger humans are killed.

In this region, the use of chili powder and oil has been tested as a deterrent in multiple forms (Langbauer et al., 2021; Osborn, 2002). In comparison to traditional deterrent methods of shouting and chasing, elephants that inhale the chili powder spend less time in fields (Osborn, 2002) and burning chili bricks results in less plant damage and a reduction in the number of visits from elephants (Karidozo & Osborn, 2005). In the early 2000s, Connected Conservation introduced chili fences, fences that have been covered with chili oil, as an effective deterrent (L. Osborn, personal communication, July 10, 2023). They have since actively promoted a wider implementation of chili fences. Problematic elephants may also be darted, anesthetized, and have their trunks covered with chili wax (Langbauer et al., 2021).

1.3 Machine learning

Machine learning (ML), a subset of artificial intelligence in which training data are used to classify or identify relations to make predictions or decisions, is increasingly common in geospatial analysis (Goodfellow et al., 2016). Machine learning algorithms are commonly used in ecological niche modeling and land cover mapping. Ecological niche models that focus specifically on predation risk through the incorporation of particular environmental factors have been used to study human-wildlife conflict using ML (Zarco-González et al., 2013). Outside of this type of modified ecological niche modeling, studies using ML to predict or understand conflict predictors in an explicitly geographic framework are relatively limited.

When ML methods have been used to study human-wildlife conflict, the methods have generally focused on regression rather than some of the more advanced techniques, such as RF, neural networks, etc. Work done in Kibale National Park, for example, used regression analysis and found the frequency of crop raids and the amount of damage caused by elephants was positively related to the

amount of guarding of a field and guarding did not result in a significant decrease in reduction in crop loss (Naughton-Treves, 1998). Authors hypothesized that this counterintuitive result is the result of farmers increasing patrols and guarding after raid events, thus fields that are more attractive to elephants are guarded as an ineffective response (Naughton-Treves, 1998). Generalized linear models were also used to determine factors related to elephant crop-raiding in the nearby Okavango Delta in Botswana (Songhurst & Coulson, 2014). Machine learning has been used to assess human-elephant conflict patterns in Asia previously and to provide suggestions for mitigating conflict (Naha et al., 2019).

Four supervised machine learning algorithms are explored in this work: support vector machines (SVM), random forest (RF), and deep learning neural network (DNN) as well as a multi-layer perceptron neural network (MLP). SVM is a kernel-based, supervised learning method. While computationally intensive, SVM works well for high-dimensional feature space and is good when decision boundaries are complex and nonlinear (Cortes & Vapnik, 1995). It is sensitive to parameter settings and the features selected and is used for classification as well as regression (Burges, 1998; Vapnik, 1999). RF uses an ensemble of trees to make decisions and splits the nodes by minimizing correlation between trees. By using multiple trees and combining their predictions, accuracy is significantly improved. RF is robust to noisy data and reduces overfitting. Neural networks mimic how brains function and are often employed when the system of interest is non-linear and involved (J.-C. Chen & Wang, 2020; Tfwala & Wang, 2016). Deep learning neural networks (DNN) contain thousands of layers between the inputs and outputs. MLP is a type of feed-forward neural network that is similar to a linear model but can be more powerful when a non-linear activation function is applied to results (Hornik et al., 1989). An MLP contains an input layer, at least one hidden layer, and an output layer that are interconnected.

1.4 Objectives

Elephants around Victoria Falls, Zimbabwe raid subsistence-level agricultural fields and come into conflict with humans in particular areas, whereas other areas remain relatively untouched and conflict free (M. Karidozo, personal communication, July 27, 2021). This work uses more advanced machine learning (ML) techniques to examine the environmental factors and potential drivers of human-elephant conflict.

2 Methods

2.1 Study site

Zimbabwe is a landlocked south African country bordered by Botswana to the west, Zambia to the north, Mozambique to the east, and South Africa to the south (Figure 4.1A). The city of Victoria Falls is in the Matabeleland North Province in the Hwange District (Figure 4.1B). The majority of the conflict data reported for elephants occurs in the communal lands to the southeast of Victoria Falls (Figure 4.1C). Like the majority of Zimbabwe, the vegetation in this area falls within the broadly defined savanna vegetation zone (Van Wyk, 2013). Dominant vegetation types are dry forests and thickets, specifically *Baikiaea* woodland interspersed with *Colophospermum* woodland (Timberlake et al., 1993). Water availability on the landscape is highly seasonal, with rivers and natural water sources significantly reduced during the dry season.

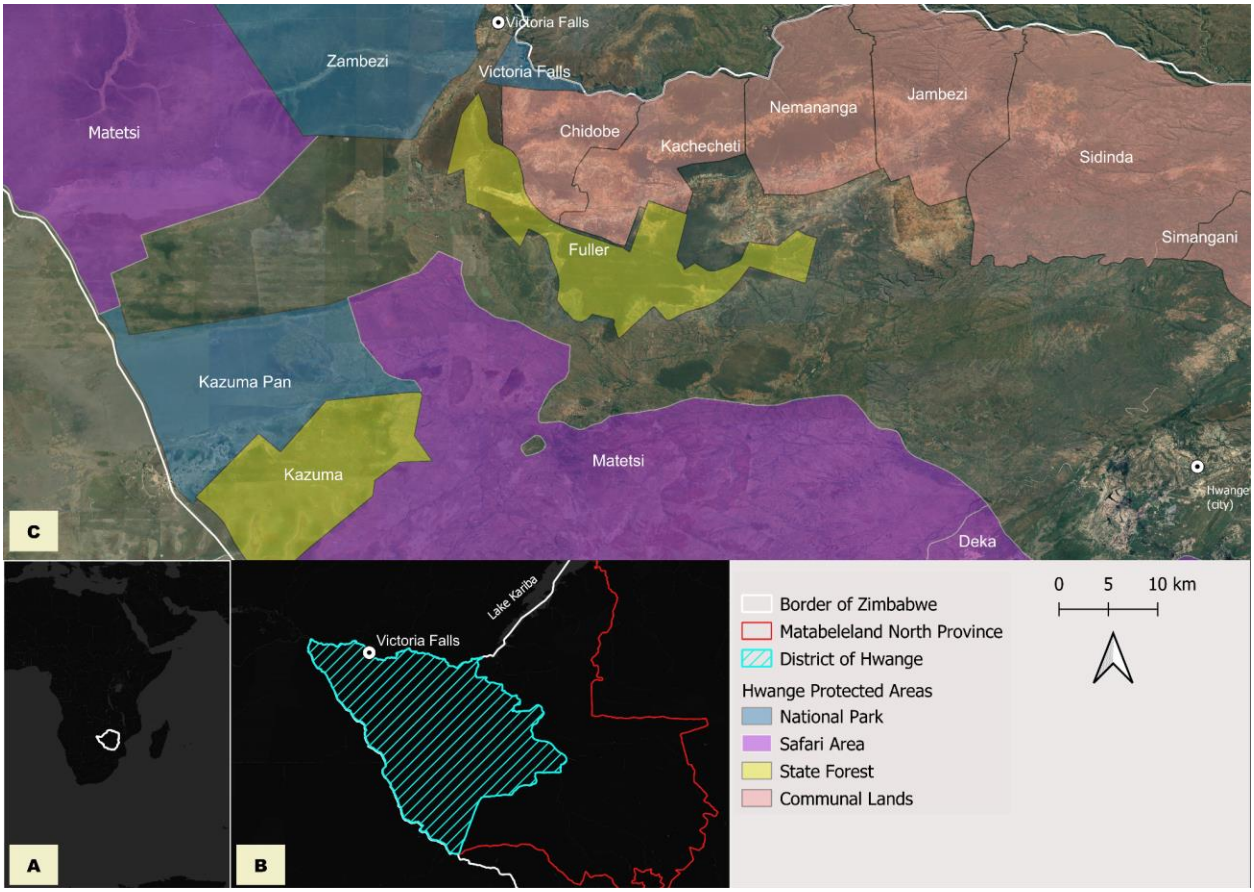

Figure 4.1. Insert map A shows Zimbabwe within the African continent. Map B shows the Matabeleland North Province outlined in red, the Hwange District is indicated by light blue lines, and the city of Victoria Falls indicated by a white circle centered around a black dot. The Zambezi River spans the northern border of Zimbabwe and flows eastward into Lake Kariba. In Map C, protected areas are labeled by name and their type identified by color. The cities of Victoria Falls and Hwange are indicated by white circles encasing a black dot. Satellite imagery is provided by Google.

The climate can be divided into two seasons based on precipitation: a rainy season starting in November and lasting through March and a dry season from April until November (Figure 4.2). Eighty percent of precipitation across Zimbabwe falls between the months of November and March, with rainfall shifting earlier during dry years (Mberego & Gwenzi, 2014). Vegetation typically responds to

precipitation by one to two months (Mberego & Gwenzi, 2014). Crop water requirements peak in December and January (Funk & Budde, 2009). Elephants are attracted to a variety of crop; some studies suggest they prefer millet, maize, sorghum (Hariohay et al., 2020; Matsika et al., 2023) whereas other studies have found no effect of crop type on raiding occurrences (Buchholtz et al., 2023).

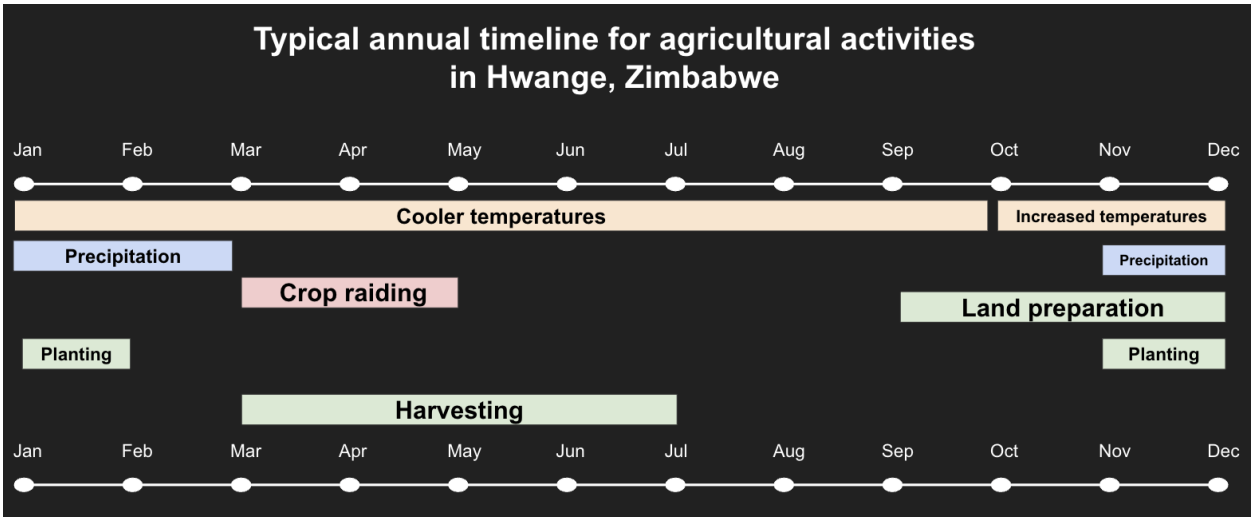

Figure 4.2. Typical annual timeline for agricultural activities in Hwange, Zimbabwe. The wet season historically began in October but has shifted later, to November, over the past two decades. The main harvesting period typically runs from April through July. Created based on conversations with in-situ collaborators and information available on Famine Early Warning Systems Network on Zimbabwe.

2.2 Crop raiding data

In total, 713 crop raiding locations from 2015-2021 were documented and georeferenced (Figure 4.3). Two hundred and eighteen locations were collected in 2021, two in 2020 due to the pandemic and lockdown, zero in 2019 also due to the pandemic and lockdown, 241 points in 2018, 95 in 2017, 124 in 2016, and 33 in 2015. These points were collected *in situ* by Victoria Falls Wildlife Trust, Hwange Rural District Council, and Connected Conservation rangers. Conflict is reported by calling the

Hwange Rural District Council. A trained enumerator records as much data about the incident as possible, potentially including crop type, estimates of kilograms of damage, the number of individual elephants and their sex, etc. If possible, the enumerator travels to the conflict location to verify. The exact data recorded has evolved over time, with more recent reports detailing mitigation methods used, and observations on the outcome.

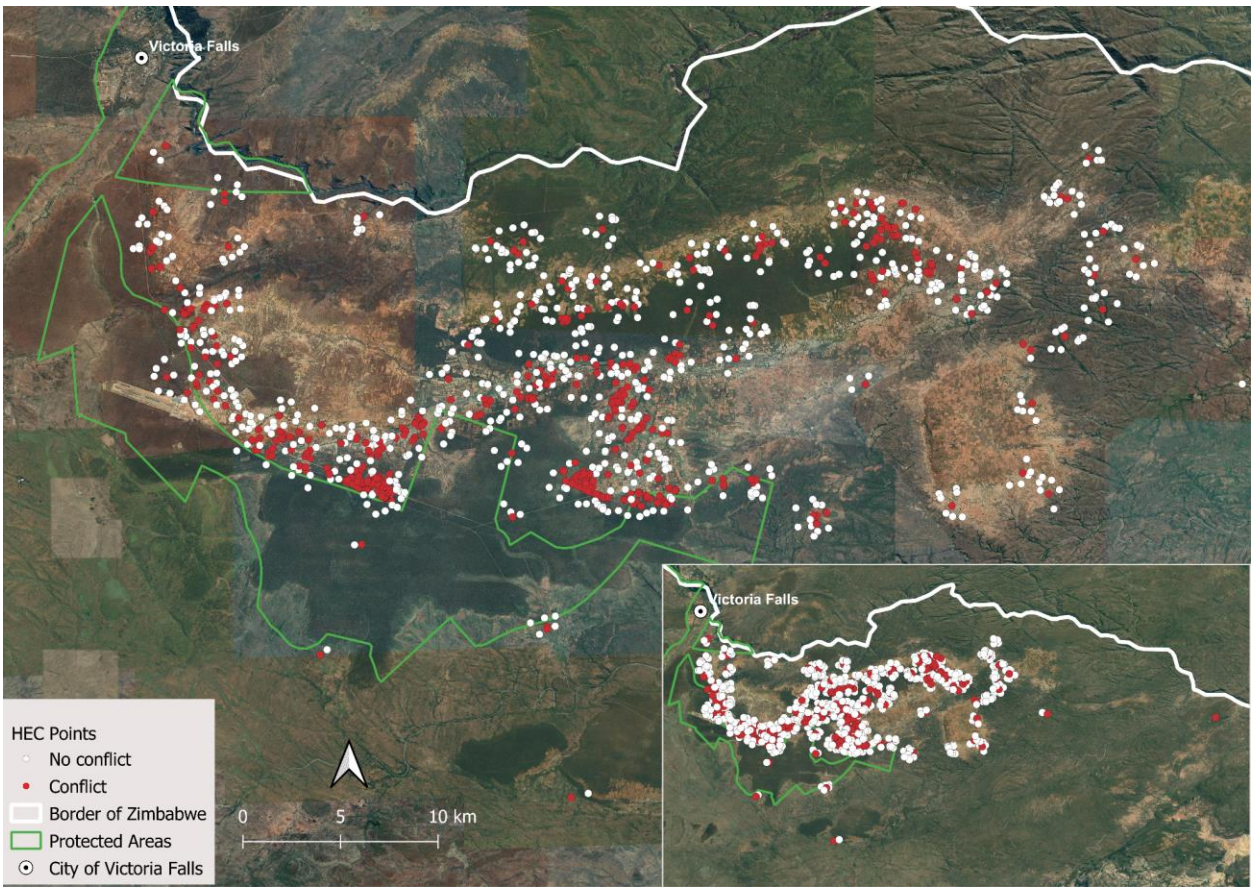

Figure 4.3. Study area. Red points are crop raiding locations. White points are absence points created randomly within 100 m to 1 km from conflict points. Victoria Falls is labeled in the upper lefthand corner and protected areas that are not mixed use are outlined in green. Country boundary of Zimbabwe with Zambia is in white. Imagery is a mosaic from Google.

2.3 Data preparation and exploratory analysis

In order to improve our understanding of the drivers of human-elephant conflict in the Victoria Falls area of northeastern Zimbabwe, we used machine learning models (explained in section "Machine learning") to identify where conflict is likely to occur. Exploratory analysis included creating heat maps of conflict reports in QGIS using Kernel Density Estimation with a radius of 15.8 degrees. Multiple predictors of human-elephant conflict were considered, including building density, distance from fences, elevation, etc. The distribution of potential predictors were plotted and visualized. All predictors were centered and scaled and correlation was calculated using Pearson's r correlation matrices (Booth et al., 1994) (Figure 4.4).

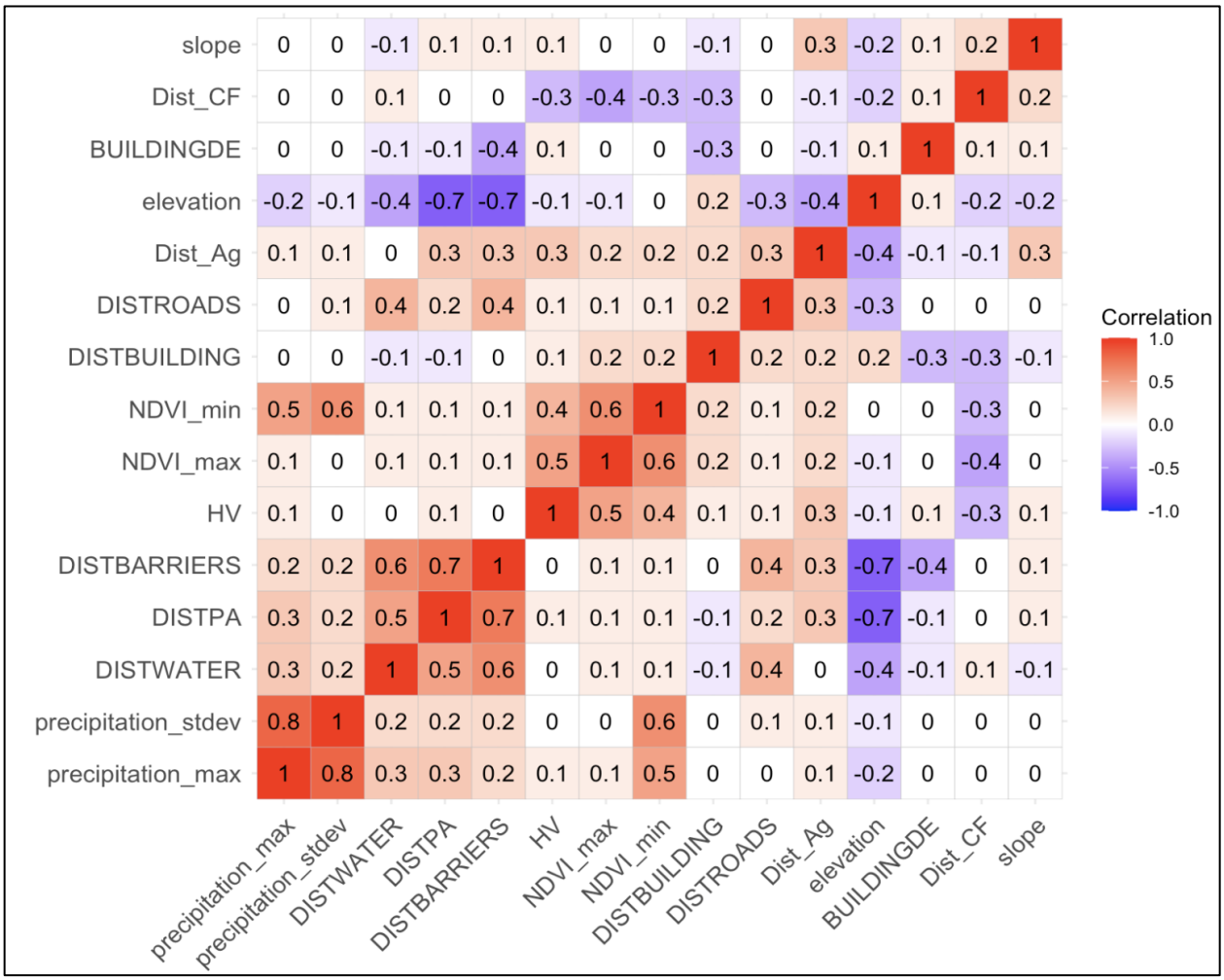

Figure 4.4. Correlation matrix of potential predictor variables. Positively correlated variables are in red and negatively correlated variables are in purple. Darker shades indicate stronger correlation. Correlation coefficients are imposed on squares. BUILDINGDE= building density, Dist_CF=distance from closed forest, Dist_Ag= distance from agriculture, DISTROADS=distance from roads, DISTBUILDING=distance from buildings, HV=HV polarization backscattering, DISTBARRIERS=distance from fences, DISTPA=distance from protected areas, DISTWATER=distance from permanent water sources.

Any potential predictors with correlation values 0.7 and higher were excluded from regression-based models, as the assumption of independence is violated, standard errors are inflated, and predictor effects can be challenging to determine (Booth et al., 1994; Dormann et al., 2013). Some machine learning algorithms are less affected by moderate collinearity, including (Breiman, 2001; Dormann et al., 2013). Support vector machines (SVM) are more susceptible to noise and can be impacted by even minimal collinearity (Anastasiadis et al., 2005; Dormann et al., 2013). Distance from barriers (fences) had a collinearity of 0.7 with distance from protected areas but was hypothesized to potentially be an informative predictor. Thus, it was added to some models and retained if accuracy improved.

Maximum precipitation, maximum normalized vegetation difference index (NDVI), and minimum NDVI during the crop raiding months*, building density, distance from buildings, from water, from roads, from protected areas, slope, HV backscattering, distance accumulation from agriculture and closed canopy forest were ultimately included as predictors (Table 4.1). *In this context, “crop raiding months” do not refer to the months indicated in Figure 4.2 but to the exact months within each year that conflict was recorded. Conflict might have started earlier or extended later than the typical crop

raiding season referred to in Figure 4.2. Machine learning methods that are less susceptible to the effects of collinearity might have included additional predictor variables (see Table 4.1).

Table 4.1. Description of data along with source, resolution, and use. Italics is used to indicate a predictor that was not used in all models.

Data	Description	Use	Resolution	Source
Crop-raiding points	Ground-based GPS point locations of crop-raiding, with crop type, amount of damage, and date recorded	Dependent variable	Temporal: 2015-2021 Spatial: N/A	Victoria Falls Wildlife Trust, Connected Conservation, & Hwange Rural District Council
Normalized Difference Vegetation Index (NDVI)	Maximum and minimum NDVI values from Landsat 8 Operational Land Imager (OLI)	Predictor variable	Temporal: 16-day repeat restricted to crop-raiding months per year Spatial: 30m	USGS satellite imagery accessed using Google Earth Engine (GEE)
Precipitation	Maximum precipitation values modeled based on satellite and ground station data	Predictor variable	Temporal: restricted to crop-raiding months per year Spatial: 0.05°	Climate Hazards Group InfraRed Precipitation with Station data (CHIRPS) through GEE
Buildings	Distance from buildings and density of buildings	Predictor variables	Temporal: Data collected 2022 Spatial: N/A	Open Street Maps
Protected areas	Boundaries of conservation areas such as national parks, forestry lands, etc.	Predictor variable	Temporal: Updated Oct, 2020 Spatial: N/A	Protected Planet

Roads	Major and secondary roads, both paved and unpaved	Predictor variable	Temporal: Not specified Spatial: N/A	Open Street Maps
Fences	Distance from barriers	Predictor variable	Temporal: Data collected 2022 Spatial: N/A	Open Street Maps
Rivers	Major rivers and streams	Predictor variable	Temporal: Not specified Spatial: N/A	HydroSheds
Land cover	Distance accumulation (elevation used as from agriculture and closed canopy forest	Predictor variables	Temporal: 2015-2021 Spatial: 30m	Created by author from Landsat 8 OLI imagery from the first quarter of each year
Digitized elevation model	Slope	Predictor variables	Temporal: 2020 Spatial: ~30m	From Shuttle Radar Topography Mission through GEE
PALSAR-2/PALSAR Yearly Mosaic, version 2	HV polarization backscattering dB	Predictor variable	Temporal: 2015-2021 Spatial: 25m	From JAXA EORC through GEE

As a measure of vegetation health, the NDVI was used with higher values indicating greener pixels. NDVI is sensitive to ecosystem conditions and is the most popular index for assessing vegetation health (Goward et al., 1985; S. Huang et al., 2021; Myneni et al., 1995; Ollinger, 2011). Using Google Earth Engine (GEE), NDVI for each pixel was calculated from Landsat 8 OLI imagery (higher resolution

Sentinel was imagery considered but is not available for 2015). In RStudio Version 1.1.423, for each year, measures of central tendency (mean, median, standard deviation, as well as maximum and minimum) for NDVI were then calculated per point. Values were extracted for months during which a conflict occurred. Precipitation values were sourced from CHIRPS, a global precipitation dataset designed for drought monitoring (Funk et al., 2015). Measures of central tendency were calculated and ultimately the maximum precipitation value during the crop raiding period was included.

Synthetic Aperture Radar (SAR), a form of active remote sensing in which radio waves are transmitted from and reflected back to the sensor, has also proved to be useful for vegetation studies as an estimate of biomass (Bouvet et al., 2018; Kasischke et al., 1997; Urbazaev et al., 2015). The PALSAR-2 annual mosaic contains an L-band with a wavelength 23.6 cm and four possible polarizations (Rosenqvist et al., 2007). The HV backscattering values were gathered per point from the PALSAR-2 Yearly Mosaic available in GEE (Shimada et al., 2014). Note that these SAR mosaics are not annual averages but single measurements per year.

Annual land cover maps were generated using a RF classification with Landsat 8 OLI imagery. From these annual maps, distance from closed canopy forest and distance from agriculture were both included in machine learning models.

2.4 Machine learning

To understand where human-elephant conflict is likely to occur, predictive models were created with the locations of elephant crop raiding as the dependent variable and potential geospatial drivers of conflict as the independent variables. Multiple supervised machine learning algorithms were tested using binary classifications to identify whether a location is likely to experience conflict. Algorithms were selected based on their suitability for binary classification and general ease of use. Pseudo absence

points were created between 100 m to 1 km from conflict points. All pseudo absences were assigned the same date as crop raiding points and an equal number of pseudo absences to crop raiding points was generated for each year.

Unless otherwise specified, 70% of points were used for training and 30% for testing. All predictors were centered and scaled before modeling using the default scale function in R (centering is done by subtracting the column means of x from their corresponding columns and then scaling by dividing the columns of x by their standard deviations). Four machine learning methods were tested: SVM, RF, DNN and MLP (workflow in Figure 4.5). These models were chosen based on their suitability for binary classification, their overall ease of use, and the nature of the predictor variables. A binomial generalized linear model (GLM) was also used to provide additional information about the relationship between predictors and crop raiding occurrence.

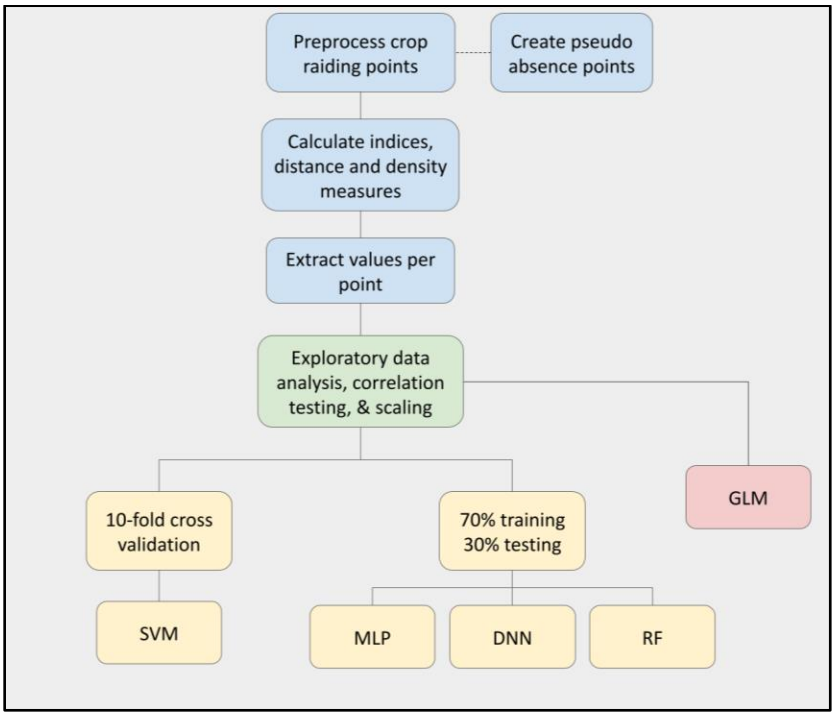

Figure 4.5. Workflow for methodology. Processes in blue are preprocessing steps to generate necessary inputs for further analysis. Exploratory data analysis consisted of plotting the distribution of variables,

checking for correlation, and normalizing the data. Processes in yellow are the ML methods along with separation of training and testing data. A binomial generalized linear model was also used to elicit further information about the relationship between conflict and predictors. For more information on methods, refer to the text.

As SVM is sensitive to parameter settings (Burges, 1998; Vapnik, 1999), different cost values and linear, polynomial, radial, and sigmoid kernel types were all evaluated to optimize model performance and accuracy. For SVM, ten-fold cross validation was used instead of partitioning the data for training and testing purposes. Thus, the entire reference dataset was randomly divided so that 1/10th of the data is reserved for testing and the remaining is used to train the model. This process is repeated ten times with a different portion of the data reserved for testing in each instance. This model was run in RStudio (Posit team, 2023) using the 'e1071' library.

The RF algorithm was also run in RStudio using the 'randomForest' library. The number of trees was adjusted to improve model accuracy and ultimately five thousand trees were employed to train 70% of the reference data. Other than the number of trees, all default model settings were used.

Both neural network algorithms were run using Jupyter Notebook 6.1.4. A DNN was created using the Keras Python and TensorFlow libraries (Bernico, 2018). A sequential model was used and various activation functions, loss functions, and optimizers, such as stochastic gradient descent, RMSprop, and Adam were tested (Duchi et al., 2011; Kingma & Ba, 2014). The batch size and the number of epochs were also evaluated to improve accuracy. For MLP, the 'sklearn' package was used. Activation functions, the number of iterations, and the number of hidden layers were tested and optimized to refine model accuracy.

3 Results

3.1 Exploratory analysis and general trends

Creating heat maps from conflict reports indicate high occurrences of conflict alongside the boundary of Fuller Forest State Park across all years for which conflict reports were recorded (Figure 4.6). Across all years, including the collected first year data for which there are only 33 reports, conflict is localized along the northern edge of Fuller Forest at the center. Areas of high conflict are more widely distributed in 2021 and extend further from Fuller Forest.

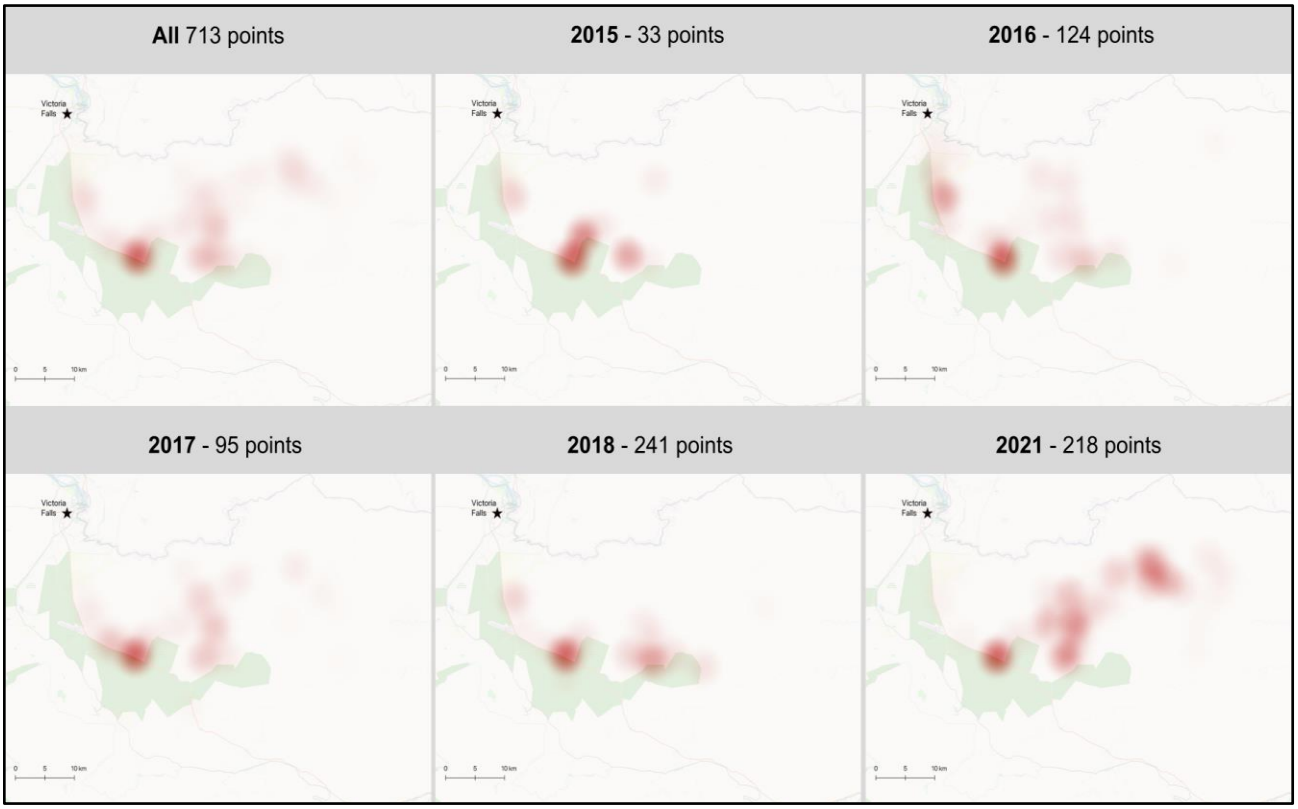

Figure 4.6. Heat Maps of conflict reports. Darker red indicates more conflict reported. Map for all reported conflict in upper left. No conflict map was created for 2020 as there were only two reports. No conflict was reported at all in 2019. Fuller Forest is in green. City of Victoria Falls is indicated by a star. Base map is from Open Street Maps.

3.2 Predictors most important to modeling conflict

RF indicates the importance of predictors within the model and GLM indicates the relationship between the predictors and the outcome. SVM, DNN, and MLP are all black box models; no information is available concerning how predictors impact model performance nor is there information on the direction of any relationships. This section reports the findings for RF and the binomial GLP.

While correlated with distance from protected areas, when the predictor variable distance from barriers was added to the model, model accuracy improved slightly, thus this predictor was included. Variable importance factors for the model found distance accumulation from agriculture to be the most important predictor variable, with a mean decrease in accuracy of 411 compared to the next most important variable, HV backscattering, which had a mean decrease in accuracy of 351. The plotted importance of all model variables can be found in Figure 4.7.

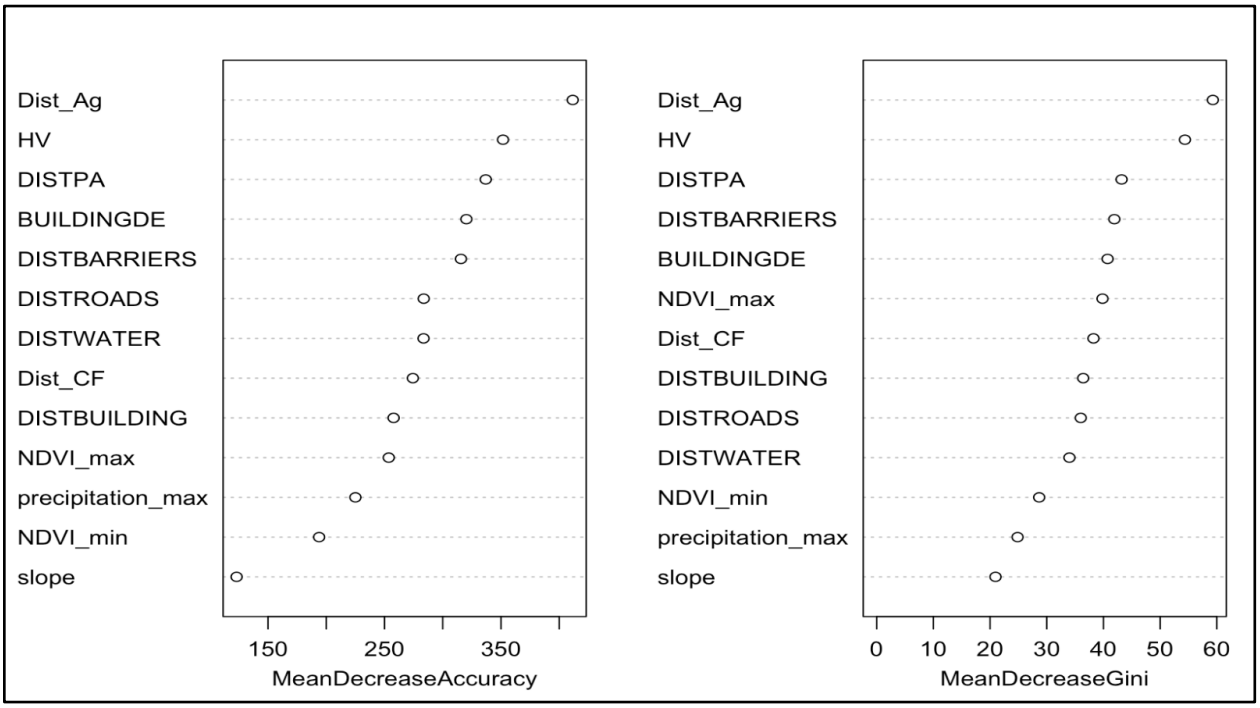

Figure 4.7. Variable Importance Plot of variables included in random forest model.

A binomial GLM using all the data available was also used to gain further insight into the relationships between predictors and crop raiding occurrence. Predictors that negatively impacted crop raiding include distance from protected areas ($P<0.001$), building density ($P<0.05$), distance from agriculture ($P<0.001$), and maximum NDVI and HV ($P<0.001$). The only predictor to contribute positively included distance from buildings ($P<0.001$). Distance from water approached but did not reach significance ($P<0.1$). Distance from barriers (fences) was not included in the binomial GLM as it violated assumptions of normality. Exploratory data analysis showed distance from fences is slightly lower for points that were raided versus absence points.

3.2 Comparison of ML outcomes

Using a C-classification type with a radial kernel, the result was an SVM model with 559 support vectors in total and a total training accuracy of 73.94%. Ten-fold cross validation was used to train the model and the highest accuracy achieved was 79.79% with a low of 69%. SVM model accuracy using testing data was 54.9%. The confusion matrix for the testing data can be found in Table 4.2 with zero indicating pseudo absence points and one indicating a point where crop raiding did occur.

Table 4.2. Confusion matrix for testing data using SVM (0=absence, 1= crop raided)

	Predicted 0	Actual 1
Actual 0	131	110

Predicted 1	83	104

RF model accuracy using training data was 82.46%. The class error rates for raided points and absences were 16.4% and 18.6% respectively using training data. Testing the model using the remainder of the data resulted in an accuracy of 81.8%. The confusion matrix (Table 4.3) for the test data is below.

Table 4.3. Confusion matrix for test data using RF (0=absence, 1= crop raided)

	Predicted 0	Actual 1
Actual 0	184	48
Predicted 1	30	166

The most successful parameterization of tested DNN models used a sequential DNN model with two layers using the rectified linear unit activation (ReLU) function, a third layer using a sigmoid activation function so that the network output is binary, and the Adam optimizer. Five thousand epochs were used and a batch size of 200. When the predictor variable distance from barriers was added to the DNN model, measures of accuracy did not differ considerably; thus, predictor variables for this model included only those with correlation coefficients below 0.7.

DNN model accuracy using training data averaged 94.9%. A total of 325 parameters were used to train the model. Accuracy using the testing data averaged 72.5%, reaching as high as 75.5% and as low as 70%. The confusion matrix for the test data is below.

Table 4.4. Confusion matrix for test data using DNN (0=absence, 1= crop raided)

	Predicted 0	Actual 1
Actual 0	144	64
Predicted 1	54	166

MLP neural network classifier defaults were used with the exception of a maximum number of iterations of 100,000 and three hidden layers with 100 neurons in each. As with the DNN model, adding distance from barriers as a predictor did not result in considerable changes to model outputs, thus for the sake of model parsimony this variable was not included. Model accuracy using training data averaged 100% and accuracy with testing data was 77.1% and ranged from 74-79%. The confusion matrix can be found in Table 4.5. below.

Table 4.5. Confusion matrix for test data using MLP neural network (0=absence, 1= crop raided)

	Predicted 0	Actual 1
Actual 0	154	67
Predicted 1	32	175

4 Discussion

Human-elephant conflict is a complicated but pressing concern throughout Africa. These megaherbivores spend a considerable portion of their day feeding and can cause significant damage to

local livelihoods when raiding crops (Ruggiero, 1992; Wyatt & Eltringham, 1974). Agricultural land across Zimbabwe is expanding (Useya et al., 2019) and the growing conditions in the Hwange region of Zimbabwe are already challenging and limited due to poor soils and erratic precipitation (Manatsa et al., 2020; Moyo, 2000; Vincent & Thomas, 1960).

Zimbabwe has an estimated carrying capacity of 45,000 elephants, but the most recent calculations place the population around 100,000 individuals, making coexistence a priority (*ZIMBABWE NATIONAL ELEPHANT MANAGEMENT PLAN (2021 – 2025)*, 2021). Elephants are intelligent creatures with exceptional long-term spatial memory (Bates et al., 2007; Fritz, 2017; Hart et al., 2008; Polansky et al., 2015), even altering their navigation strategies dependent on habitat familiarity (Presotto et al., 2019). Experimental methods hailed as effective deterrents often become ineffective with time, as elephants learn when threats are empty (Davies et al., 2011; O'Connell-Rodwell et al., 2000; Osborn, 2010). There are reports that elephants retaliate against crop-raiding prevention methods and retaliate after previous confrontations (Barua, 2014; Mwamidi et al., 2012; Zimmermann et al., 2023). Further complicating human-elephant interactions are restrictions by international organizations that reduce local agency to manage elephant populations and conflict (Naughton-Treves & Treves, 2005; O'Connell-Rodwell et al., 2000). It is in this matrix of international and national policies, local livelihoods, challenging agricultural conditions, and dynamic climate that humans and elephants find themselves sharing space and resources. As development continues, understanding human-elephant conflict in this region becomes more urgent.

This study analyzed reported human-elephant conflict from 2015 to 2021 southeast of the city of Victoria Falls using machine learning techniques to understand where conflict is likely to occur. When tested with data not used to train the model, MLP neural network and DNN models predicted conflict occurrence at accuracies of 77.1 and 72.5% respectively. SVM was able to predict crop raiding only slightly better than at random, obtaining an accuracy of only 54.9% when using the testing data. RF

performed the best out of the machine learning models appraised, scoring an accuracy of 81.8% when tested. Variables that contributed most to the RF model were distance from agriculture, maximum HV backscattering (indicator of biomass), and distance from protected areas. Thus, while also having the advantage of providing more information than the other ML algorithms tested, RF was also the best performing algorithm. The most statistically significant relationships ($P<0.001$) discovered through binomial regression were NDVI max, distance from protected areas, distance from buildings, distance from agricultural area, and HV backscattering values.

Studies of human-elephant conflict in African savanna environments have found that risk of crop raiding increases closer to protected areas or refuge (M. D. Graham et al., 2010; Hariohay et al., 2020; Oppong et al., 2008; Sanare et al., 2022). Our findings align with these results, as evidenced by the negative relationship between distance from protected area and crop raiding occurrence. As expected, as distance to cultivated areas decreases, the likelihood of crop raiding increases in this study and in previous work in Kenya (M. D. Graham et al., 2010; Tiller et al., 2021). At the village scale, higher density of households reduces the risk of raiding in Tanzania (Hariohay et al., 2020), which aligns with our finding that higher building density areas are less likely to be raided. Research in Kenya found the relationship with settlement density was more complex with low risk at low dwelling density, high risk at densities of 5-15 dwellings per km^2, and low risk again at a threshold of 20 dwellings per km^2 (M. D. Graham et al., 2010). The distance from settlements is an additional contributing factor, with conflict in Hwange occurring further from buildings, concurring with results from Kenya (Sitati et al., 2005) and similar to results from Botswana where likelihood increases further from village (Songhurst & Coulson, 2014). Figure 4.8 shows crop raiding locations for the first quarter of 2021 along with building density and areas classified as agriculture in 2021. Much of the conflict appears at the edge of agricultural areas and often in areas where building density is somewhat lower. Our findings indicate that elephants to the

south of Victoria Falls are more likely to raid in areas with comparatively lower risk, as indicated by a lower presence of human activity.

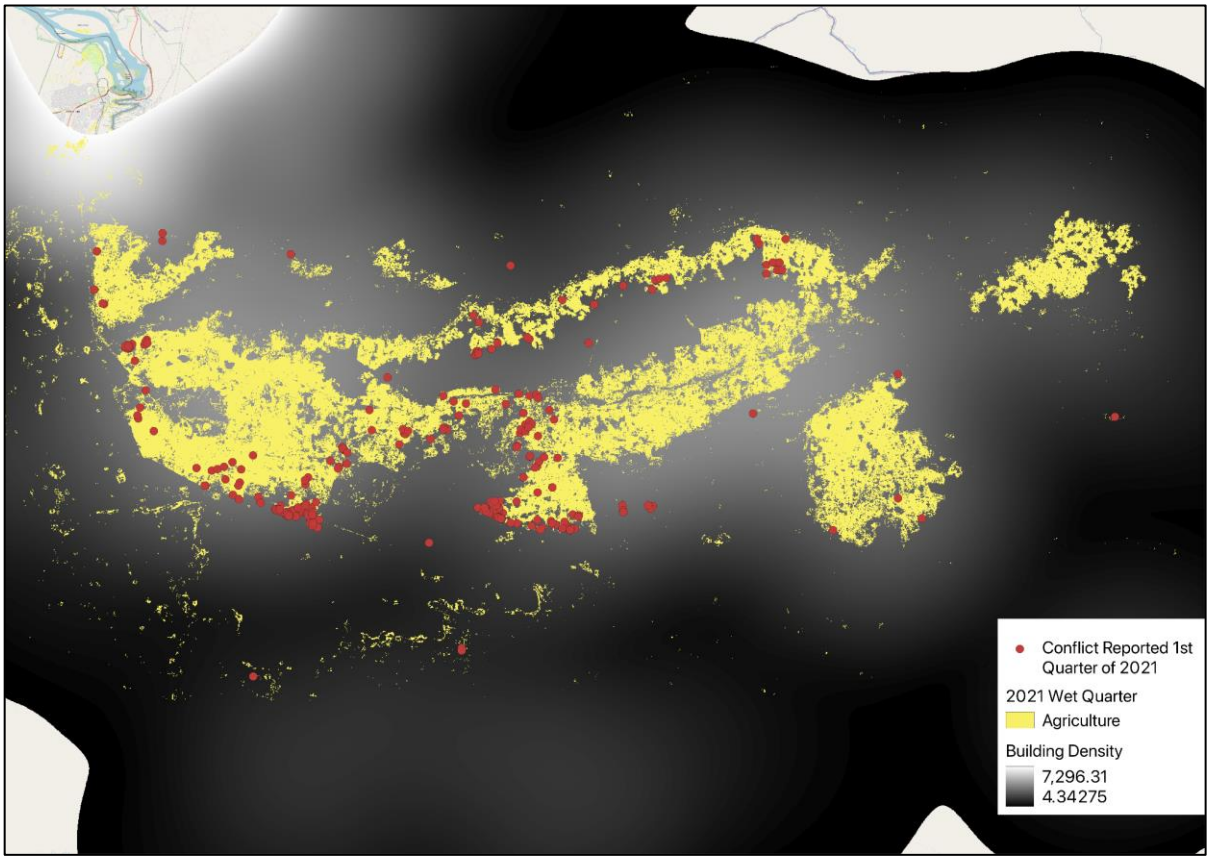

Figure 4.8. Conflict in the first quarter of 2021 shown as red points. Area classified as agriculture in 2021 is shown in yellow. Darker areas indicate lower building density whereas lighter areas indicate higher density of buildings. Basemap is from Open Street Maps.

Fences are occasionally a barrier to elephants. In this study area, distance from fences was correlated with distance from protected areas. This is not unsurprising, as our data did not discriminate if fences were erected around crops and pastures or if they were erected alongside or in parks, important areas such as the trash dump, or the airport. Previous work has found that fenced crops actually increase the likelihood of raiding, likely because fences are associated with a decrease in

guarding effort from farmers (Sitati et al., 2005). Fences were included in our models and were the fifth most important predictor in the RF model.

Our results on vegetation health, as indicated by maximum NDVI values during the crop raiding period and HV backscattering coefficients, differ from previously reported results. This is likely due to the exact measurements used and their temporal scale. While we found that areas with lower maximum NDVI values are associated with crop raiding, work in Tanzania from roughly the same time period (2016-2020) found crop raiding increased as average NDVI from 2016-2019 increased (Sanare et al., 2022). As NDVI declines in protected areas and crops mature, crop raiding increases in Mozambique (Branco et al., 2019).

Human-elephant conflict occurs in a variety of situations influenced by a myriad of factors operating at varying scales. This study used pseudo absences of conflict to identify patterns of conflict in this region. Using reported absences with information concerning whether or not crops were actively being cultivated, their plant growth stage, any elephant deterrents in use, as well as the planting and conflict history of that field would be ideal. Such information would provide important context and help elucidate why elephants raid and cause conflict in some areas but not others.

Data collection efforts were obviously impacted by the COVID-19 pandemic and shutdown of services in Zimbabwe. Southeast of Victoria Falls, the crop raiding period typically lasts a few months. The first year in which data collection returned to normal following the end of the COVID-19 shutdown was 2021, and conflict was reported in 11 out of 12 months (Figure 4.9). Reports from residents indicate that elephants and wildlife in general have been much more active in anthropogenic areas and much bolder in their behavior in comparison to pre-COVID-19 pandemic levels. Thus, data from 2021 might not represent typical patterns for this region. It is possible levels of conflict will decline gradually over time and patterns of conflict will return to normal.

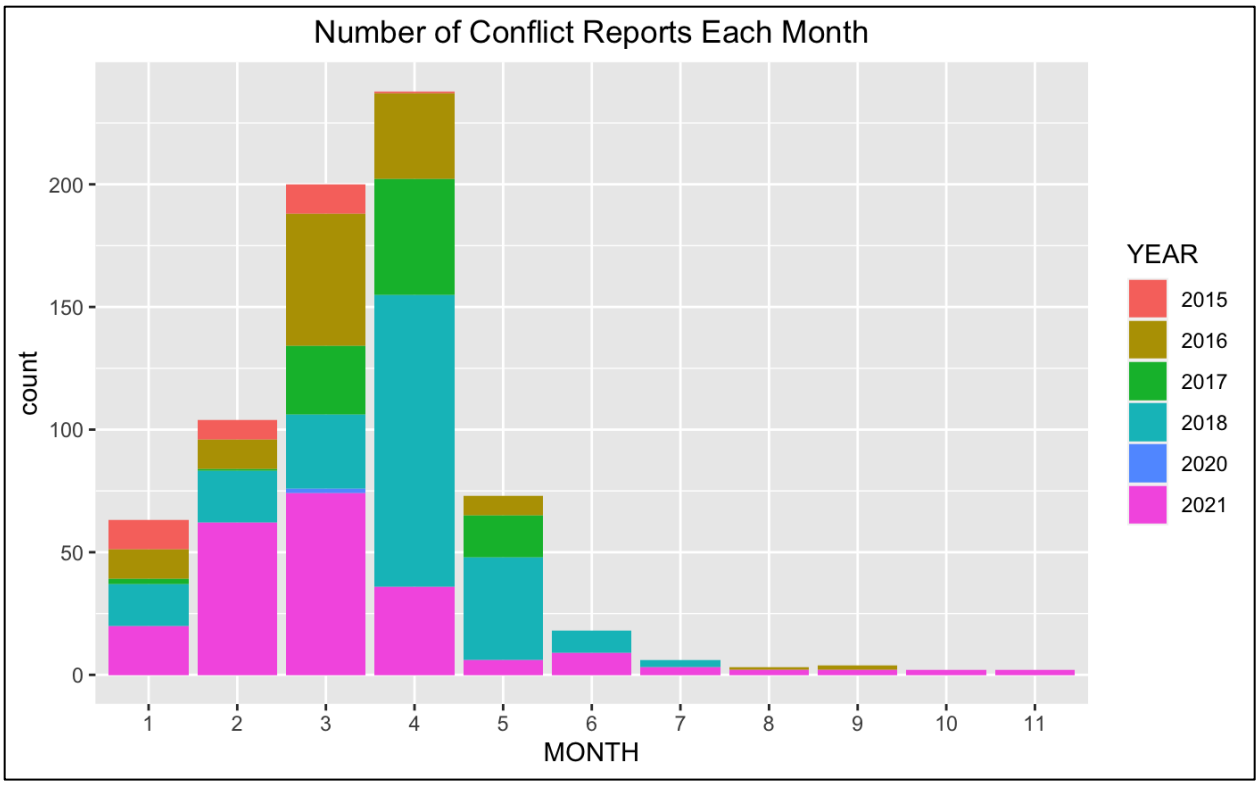

Figure 4.9. Number of human-elephant conflicts reported each month over the duration of study. Note that there are no conflict reports in 2019 due to the COVID-19 pandemic and subsequent shutdown. Refer to the "Crop raiding data" section in "Methods" for more information on the number of conflict reports per year.

Fraction of Photosynthetically Active Radiation (FPAR) has been found to be a more accurate predictor of herbaceous and dry forage biomass compared to NDVI (Machwitz et al., 2015; Tsalyuk et al., 2019). Future work could explore calculating FPAR for the area to test if it is a stronger predictor than NDVI. As elephants have impressive long term memories in regards to their use of space (Fishlock et al., 2016; Polansky et al., 2015; Presotto et al., 2019), the temporal scale at which vegetation health was measured chosen in this work might not be the best predictor of the likelihood of conflict. Our conflict models might be improved by including other measures of vegetation health and/or considering a different temporal scale for these particular predictors.

The history of a given agricultural field is also important when modeling human-elephant conflict, with those raided more frequently in the past more likely to be raided again (Sitati et al., 2005; Songhurst & Coulson, 2014). Farms with greater crop diversity have been shown at greater risk (Oppong et al., 2008) as have larger farms (Oppong et al., 2008; Sitati et al., 2005). Future work could measure if conflict points overlap with points from previous years.

Predicting human-elephant conflict is complicated and dependent on the temporal scale of data collected (Buchholtz et al., 2023; Pozo et al., 2017). As elephant populations rise in Zimbabwe, understanding human-elephant conflict in this region grows urgent. Results presented in this work should provide local context and specifics on where conflict is likely to occur south of Victoria Falls. This information can be used to inform wildlife management but also agricultural planning.

5 Conclusion

In studying human-elephant conflict, NDVI max, distance from protected areas, distance from buildings, distance from agricultural area, and HV backscattering values proved important predictors modeling where conflict would occur. Out of the machine learning algorithms tested, RF performed the best. Variables that contributed most to the RF model were distance from agriculture, maximum HV backscattering (indicator of biomass), and distance from protected areas. RF also provides more information than the other algorithms tested. The most statistically significant relationships discovered through binomial regression were NDVI max, distance from protected areas, distance from buildings, distance from agricultural area, and HV backscattering values. South of Victoria Falls, conflict is more likely to occur as one moves closer to agricultural land and protected areas, and further from buildings. As maximum NDVI during the crop raiding season declines, the likelihood of conflict increases, potentially indicating that this measure of vegetation health is not the most suitable for monitoring in relation to conflict or suggesting the temporal scale at which measurements are being collected is insufficient.

5 CONCLUSION

Conservation science's understanding of broad ecological patterns and theories is constructed by examining local patterns and principles. As such, wildlife coexistence should be studied with careful attention to scale. The region south of Victoria Falls in Zimbabwe frequently experiences conflict between humans and elephants. Crop-raiding occurs when forage is limited in natural vegetation but high in agricultural areas. Which farms are likely to be raided is unsettled, as elephants will raid particular fields and leave others untouched. The overarching issue of monitoring land cover and vegetation health to inform our knowledge of human-elephant conflict is well-suited to geospatial analysis. Through the analyses performed in this research, we sought to ameliorate human-elephant conflict by using multi-scalar remote sensing and geospatial analysis. Chapter Two reviewed scaling methods for remotely sensed data to show how scaling data permeates landscape-scale wildlife studies. Chapter Three examined land cover in the Victoria Falls region to discern whether seasonal and remotely sensed imagery resolution potentially occlude or complicate land cover classification. Finally, Chapter Four modeled human-elephant conflict to determine which underlying spatial factors are most germane to predicting conflict.

Remotely sensed data and derived products are key components of landscape analysis, but often need to be scaled to meet modeling or analysis assumptions. A plethora of scaling methods are available ranging from simple techniques with limited computational demands to more advanced methods that use deep learning algorithms. However, recognizing the advantages and limitations of different scaling methods as well as the differences between techniques is obligatory for landscape ecologists studying spatial patterns. Scale biases can add significant uncertainty and inaccuracies to an analysis. Neglecting these potential effects can complicate spatial pattern analysis and obfuscate results.

We reviewed the methods available for upscaling and downscaling remote sensing data and identified the following key findings.

First, with both upscaling and downscaling, there is no single appropriate scaling method, and so there are always tradeoffs that must be considered. While a diversity of scaling methods are available to landscape ecologists, work remains to integrate these into spatial pattern analyses. Second, landscape ecologists must be particularly aware of how scaling impacts patch richness and abundance, as these pillars of landscape diversity will be impacted differently by different scaling methods (e.g., through the elimination of patches, promoting dominance of one class. etc.). Third, methods that preserve heterogeneity, such as moving window or object-based approaches, may ultimately be better suited for spatial pattern analysis, but more work is needed to understand how heterogeneity is impacted by scaling and vice versa. Fourth, the field can focus on leveraging technological advances in machine learning and deep learning and methodological innovations in computer vision and signal processing. Lastly, plenty of scaling techniques exist, but it appears many are not widely applied in landscape ecology. We can suggest more collaborations with remote sensing and signal processing scientists, but ultimately, the path forward is to ensure landscape ecologists know about the different options, understand the potential benefits of scaling data (particularly for downscaling), and feel comfortable determining an appropriate method.

In general, land cover maps produced using Landsat, Sentinel, and Planet imagery had high accuracy, with kappa scores between 0.82 to 0.95 and total accuracies between 0.84 and 0.9, regardless of season. Accuracy was generally more consistent using Landsat compared to Sentinel or Planet. In regards to top performing models, NGRDI was of high importance when modeling land cover, as was NDVI. Top performing land cover maps created from Landsat and Sentinel imagery were improved with a short wave infrared band. Vegetation health follows well-established seasonal patterns when measured using NDVI, with forest and agricultural land much greener in the wet quarter compared to

the dry quarter. The opposite pattern was found using NGRDI, suggesting NGRDI is not a suitable indicator of vegetation health for monitoring the communal lands south of Victoria Falls. The amount of edge and the complexity of patch shapes were not greatly influenced by the spatial and spectral resolution of the land cover maps. Forest connectivity in the region is relatively high and landscape patches are of moderate complexity. When specifically examining hotspots of human-elephant conflict for differences in land cover between maps produced using Landsat, Sentinel, and Planet imagery, forest classified using the higher resolution of Sentinel and Planet imagery becomes apparent adjacent to many conflict points. Sentinel and Planet appear to be alike in land classified as forest. Thus Sentinel, with its higher spectral resolution and lack of cost, may produce land cover maps best suited to monitoring human-elephant conflict rather than maps modeled from Landsat or Planet imagery.

In studying human-elephant conflict, NDVI max, distance from protected areas, distance from buildings, distance from agricultural area, and HV backscattering values proved important predictors in predicting where conflict would occur. Out of the machine learning algorithms tested (support vector machines, multilayer perceptron neural network, deep learning neural network, and random forest), random forest performed the best. Variables that contributed most to the random forest model were distance from agriculture, maximum HV backscattering (indicator of biomass), and distance from protected areas. Random forest also provides more information than the other algorithms tested. The most statistically significant relationships discovered through binomial regression were NDVI max, distance from protected areas, distance from buildings, distance from agricultural area, and HV backscattering values. South of Victoria Falls, conflict is more likely to occur as one moves closer to agricultural land and protected areas, and further from buildings. As maximum NDVI during the crop raiding season declines, the likelihood of conflict increases, potentially indicating that this measure of vegetation health is not the most suitable for monitoring in relation to conflict or suggesting the temporal scale at which measurements are being collected is insufficient.

While remotely sensed data and derived products can be scaled in multiple ways and there is no single correct way to scale, landscape ecologists and wildlife conservation scientists must be cognizant of the limitations of their chosen method and of potential scale biases. As demonstrated when using imagery of differing grain size for land cover classification and subsequent analysis of vegetation and landscape connectivity, the spatial scale matters. Conducting an assessment of various scales and subsequently determining the one that is most suitable for the study organism(s) and the question(s) under consideration is an essential component of proficient landscape ecology. Human-elephant conflict south of Victoria Falls Findings should engender greater precision in conflict mitigation efforts and bolster scientific understanding of scaling processes and human-elephant relations.

REFERENCES

Addison, L. (2019). The fragility of empowerment: Changing gender relations in a Zimbabwean resettlement area. *Review of African Political Economy*, *46*(159), 101–116. https://doi.org/10.1080/03056244.2019.1610939

Adelabu, S., Mutanga, O., & Adam, E. (2014). Evaluating the impact of red-edge band from Rapideye image for classifying insect defoliation levels. *ISPRS Journal of Photogrammetry and Remote Sensing*, *95*, 34–41. https://doi.org/10.1016/j.isprsjprs.2014.05.013

Allen, T. F. H., & Hoekstra, T. W. (1991). Role of Heterogeneity in Scaling of Ecological Systems Under Analysis. In J. Kolasa & S. T. A. Pickett (Eds.), *Ecological Heterogeneity* (pp. 47–68). Springer. https://doi.org/10.1007/978-1-4612-3062-5_3

Allen, T. F., & Starr, T. B. (1982). *Hierarchy: Perspectives for ecological complexity*. University of Chicago Press Illinois.

Alvarez-Vanhard, E., Corpetti, T., & Houet, T. (2021). UAV & satellite synergies for optical remote sensing applications: A literature review. *Science of Remote Sensing*, *3*, 100019. https://doi.org/10.1016/j.srs.2021.100019

Anastasiadis, A. D., Magoulas, G. D., & Vrahatis, M. N. (2005). New globally convergent training scheme based on the resilient propagation algorithm. *Neurocomputing*, *64*, 253–270. https://doi.org/10.1016/j.neucom.2004.11.016

Argañaraz, J. P., & Entraigas, I. (2014). Scaling functions evaluation for estimation of landscape metrics at higher resolutions. *Ecological Informatics*, *22*, 1–12. https://doi.org/10.1016/j.ecoinf.2014.02.004

Armstrong, C. (2019). Sharing conservation burdens fairly. *Conservation Biology*, *33*(3), 554–560. https://doi.org/10.1111/cobi.13260

Arnot, C., Fisher, P. F., Wadsworth, R., & Wellens, J. (2004). Landscape metrics with ecotones: Pattern under uncertainty. *Landscape Ecology*, *19*(2), 181–195.

Atkinson, P. M. (2013). Downscaling in remote sensing. *International Journal of Applied Earth Observation and Geoinformation*, *22*, 106–114. https://doi.org/10.1016/j.jag.2012.04.012

Attorre, F., Alfò, M., De Sanctis, M., Francesconi, F., Valenti, R., Vitale, M., & Bruno, F. (2011). Evaluating the effects of climate change on tree species abundance and distribution in the Italian peninsula. *Applied Vegetation Science*, *14*(2), 242–255. https://www.jstor.org/stable/41058163

Azarang, A., & Ghassemian, H. (2017). A new pansharpening method using multi resolution analysis framework and deep neural networks. *2017 3rd International Conference on Pattern Recognition and Image Analysis (IPRIA)*, 1–6. https://doi.org/10.1109/PRIA.2017.7983017

Baraldi, A., & Panniggiani, F. (1995). An investigation of the textural characteristics associated with gray level cooccurrence matrix statistical parameters. *IEEE Transactions on Geoscience and Remote Sensing*, *33*(2), 293–304. https://doi.org/10.1109/TGRS.1995.8746010

Barnes, E. M., Clarke, T. R., Richards, S. E., Colaizzi, P. D., Haberland, J., Kostrzewski, M., Waller, P., Choi, C., Riley, E., & Thompson, T. (2000). Coincident detection of crop water stress, nitrogen status and canopy density using ground based multispectral data. *Proceedings of the Fifth International Conference on Precision Agriculture*, *1619*, 6.

Barnes, R. F. W. (1982). Elephant feeding behaviour in Ruaha National Park, Tanzania*. *African Journal of Ecology*, *20*(2), 123–136. https://doi.org/10.1111/j.1365-2028.1982.tb00282.x

Barua, M. (2014). Bio-Geo-Graphy: Landscape, Dwelling, and the Political Ecology of Human-Elephant Relations. *Environment and Planning D: Society and Space*, *32*(5), 915–934. https://doi.org/10.1068/d4213

Bates, L. A., Sayialel, K. N., Njiraini, N. W., Poole, J. H., Moss, C. J., & Byrne, R. W. (2007). African elephants have expectations about the locations of out-of-sight family members. *Biology Letters*, *4*(1), 34–36. https://doi.org/10.1098/rsbl.2007.0529

Beck, H. E., Zimmermann, N. E., McVicar, T. R., Vergopolan, N., Berg, A., & Wood, E. F. (2018). Present and future Köppen-Geiger climate classification maps at 1-km resolution. *Scientific Data*, *5*(1), Article 1. https://doi.org/10.1038/sdata.2018.214

Benson, B. J., & MacKenzie, M. D. (1995). Effects of sensor spatial resolution on landscape structure parameters. *Landscape Ecology*, *10*(2), 113–120.

Bernico, M. (2018). *Deep Learning Quick Reference: Useful hacks for training and optimizing deep neural networks with TensorFlow and Keras*. Packt Publishing Ltd.

Bhatasara, S., & Chiweshe, M. K. (2017). Beyond gender: Interrogating women's experiences in FTLRP in Zimbabwe. *Africa Review*, *9*(2), 154–172. https://doi.org/10.1080/09744053.2017.1329808

Bian, L., & Butler, R. (1999). Comparing effects of aggregation methods on statistical and spatial properties of simulated spatial data. *Photogrammetric Engineering and Remote Sensing*, *65*, 73–84.

Bihamta Toosi, N., Soffianian, A. R., Fakheran, S., Pourmanafi, S., Ginzler, C., & T. Waser, L. (2020). Land Cover Classification in Mangrove Ecosystems Based on VHR Satellite Data and Machine Learning—An Upscaling Approach. *Remote Sensing*, *12*(17), Article 17. https://doi.org/10.3390/rs12172684

Bohrer, G., Beck, P. S., Ngene, S. M., Skidmore, A. K., & Douglas-Hamilton, I. (2014). Elephant movement closely tracks precipitation-driven vegetation dynamics in a Kenyan forest-savanna landscape. *Movement Ecology*, *2*(1), 2. https://doi.org/10.1186/2051-3933-2-2

Booth, G. D., Niccolucci, M. J., & Schuster, E. G. (1994). *Identifying proxy sets in multiple linear regression: An aid to better coefficient interpretation* [Research paper INT]. US Dept of Agriculture Forest Service.

Boucher, A., & Kyriakidis, P. C. (2006). Super-resolution land cover mapping with indicator geostatistics. *Remote Sensing of Environment*, *104*(3), 264–282. https://doi.org/10.1016/j.rse.2006.04.020

Bouvet, A., Mermoz, S., Le Toan, T., Villard, L., Mathieu, R., Naidoo, L., & Asner, G. P. (2018). An above-ground biomass map of African savannahs and woodlands at 25m resolution derived from ALOS PALSAR. *Remote Sensing of Environment*, *206*, 156–173. https://doi.org/10.1016/j.rse.2017.12.030

Boyle, S. A., Kennedy, C. M., Torres, J., Colman, K., Pérez-Estigarribia, P. E., & Sancha, N. U. de la. (2014). High-Resolution Satellite Imagery Is an Important yet Underutilized Resource in Conservation Biology. *PLOS ONE*, *9*(1), e86908. https://doi.org/10.1371/journal.pone.0086908

Branco, P. S., Merkle, J. A., Pringle, R. M., Pansu, J., Potter, A. B., Reynolds, A., Stalmans, M., & Long, R. A. (2019). Determinants of elephant foraging behaviour in a coupled human-natural system: Is brown the new green? *Journal of Animal Ecology*, *88*(5), 780–792. https://doi.org/10.1111/1365-2656.12971

Breiman, L. (2001). Random Forests. *Machine Learning*, *45*, 5–32. https://doi.org/10.1023/A:1010933404324

Brown, J. H., Gillooly, J. F., Allen, A. P., Savage, V. M., & West, G. B. (2004). Toward a Metabolic Theory of Ecology. *Ecology*, *85*(7), 1771–1789. https://doi.org/10.1890/03-9000

Brunsdon, C., & Comber, A. (2020). Opening practice: Supporting reproducibility and critical spatial data science. *Journal of Geographical Systems*. https://doi.org/10.1007/s10109-020-00334-2

Buchanan, G. M., Nelson, A., Mayaux, P., Hartley, A., & Donald, P. F. (2009). Delivering a Global, Terrestrial, Biodiversity Observation System through Remote Sensing. *Conservation Biology*, *23*(2), 499–502. https://doi.org/10.1111/j.1523-1739.2008.01083.x

Buchholtz, E. K., McDaniels, M., McCulloch, G., Songhurst, A., & Stronza, A. (2023). A mixed-methods assessment of human-elephant conflict in the Western Okavango Panhandle, Botswana. *People and Nature*, *5*(2), 557–571. https://doi.org/10.1002/pan3.10443

Burges, C. J. C. (1998). A Tutorial on Support Vector Machines for Pattern Recognition. *Data Mining and Knowledge Discovery*, *2*(2), 121–167. https://doi.org/10.1023/A:1009715923555

Chamaillé-Jammes, S., Mtare, G., Makuwe, E., & Fritz, H. (2013). African Elephants Adjust Speed in Response to Surface-Water Constraint on Foraging during the Dry-Season. *PLOS ONE*, *8*(3), e59164. https://doi.org/10.1371/journal.pone.0059164

Chambers, C. L., Cushman, S. A., Medina-Fitoria, A., Martínez-Fonseca, J., & Chávez-Velásquez, M. (2016). Influences of scale on bat habitat relationships in a forested landscape in Nicaragua. *Landscape Ecology*, *31*(6), 1299–1318. https://doi.org/10.1007/s10980-016-0343-4

Chapin, F. S., Zavaleta, E. S., Eviner, V. T., Naylor, R. L., Vitousek, P. M., Reynolds, H. L., Hooper, D. U., Lavorel, S., Sala, O. E., Hobbie, S. E., Mack, M. C., & Díaz, S. (2000). Consequences of changing biodiversity. *Nature*, *405*(6783), 234–242. https://doi.org/10.1038/35012241

Chen, C., Wang, L., Myneni, R. B., & Li, D. (2020). Attribution of Land-Use/Land-Cover Change Induced Surface Temperature Anomaly: How Accurate Is the First-Order Taylor Series Expansion? *Journal of Geophysical Research: Biogeosciences*, *125*(9), e2020JG005787. https://doi.org/10.1029/2020JG005787

Chen, J.-C., & Wang, Y.-M. (2020). Comparing Activation Functions in Modeling Shoreline Variation Using Multilayer Perceptron Neural Network. *Water*, *12*(5), Article 5. https://doi.org/10.3390/w12051281

Chipenda, C. (2018). *After land reform in Zimbabwe: What about the youth?* Emancipatory Rural Politics Initiative (ERPI) 2018 Conference: "Authoritarian Populism and the Rural World."

Chiweshe, M. K., & Chabata, T. (2019). The complexity of farmworkers' livelihoods in Zimbabwe after the Fast Track Land Reform: Experiences from a farm in Chinhoyi, Zimbabwe. *Review of African Political Economy*, *46*(159), 55–70. https://doi.org/10.1080/03056244.2019.1609920

Chiyo, P. I., Moss, C. J., Archie, E. A., Hollister-Smith, J. A., & Alberts, S. C. (2011). Using molecular and observational techniques to estimate the number and raiding patterns of crop-raiding elephants. *Journal of Applied Ecology*, *48*(3), 788–796. https://doi.org/10.1111/j.1365-2664.2011.01967.x

Cihlar, J. (2000). Land cover mapping of large areas from satellites: Status and research priorities. *International Journal of Remote Sensing*, *21*(6–7), 1093–1114. https://doi.org/10.1080/014311600210092

CITES implementation report (Implementation Report 08/03/21e). (2021). Zimbabwe Parks and Wildlife Management Authority. https://cites.org/sites/default/files/documents/19-21Zimbabwe.pdf

Congalton, R. G. (1991). A review of assessing the accuracy of classifications of remotely sensed data. *Remote Sensing of Environment*, *37*(1), 35–46. https://doi.org/10.1016/0034-4257(91)90048-B

Congalton, R. G., & Green, K. (1999). *Assessing the Accuracy of Remotely Sensed Data: Principles and Practices.* Lewis Publishers.

Cook, R. M., Witkowski, E. T. F., Helm, C. V., Henley, M. D., & Parrini, F. (2017). Recent exposure to African elephants after a century of exclusion: Rapid accumulation of marula tree impact and mortality, and poor regeneration. *Forest Ecology and Management*, *401*, 107–116. https://doi.org/10.1016/j.foreco.2017.07.006

Cortes, C., & Vapnik, V. (1995). Support-vector networks. *Machine Learning*, *20*(3), 273–297. https://doi.org/10.1007/BF00994018

Cracknell, A. P. (1998). Synergy in remote sensing-what's in a pixel? *International Journal of Remote Sensing*, *19*(11), 2025–2047. https://doi.org/10.1080/014311698214848

Davies, T. E., Wilson, S., Hazarika, N., Chakrabarty, J., Das, D., Hodgson, D. J., & Zimmermann, A. (2011). Effectiveness of intervention methods against crop-raiding elephants. *Conservation Letters*, *4*(5), 346–354. https://doi.org/10.1111/j.1755-263X.2011.00182.x

de Klerk, H. M., & Buchanan, G. (2017). Remote sensing training in African conservation. *Remote Sensing in Ecology and Conservation*, *3*(1), 7–20. https://doi.org/10.1002/rse2.36

Dejene, S. W., Mpakairi, K. S., Kanagaraj, R., Wato, Y. A., & Mengistu, S. (2021). Modelling continental range shift of the African elephant (Loxodonta africana) under a changing climate and land cover: Implications for future conservation of the species. *African Zoology*, *56*(1), 25–34. https://doi.org/10.1080/15627020.2020.1846617

Delegido, J., Verrelst, J., Alonso, L., & Moreno, J. (2011). Evaluation of Sentinel-2 Red-Edge Bands for Empirical Estimation of Green LAI and Chlorophyll Content. *Sensors*, *11*(7), Article 7. https://doi.org/10.3390/s110707063

Dendoncker, N., Bogaert, P., & Rounsevell, M. (2006). A statistical method to downscale aggregated land use data and scenarios. *Journal of Land Use Science*, *1*(2–4), 63–82. https://doi.org/10.1080/17474230601058302

Dickman, A. J. (2010). Complexities of conflict: The importance of considering social factors for effectively resolving human–wildlife conflict. *Animal Conservation*, *13*(5), 458–466. https://doi.org/10.1111/j.1469-1795.2010.00368.x

Dormann, C. F., Elith, J., Bacher, S., Buchmann, C., Carl, G., Carré, G., Marquéz, J. R. G., Gruber, B., Lafourcade, B., Leitão, P. J., Münkemüller, T., McClean, C., Osborne, P. E., Reineking, B., Schröder, B., Skidmore, A. K., Zurell, D., & Lautenbach, S. (2013). Collinearity: A review of methods to deal with it and a simulation study evaluating their performance. *Ecography*, *36*(1), 27–46. https://doi.org/10.1111/j.1600-0587.2012.07348.x

Doyog, N. D., Lin, C., Lee, Y. J., Lumbres, R. I. C., Daipan, B. P. O., Bayer, D. C., & Parian, C. P. (2021). Diagnosing pristine pine forest development through pansharpened-surface-reflectance Landsat image derived aboveground biomass productivity. *Forest Ecology and Management*, *487*, 119011. https://doi.org/10.1016/j.foreco.2021.119011

Dube, K., & Nhamo, G. (2019). Climate change and potential impacts on tourism: Evidence from the Zimbabwean side of the Victoria Falls. *Environment, Development and Sustainability*, *21*(4), 2025–2041. https://doi.org/10.1007/s10668-018-0118-y

Dublin, H. T., Sinclair, A. R. E., & McGlade, J. (1990). Elephants and Fire as Causes of Multiple Stable States in the Serengeti-Mara Woodlands. *Journal of Animal Ecology*, *59*(3), 1147–1164. https://doi.org/10.2307/5037

Duchi, J., Hazan, E., & Singer, Y. (2011). Adaptive Subgradient Methods for Online Learning and Stochastic Optimization. *Journal of Machine Learning Research*, *12*(7).

Duporge, I., Isupova, O., Reece, S., Macdonald, D. W., & Wang, T. (2020). Using very-high-resolution satellite imagery and deep learning to detect and count African elephants in heterogeneous landscapes. *Remote Sensing in Ecology and Conservation*, *n/a*(n/a). https://doi.org/10.1002/rse2.195

Dutilleul, P., & Legendre, P. (1993). Spatial heterogeneity against heteroscedasticity: An ecological paradigm versus a statistical concept. *Oikos*, 152–171.

Dymond, C. C., Mladenoff, D. J., & Radeloff, V. C. (2002). Phenological differences in Tasseled Cap indices improve deciduous forest classification. *Remote Sensing of Environment*, *80*(3), 460–472. https://doi.org/10.1016/S0034-4257(01)00324-8

Eilola, S., Käyhkö, N., & Fagerholm, N. (2021). Lessons learned from participatory land use planning with high-resolution remote sensing images in Tanzania: Practitioners' and participants' perspectives. *Land Use Policy*, *109*, 105649. https://doi.org/10.1016/j.landusepol.2021.105649

Eitel, J. U. H., Vierling, L. A., Litvak, M. E., Long, D. S., Schulthess, U., Ager, A. A., Krofcheck, D. J., & Stoscheck, L. (2011). Broadband, red-edge information from satellites improves early stress detection in a New Mexico conifer woodland. *Remote Sensing of Environment*, *115*(12), 3640–3646. https://doi.org/10.1016/j.rse.2011.09.002

Elephant Kills Vic Falls Mentally Ill Homeless Man. (2020, June 18). *NewZimbabwe.Com*. https://www.newzimbabwe.com/elephant-kills-vic-falls-mentally-ill-homeless-man/

Fishlock, V., Caldwell, C., & Lee, P. C. (2016). Elephant resource-use traditions. *Animal Cognition*, *19*(2), 429–433. https://doi.org/10.1007/s10071-015-0921-x

Fortin, D., Bérubé, A.-J., Boudreau, S., Shrader, A., & Ward, D. (2022). Density-dependent habitat selection varies between male and female African elephants. *Biological Conservation*, *276*, 109794. https://doi.org/10.1016/j.biocon.2022.109794

Frazier, A. E. (2014). A new data aggregation technique to improve landscape metric downscaling. *Landscape Ecology*, *29*(7), 1261–1276. https://doi.org/10.1007/s10980-014-0066-3

Frazier, A. E. (2015a). Landscape heterogeneity and scale considerations for super-resolution mapping. *International Journal of Remote Sensing*, *36*(9), 2395–2408. https://doi.org/10.1080/2150704X.2015.1040130

Frazier, A. E. (2015b). Landscape heterogeneity and scale considerations for super-resolution mapping. *International Journal of Remote Sensing*, *36*(9), 2395–2408. https://doi.org/10.1080/2150704X.2015.1040130

Frazier, A. E. (2015c). Landscape heterogeneity and scale considerations for super-resolution mapping. *International Journal of Remote Sensing*, *36*(9), 2395–2408. https://doi.org/10.1080/2150704X.2015.1040130

Frazier, A. E. (2016). Surface metrics: Scaling relationships and downscaling behavior. *Landscape Ecology*, *31*(2), 351–363. https://doi.org/10.1007/s10980-015-0248-7

Frazier, A. E., & Kedron, P. (2017). Landscape Metrics: Past Progress and Future Directions. *Current Landscape Ecology Reports*, *2*(3), 63–72. https://doi.org/10.1007/s40823-017-0026-0

Frazier, A. E., Kedron, P., Ovando-Montejo, G. A., & Zhao, Y. (2021). Scaling spatial pattern metrics: Impacts of composition and configuration on downscaling accuracy. *Landscape Ecology*. https://doi.org/10.1007/s10980-021-01349-w

Frazier, A. E., & Wang, L. (2011). Characterizing spatial patterns of invasive species using sub-pixel classifications. *Remote Sensing of Environment*, *115*(8), 1997–2007.

Frischen, J., Meza, I., Rupp, D., Wietler, K., & Hagenlocher, M. (2020). Drought Risk to Agricultural Systems in Zimbabwe: A Spatial Analysis of Hazard, Exposure, and Vulnerability. *Sustainability*, *12*(3), Article 3. https://doi.org/10.3390/su12030752

Fritz, H. (2017). Long-term field studies of elephants: Understanding the ecology and conservation of a long-lived ecosystem engineer. *Journal of Mammalogy*, *98*(3), 603–611. https://doi.org/10.1093/jmammal/gyx023

Fu, Y., Wu, X.-J., & Durrani, T. (2021). Image fusion based on generative adversarial network consistent with perception. *Information Fusion*, *72*, 110–125. https://doi.org/10.1016/j.inffus.2021.02.019

Funk, C., & Budde, M. E. (2009). Phenologically-tuned MODIS NDVI-based production anomaly estimates for Zimbabwe. *Remote Sensing of Environment*, *113*(1), 115–125.

Funk, C., Peterson, P., Landsfeld, M., Pedreros, D., Verdin, J., Shukla, S., Husak, G., Rowland, J., Harrison, L., Hoell, A., & Michaelsen, J. (2015). The climate hazards infrared precipitation with stations—A new environmental record for monitoring extremes. *Scientific Data*, *2*(1), Article 1. https://doi.org/10.1038/sdata.2015.66

Galpern, P., & Manseau, M. (2013). Finding the functional grain: Comparing methods for scaling resistance surfaces. *Landscape Ecology*, *28*(7), 1269–1281.

Gao, F., Hilker, T., Zhu, X., Anderson, M., Masek, J., Wang, P., & Yang, Y. (2015). Fusing Landsat and MODIS Data for Vegetation Monitoring. *IEEE Geoscience and Remote Sensing Magazine*, *3*(3), 47–60. https://doi.org/10.1109/MGRS.2015.2434351

Gao, Q., Yu, M., Yang, X., & Wu, J. (2001). Scaling simulation models for spatially heterogeneous ecosystems with diffusive transportation. *Landscape Ecology*, *16*(4), 289–300.

García-Gigorro, S., & Saura, S. (2005). Forest fragmentation estimated from remotely sensed data: Is comparison across scales possible? *Forest Science*, *51*(1), 51–63.

Gardner, R. H., Lookingbill, T. R., Townsend, P. A., & Ferrari, J. (2008). A new approach for rescaling land cover data. *Landscape Ecology*, *23*(5), 513–526.

Garrigues, S., Allard, D., Baret, F., & Weiss, M. (2006). Influence of landscape spatial heterogeneity on the non-linear estimation of leaf area index from moderate spatial resolution remote sensing data. *Remote Sensing of Environment*, *105*(4), 286–298. https://doi.org/10.1016/j.rse.2006.07.013

Ge, Y., Jin, Y., Stein, A., Chen, Y., Wang, J., Wang, J., Cheng, Q., Bai, H., Liu, M., & Atkinson, P. M. (2019). Principles and methods of scaling geospatial Earth science data. *Earth-Science Reviews*, *197*, 102897. https://doi.org/10.1016/j.earscirev.2019.102897

GEOGLAM Crop Monitors. (2020). *Consecutive years of record below-average rainfall affecting crops in Zimbabwe* (Special Report-Zimbabwe, p. 5). Global Agricultural Monitoring. https://cropmonitor.org/documents/SPECIAL/reports/Special_Report_20200201_Zimbabwe.pdf

Geza, S. (1986). The Role of Resettlement in Social Development in Africa. *Journal of Social Development in Africa*, *1*(1), 35–42. https://www.africabib.org/rec.php?RID=W00075535

Gillespie, A. R., Kahle, A. B., & Walker, R. E. (1987). Color enhancement of highly correlated images. II. Channel ratio and "chromaticity" transformation techniques. *Remote Sensing of Environment*, *22*(3), 343–365.

Golibagh Mahyari, A., & Yazdi, M. (2011). Panchromatic and Multispectral Image Fusion Based on Maximization of Both Spectral and Spatial Similarities. *IEEE Transactions on Geoscience and Remote Sensing*, *49*(6), 1976–1985. https://doi.org/10.1109/TGRS.2010.2103944

Goodchild, M., & Quattrochi, D. A. (1997). Introduction: Scale, Multiscaling, Remote Sensing, and GIS. In *Scale in Remote Sensing and GIS* (pp. 1–13). CRC Press.

Goodfellow, I., Bengio, Y., & Courville, A. (2016). *Deep Learning*. MIT Press.

Goovaerts, P. (2006). Geostatistical analysis of disease data: Accounting for spatial support and population density in the isopleth mapping of cancer mortality risk using area-to-point Poisson kriging. *International Journal of Health Geographics*, *5*(1), 52. https://doi.org/10.1186/1476-072X-5-52

Gordon, C., Greve, M., Henley, M., Bedetti, A., Allin, P., & Svenning, J.-C. (2023). Elephant rewilding affects landscape openness and fauna habitat across a 92-year period. *Ecological Applications*, *33*(3). https://doi.org/10.1002/eap.2810

Goward, S. N., Tucker, C. J., & Dye, D. G. (1985). North American vegetation patterns observed with the NOAA-7 advanced very high resolution radiometer. *Vegetatio*, *64*(1), 3–14. https://doi.org/10.1007/BF00033449

Graham, L. J., Spake, R., Gillings, S., Watts, K., & Eigenbrod, F. (2019). Incorporating fine-scale environmental heterogeneity into broad-extent models. *Methods in Ecology and Evolution*, *10*(6), 767–778. https://doi.org/10.1111/2041-210X.13177

Graham, M. D., Notter, B., Adams, W. M., Lee, P. C., & Ochieng, T. N. (2010). Patterns of crop-raiding by elephants, Loxodonta africana, in Laikipia, Kenya, and the management of human–elephant conflict. *Systematics and Biodiversity*, *8*(4), 435–445.

Green, K., Kempka, D., & Lackey, L. (1994). Using remote sensing to detect and monitor land-cover and land-use change. *Photogrammetric Engineering and Remote Sensing*, *60*(3), 331–337.

Gregory, R. (2000). Using Stakeholder Values to Make Smarter Environmental Decisions. *Environment: Science and Policy for Sustainable Development*, *42*(5), 34–44. https://doi.org/10.1080/00139150009604888

Grunwald, S., Vasques, G. M., & Rivero, R. G. (2015). Chapter One — Fusion of Soil and Remote Sensing Data to Model Soil Properties. In D. L. Sparks (Ed.), *Advances in Agronomy* (Vol. 131, pp. 1–109). Academic Press. https://doi.org/10.1016/bs.agron.2014.12.004

Guerbois, C., Chapanda, E., & Fritz, H. (2012). Combining multi-scale socio-ecological approaches to understand the susceptibility of subsistence farmers to elephant crop raiding on the edge of a protected area. *Journal of Applied Ecology*, *49*(5), 1149–1158.

Guldemond, R., & Van Aarde, R. (2008). A meta-analysis of the impact of African elephants on savanna vegetation. *The Journal of Wildlife Management*, *72*(4), 892–899.

Gupta, R. K., Prasad, T. S., Krishna Rao, P. V., & Bala Manikavelu, P. M. (2000). Problems in upscaling of high resolution remote sensing data to coarse spatial resolution over land surface. *Advances in Space Research*, *26*(7), 1111–1121. https://doi.org/10.1016/S0273-1177(99)01127-8

Guy, P. R. (1976). The feeding behaviour of elephant (Loxodonta africana) in the Sengwa area Rhodesia. *South African Journal of Wildlife Research*, *6*(1), 55–63.

Ha, W., Gowda, P. H., & Howell, T. A. (2013). A review of downscaling methods for remote sensing-based irrigation management: Part I. *Irrigation Science*, *31*(4), 831–850. https://doi.org/10.1007/s00271-012-0331-7

Hall, O., Hay, G. J., Bouchard, A., & Marceau, D. J. (2004). Detecting dominant landscape objects through multiple scales: An integration of object-specific methods and watershed segmentation. *Landscape Ecology*, *19*(1), 59–76. https://doi.org/10.1023/B:LAND.0000018371.43447.1f

Hammar, A., Raftopoulos, B., & Jensen, S. (2003). *Zimbabwe's unfinished business: Rethinking land, state and nation in the context of crisis*. Weaver Press. https://cir.nii.ac.jp/crid/1130282270656984832

Haralick, R., Shanmugam, K., & Dinstein, I. (1973). Textural Features for Image Classification. *IEEE Transactions on Systems, Man, and Cybernetics*, *SMC-3*(6), 610–621. https://ieeexplore.ieee.org/document/4309314

Hariohay, K. M., Fyumagwa, R. D., Kideghesho, J. R., & Røskaft, E. (2018). Awareness and attitudes of local people toward wildlife conservation in the Rungwa Game Reserve in Central Tanzania. *Human Dimensions of Wildlife*, *23*(6), 503–514. https://doi.org/10.1080/10871209.2018.1494866

Hariohay, K. M., Munuo, W. A., & Røskaft, E. (2020). Human–elephant interactions in areas surrounding the Rungwa, Kizigo, and Muhesi Game Reserves, central Tanzania. *Oryx*, *54*(5), 612–620. https://doi.org/10.1017/S003060531800128X

Hart, B. L., Hart, L. A., & Pinter-Wollman, N. (2008). Large brains and cognition: Where do elephants fit in? *Neuroscience & Biobehavioral Reviews*, *32*(1), 86–98. https://doi.org/10.1016/j.neubiorev.2007.05.012

Hay, G. J., Marceau, D. J., Dubé, P., & Bouchard, A. (2001). A multiscale framework for landscape analysis: Object-specific analysis and upscaling. *Landscape Ecology*, *16*(6), 471–490. https://doi.org/10.1023/A:1013101931793

Hay, G. J., Niernann, K. O., & Goodenough, D. G. (1997). Spatial thresholds, image-objects, and upscaling: A multiscale evaluation. *Remote Sensing of Environment*, *62*(1), 1–19.

Haydn, R., Dalke, G. W., Henkel, J., & Bare, J. E. (1982). Application of the IHS color transform to the processing of multisensor data and image enhancement. *Proceedings of the International Symposium on Remote Sensing of Environment, First Thematic Conference: Remote Sensing of Arid and Semi-Arid Lands*.

He, H. S., Ventura, S. J., & Mladenoff, D. J. (2002). Effects of spatial aggregation approaches on classified satellite imagery. *International Journal of Geographical Information Science*, *16*(1), 93–109. https://doi.org/10.1080/13658810110075978

Hoare, R. E. (1999). Determinants of human–elephant conflict in a land-use mosaic. *Journal of Applied Ecology*, *36*(5), 689–700.

Holt, D., Steel, D. G., Tranmer, M., & Wrigley, N. (1996). Aggregation and Ecological Effects in Geographically Based Data. *Geographical Analysis*, *28*(3), 244–261. https://doi.org/10.1111/j.1538-4632.1996.tb00933.x

Hornik, K., Stinchcombe, M., & White, H. (1989). Multilayer feedforward networks are universal approximators. *Neural Networks*, *2*(5), 359–366. https://doi.org/10.1016/0893-6080(89)90020-8

Hoskins, A. J., Bush, A., Gilmore, J., Harwood, T., Hudson, L. N., Ware, C., Williams, K. J., & Ferrier, S. (2016). Downscaling land-use data to provide global 30″ estimates of five land-use classes. *Ecology and Evolution*, *6*(9), 3040–3055. https://doi.org/10.1002/ece3.2104

Hu, Z., & Islam, S. (1997). A framework for analyzing and designing scale invariant remote sensing algorithms. *IEEE Transactions on Geoscience and Remote Sensing*, *35*(3), 747–755. https://doi.org/10.1109/36.581996

Huang, S., Tang, L., Hupy, J. P., Wang, Y., & Shao, G. (2021). A commentary review on the use of normalized difference vegetation index (NDVI) in the era of popular remote sensing. *Journal of Forestry Research*, *32*(1), 1–6. https://doi.org/10.1007/s11676-020-01155-1

Huang, W., Xiao, L., Wei, Z., Liu, H., & Tang, S. (2015). A New Pan-Sharpening Method With Deep Neural Networks. *IEEE Geoscience and Remote Sensing Letters*, *12*(5), 1037–1041. https://doi.org/10.1109/LGRS.2014.2376034

Hulsman, P., Savenije, H. H. G., & Hrachowitz, M. (2021). Satellite-based drought analysis in the Zambezi River Basin: Was the 2019 drought the most extreme in several decades as locally perceived? *Journal of Hydrology: Regional Studies*, *34*, 100789. https://doi.org/10.1016/j.ejrh.2021.100789

Hunt, E. R., Cavigelli, M., Daughtry, C. S. T., Mcmurtrey, J. E., & Walthall, C. L. (2005). Evaluation of Digital Photography from Model Aircraft for Remote Sensing of Crop Biomass and Nitrogen Status. *Precision Agriculture*, *6*(4), 359–378. https://doi.org/10.1007/s11119-005-2324-5

Hurni, K., Hett, C., Epprecht, M., Messerli, P., & Heinimann, A. (2013). A Texture-Based Land Cover Classification for the Delineation of a Shifting Cultivation Landscape in the Lao PDR Using Landscape Metrics. *Remote Sensing*, *5*(7), Article 7. https://doi.org/10.3390/rs5073377

Husak, G., Harrison, L., Magadzire, T., Funk, C., & Way-Henthorne, J. (2020, February 13). Rainfall performance for 2019/20 season over Zimbabwe falling short for the fourth time in five years. *Climate Hazards Center*. http://blog.chc.ucsb.edu/?p=695

Jannoura, R., Brinkmann, K., Uteau, D., Bruns, C., & Joergensen, R. G. (2015). Monitoring of crop biomass using true colour aerial photographs taken from a remote controlled hexacopter. *Biosystems Engineering*, *129*, 341–351. https://doi.org/10.1016/j.biosystemseng.2014.11.007

Jelinski, D. E., & Wu, J. (1996). The modifiable areal unit problem and implications for landscape ecology. *Landscape Ecology*, *11*(3), 129–140. https://doi.org/10.1007/BF02447512

Jensen, J. (2016). *Introductory Digital Image Processing: A Remote Sensing Perspective* (4th ed.). Pearson.

Jia, D., Song, C., Cheng, C., Shen, S., Ning, L., & Hui, C. (2020). A Novel Deep Learning-Based Spatiotemporal Fusion Method for Combining Satellite Images with Different Resolutions Using a Two-Stream Convolutional Neural Network. *Remote Sensing*, *12*(4), Article 4. https://doi.org/10.3390/rs12040698

Jin, Y., Ge, Y., Wang, J., Heuvelink, G. B. M., & Wang, L. (2018). Geographically Weighted Area-to-Point Regression Kriging for Spatial Downscaling in Remote Sensing. *Remote Sensing*, *10*(4), Article 4. https://doi.org/10.3390/rs10040579

Jones, D. A., Hansen, A. J., Bly, K., Doherty, K., Verschuyl, J. P., Paugh, J. I., Carle, R., & Story, S. J. (2009). Monitoring land use and cover around parks: A conceptual approach. *Remote Sensing of Environment*, *113*(7), 1346–1356. https://doi.org/10.1016/j.rse.2008.08.018

Ju, J., Gopal, S., & Kolaczyk, E. D. (2005). On the choice of spatial and categorical scale in remote sensing land cover classification. *Remote Sensing of Environment*, *96*(1), 62–77. https://doi.org/10.1016/j.rse.2005.01.016

Kaheil, Y. H., Rosero, E., Gill, M. K., McKee, M., & Bastidas, L. A. (2008). Downscaling and Forecasting of Evapotranspiration Using a Synthetic Model of Wavelets and Support Vector Machines. *IEEE Transactions on Geoscience and Remote Sensing*, *46*(9), 2692–2707. https://doi.org/10.1109/TGRS.2008.919819

Kamwi, J. M., Cho, M. A., Kaetsch, C., Manda, S. O., Graz, F. P., & Chirwa, P. W. (2018). Assessing the Spatial Drivers of Land Use and Land Cover Change in the Protected and Communal Areas of the Zambezi Region, Namibia. *Land*, *7*(4), Article 4. https://doi.org/10.3390/land7040131

Karidozo, M., & Osborn, F. (2005). Can Bees deter elephants from raiding crops? An experiment in the communal lands of Zimbabwe, Pachyderm 39: 26-32. *Pachyderm*, *9*.

Karidozo, M., & Osborn, F. (2015). Community Based Conflict Mitigation Trials: Results of Field Tests of Chilli as an Elephant Deterrent. *Journal of Biodiversity & Endangered Species*, *3*(1). https://doi.org/10.4172/2332-2543.1000144

Kasischke, E. S., Melack, J. M., & Craig Dobson, M. (1997). The use of imaging radars for ecological applications—A review. *Remote Sensing of Environment*, *59*(2), 141–156. https://doi.org/10.1016/S0034-4257(96)00148-4

Kaur, G., Saini, K. S., Singh, D., & Kaur, M. (2021). A Comprehensive Study on Computational Pansharpening Techniques for Remote Sensing Images. *Archives of Computational Methods in Engineering*. https://doi.org/10.1007/s11831-021-09565-y

Ke, Y., Im, J., Park, S., & Gong, H. (2017). Spatiotemporal downscaling approaches for monitoring 8-day 30m actual evapotranspiration. *ISPRS Journal of Photogrammetry and Remote Sensing*, *126*, 79–93. https://doi.org/10.1016/j.isprsjprs.2017.02.006

Kedron, P. J., Frazier, A. E., Ovando-Montejo, G. A., & Wang, J. (2018). Surface metrics for landscape ecology: A comparison of landscape models across ecoregions and scales. *Landscape Ecology*, *33*(9), 1489–1504. https://doi.org/10.1007/s10980-018-0685-1

Keep Victoria Falls Wild. (2023). *THE VICTORIA FALLS WORLD HERITAGE SITE 2023 STATE OF DEVELOPMENT* (p. 18) [Summary Report]. http://keepvictoriafallswild.com/downloads/KVFW2023StateofDevelopmentSummaryReport.pdf

Kerley, G., & Landman, M. (2006). The impacts of elephants on biodiversity in the Eastern Cape Subtropical Thickets: Elephant conservation. *South African Journal of Science*, *102*(9), 395–402. https://doi.org/10.10520/EJC96608

Keshava, N., & Mustard, J. F. (2002). Spectral unmixing. *IEEE Signal Processing Magazine*, *19*(1), 44–57. https://doi.org/10.1109/79.974727

Kileo, L. E., & Mbije, N. E. (2021). Land Use Practices along Saadani-Wami-Mbiki Wildlife Corridor and their Implications to Wildlife Conservation. *Asian Journal of Environment & Ecology*, *16*(4), 126–143. https://doi.org/10.9734/ajee/2021/v16i430264

King, L. E., Douglas-Hamilton, I., & Vollrath, F. (2007). African elephants run from the sound of disturbed bees. *Current Biology*, *17*(19), R832–R833. https://doi.org/10.1016/j.cub.2007.07.038

Kingma, D. P., & Ba, J. (2014). *Adam: A Method for Stochastic Optimization* (arXiv:1412.6980). arXiv. https://doi.org/10.48550/arXiv.1412.6980

Knight, A. T., Cowling, R. M., & Campbell, B. M. (2006). An Operational Model for Implementing Conservation Action. *Conservation Biology*, *20*(2), 408–419. https://doi.org/10.1111/j.1523-1739.2006.00305.x

Kolasa, J., & Pickett, S. T. (Eds.). (1991). *Ecological heterogeneity* (Vol. 572). Springer.

Kupfer, J. A. (2012). Landscape ecology and biogeography: Rethinking landscape metrics in a post-FRAGSTATS landscape. *Progress in Physical Geography*, *36*(3), 400–420.

Kyriakidis, P. C. (2004). A Geostatistical Framework for Area-to-Point Spatial Interpolation. *Geographical Analysis*, *36*(3), 259–289. https://doi.org/10.1111/j.1538-4632.2004.tb01135.x

Landis, J. R., & Koch, G. G. (1977a). A one-way components of variance model for categorical data. *Biometrics*, 671–679.

Landis, J. R., & Koch, G. G. (1977b). The Measurement of Observer Agreement for Categorical Data. *Biometrics*, *33*(1), 159–174. https://doi.org/10.2307/2529310

Lang, S. (2008). Object-based image analysis for remote sensing applications: Modeling reality – dealing with complexity. In T. Blaschke, S. Lang, & G. J. Hay (Eds.), *Object-Based Image Analysis: Spatial Concepts for Knowledge-Driven Remote Sensing Applications* (pp. 3–27). Springer. https://doi.org/10.1007/978-3-540-77058-9_1

Lang, S., Hay, G. J., Baraldi, A., Tiede, D., & Blaschke, T. (2019). GEOBIA Achievements and Spatial Opportunities in the Era of Big Earth Observation Data. *ISPRS International Journal of Geo-Information*, *8*(11), Article 11. https://doi.org/10.3390/ijgi8110474

Langbauer, W., Karidozo, M., Madden, M., Parry, R., Koehler, S., Fillebrown, J., Wehlan, T., Osborn, F., & Presotto, A. (2021). From elephant memory to conservation action: Using chili oil to mitigate conflict one elephant at a time. *Animal Conservation*, *25*. https://doi.org/10.1111/acv.12747

Laursen, L., & Bekoff, M. (1978). Loxodonta africana. *Mammalian Species*, *92*, 1–8. https://doi.org/10.2307/3503889

Lausch, A., & Herzog, F. (2002). Applicability of landscape metrics for the monitoring of landscape change: Issues of scale, resolution and interpretability. *Ecological Indicators*, *2*(1), 3–15. https://doi.org/10.1016/S1470-160X(02)00053-5

Laws, R. M., Parker, I. S. C., & Johnstone, R. C. B. (1975). Elephants and their habitats. In *The ecology of elephants in North Bunyoro, Uganda*. Clarendon Press.

Levin, S. A. (1992). The Problem of Pattern and Scale in Ecology: The Robert H. MacArthur Award Lecture. *Ecology*, *73*(6), 1943–1967. https://doi.org/10.2307/1941447

Li, H., & Reynolds, J. F. (1995). On Definition and Quantification of Heterogeneity. *Oikos*, *73*(2), 280. https://doi.org/10.2307/3545921

Li, H., & Wu, X.-J. (2019). DenseFuse: A Fusion Approach to Infrared and Visible Images. *IEEE Transactions on Image Processing*, *28*(5), 2614–2623. https://doi.org/10.1109/TIP.2018.2887342

Li, X., Du, Y., & Ling, F. (2014). Super-Resolution Mapping of Forests With Bitemporal Different Spatial Resolution Images Based on the Spatial-Temporal Markov Random Field. *IEEE Journal of Selected Topics in Applied Earth Observations and Remote Sensing*, *7*(1), 29–39. https://doi.org/10.1109/JSTARS.2013.2264828

Li, Z., Zhang, H. K., Roy, D. P., Yan, L., Huang, H., & Li, J. (2017). Landsat 15-m Panchromatic-Assisted Downscaling (LPAD) of the 30-m Reflective Wavelength Bands to Sentinel-2 20-m Resolution. *Remote Sensing*, *9*(7), Article 7. https://doi.org/10.3390/rs9070755

Ling, F., & Foody, G. M. (2019). Super-resolution land cover mapping by deep learning. *Remote Sensing Letters*, *10*(6), 598–606. https://doi.org/10.1080/2150704X.2019.1587196

Linkie, M., Dinata, Y., Nofrianto, A., & Leader-Williams, N. (2007). Patterns and perceptions of wildlife crop raiding in and around Kerinci Seblat National Park, Sumatra. *Animal Conservation*, *10*(1), 127–135. https://doi.org/10.1111/j.1469-1795.2006.00083.x

Liu, X. H., Kyriakidis, P. C., & Goodchild, M. F. (2008). Population-density estimation using regression and area-to-point residual kriging. *International Journal of Geographical Information Science*, *22*(4), 431–447. https://doi.org/10.1080/13658810701492225

Loarie, S. R., Aarde, R. J. V., & Pimm, S. L. (2009). Fences and artificial water affect African savannah elephant movement patterns. *Biological Conservation*, *142*(12), 3086–3098. https://doi.org/10.1016/j.biocon.2009.08.008

Ma, L., Liu, Y., Zhang, X., Ye, Y., Yin, G., & Johnson, B. A. (2019). Deep learning in remote sensing applications: A meta-analysis and review. *ISPRS Journal of Photogrammetry and Remote Sensing*, *152*, 166–177. https://doi.org/10.1016/j.isprsjprs.2019.04.015

Machwitz, M., Gessner, U., Conrad, C., Falk, U., Richters, J., & Dech, S. (2015). Modelling the Gross Primary Productivity of West Africa with the Regional Biomass Model RBM+, using optimized 250m MODIS FPAR and fractional vegetation cover information. *International Journal of Applied Earth Observation and Geoinformation*, *43*, 177–194. https://doi.org/10.1016/j.jag.2015.04.007

Madden, F. (2004). Creating Coexistence between Humans and Wildlife: Global Perspectives on Local Efforts to Address Human–Wildlife Conflict. *Human Dimensions of Wildlife*, *9*(4), 247–257. https://doi.org/10.1080/10871200490505675

Makuwerere Dube, L. (2021). Race, Entitlement, and Belonging: A Discursive Analysis of the Political Economy of Land in Zimbabwe. *Journal of Black Studies*, *52*(1), 24–49. https://doi.org/10.1177/0021934720946448

Malenovský, Z., Bartholomeus, H. M., Acerbi-Junior, F. W., Schopfer, J. T., Painter, T. H., Epema, G. F., & Bregt, A. K. (2007). Scaling dimensions in spectroscopy of soil and vegetation. *International Journal of Applied Earth Observation and Geoinformation*, *9*(2), 137–164. https://doi.org/10.1016/j.jag.2006.08.003

Mamombe, V., Kim, W., & Choi, Y.-S. (2017). Rainfall variability over Zimbabwe and its relation to large-scale atmosphere–ocean processes. *International Journal of Climatology*, *37*(2), 963–971. https://doi.org/10.1002/joc.4752

Manatsa, D., Mushore, T., Gwitira, I., Wuta, M., Chemura, A., Shekede, M., Mugandani, R., Sakala, L., Ali, L., Masukwedza, G., Mupuro, J., & Muzira, N. (2020). *Revision of Zimbabwe's Agro-Ecological Zones* (pp. 1–94). https://www.researchgate.net/publication/347966377_Report_on_Revised_Agroecological_Zones_of_Zimbabwe_in_press

Mapaure, I. N., & Campbell, B. M. (2002). Changes in miombo woodland cover in and around Sengwa Wildlife Research Area, Zimbabwe, in relation to elephants and fire. *African Journal of Ecology*, *40*(3), 212–219. https://doi.org/10.1046/j.1365-2028.2002.00355.x

Marx, A., & Kleinschmit, B. (2017). Sensitivity analysis of RapidEye spectral bands and derived vegetation indices for insect defoliation detection in pure Scots pine stands. *IForest - Biogeosciences and Forestry*, *10*(4), 659. https://doi.org/10.3832/ifor1727-010

Matabeleland North Correspondent. (2021, May 21). Zanu PF's Hwange DCC Member's Son Trampled to Death By Elephant. *New Zimbabwe*. https://www.newzimbabwe.com/zanu-pfs-hwange-dcc-members-son-trampled-to-death-by-elephant/

Matondi, P. B. (2012). *Zimbabwe's Fast Track Land Reform*. Bloomsbury Publishing. https://www.diva-portal.org/smash/get/diva2:563712/FULLTEXT01.pdf

Matsika, T. A., Masunga, G. S., Makati, A., McCulloch, G., Stronza, A., Songhurst, A. C., Adjetey, J. A., & Obopile, M. (2023). Crop diversity and susceptibility of crop fields to elephant raids in eastern Okavango Panhandle, northern Botswana. *Ecology and Evolution*, *13*(3), e9910. https://doi.org/10.1002/ece3.9910

Matton, N., Canto, G. S., Waldner, F., Valero, S., Morin, D., Inglada, J., Arias, M., Bontemps, S., Koetz, B., & Defourny, P. (2015). An Automated Method for Annual Cropland Mapping along the Season for Various Globally-Distributed Agrosystems Using High Spatial and Temporal Resolution Time Series. *Remote Sensing*, *7*(10), Article 10. https://doi.org/10.3390/rs71013208

Mazvimavi, D. (2010). Investigating changes over time of annual rainfall in Zimbabwe. *Hydrology and Earth System Sciences*, *14*(12), 2671–2679. https://doi.org/10.5194/hess-14-2671-2010

Mberego, S., & Gwenzi, J. (2014). Temporal patterns of precipitation and vegetation variability over Zimbabwe during extreme dry and wet rainfall seasons. *Journal of Applied Meteorology and Climatology*, *53*(12), 2790–2804.

McGarigal, K., Cushman, S. A., & Ene, E. (2023). *FRAGSTATS: Spatial Pattern Analysis Program for Categorical Maps* (Version 4). https://www.fragstats.org

McGarigal, K., Tagil, S., & Cushman, S. A. (2009). Surface metrics: An alternative to patch metrics for the quantification of landscape structure. *Landscape Ecology*, *24*(3), 433–450. https://doi.org/10.1007/s10980-009-9327-y

Meentemeyer, V. (1989). Geographical perspectives of space, time, and scale. *Landscape Ecology*, *3*(3), 163–173. https://doi.org/10.1007/BF00131535

Meentemeyer, V., & Box, E. O. (1987). Scale Effects in Landscape Studies. In M. G. Turner (Ed.), *Landscape Heterogeneity and Disturbance* (pp. 15–34). Springer. https://doi.org/10.1007/978-1-4612-4742-5_2

Mertz, O., Ravnborg, H. M., Lövei, G. L., Nielsen, I., & Konijnendijk, C. C. (2007). Ecosystem services and biodiversity in developing countries. *Biodiversity and Conservation*, *16*(10), 2729–2737. https://doi.org/10.1007/s10531-007-9216-0

Midgley, J. J., Coetzee, B. W. T., Tye, D., & Kruger, L. M. (2020). Mass sterilization of a common palm species by elephants in Kruger National Park, South Africa. *Scientific Reports*, *10*(1), Article 1. https://doi.org/10.1038/s41598-020-68679-8

Mkodzongi, G. (2013). New People, New Land and New Livelihoods: A Micro-study of Zimbabwe's Fast-track Land Reform. *Agrarian South: Journal of Political Economy*, *2*(3), 345–366. https://doi.org/10.1177/2277976013517320

Mlambo, L., Shekede, M. D., Adam, E., Odindi, J., & Murwira, A. (2021). Home range and space use by African elephants (Loxodonta africana) in Hwange National Park, Zimbabwe. *African Journal of Ecology*, *59*(4), 842–853. https://doi.org/10.1111/aje.12890

Moody, A., & Woodcock, C. E. (1995). The influence of scale and the spatial characteristics of landscapes on land-cover mapping using remote sensing. *Landscape Ecology*, *10*(6), 363–379. https://doi.org/10.1007/BF00130213

Moss, C. J., & Poole, J. H. (1983). Relationships and social structure of African elephants. In R. A. Hinde (Ed.), *Primate social relations: An integrated approach* (pp. 315–325). Blackwell Scientific Publications.

Motohka, T., Nasahara, K. N., Oguma, H., & Tsuchida, S. (2010). Applicability of Green-Red Vegetation Index for Remote Sensing of Vegetation Phenology. *Remote Sensing*, *2*(10), Article 10. https://doi.org/10.3390/rs2102369

Moyo, S. (2000). The Political Economy of Land Acquisition and Redistribution in Zimbabwe, 1990-1999. *Journal of Southern African Studies*, *26*(1), 5–28. https://doi.org/10.1080/030570700108351

Moyo, S. (2011). Changing agrarian relations after redistributive land reform in Zimbabwe. *The Journal of Peasant Studies*, *38*(5), 939–966. https://doi.org/10.1080/03066150.2011.634971

Muad, A. M., & Foody, G. M. (2012). Super-resolution mapping of lakes from imagery with a coarse spatial and fine temporal resolution. *International Journal of Applied Earth Observation and Geoinformation*, *15*, 79–91. https://doi.org/10.1016/j.jag.2011.06.002

Mudimu, G. T., Zuo, T., Shah, A. A., Nalwimba, N., & Ado, A. M. (2020). Land leasing in a post-land reform context: Insights from Zimbabwe. *GeoJournal*. https://doi.org/10.1007/s10708-020-10219-y

Murisa, T. (2010). *Social Development in Zimbabwe* (p. 25) [Discussion Paper prepared for the Development Foundation for Zimbabwe]. https://www.dfzim.com/wp-content/downloads/Social_Development_in_Zimbabwe_by_Dr_T_Murisa.pdf

Murwendo, T., Murwira, A., & Masocha, M. (2021). Vegetation phenology dynamics as an indicator of energy and productivity functions in semi-arid savannah protected areas: A case study of Gonarezhou National Park in south-eastern Zimbabwe. *Transactions of the Royal Society of South Africa*, *76*(3), 291–299. https://doi.org/10.1080/0035919X.2021.1934184

Musakwa, W., & Wang, S. (2018). Landscape change and its drivers: A Southern African perspective. *Current Opinion in Environmental Sustainability*, *33*, 80–86. https://doi.org/10.1016/j.cosust.2018.05.001

Mushonga, T., & Matose, F. (2020). Dimensions and corollaries of violence in Zimbabwe's protected forests. *Geoforum*, *117*, 216–224. https://doi.org/10.1016/j.geoforum.2020.10.005

Mutekwa, V. T., & Gambiza, J. (2016). Assessment of governance principles application in forest protected areas: The case of six state forests in western Zimbabwe. *International Forestry Review*, *18*(4), 466–484. https://doi.org/10.1505/146554816820127613

Mwamidi, D., Mwasi, S. M., & Nunow, A. (2012). THE USE OF INDIGENOUS KNOWLEDGE IN MINIMIZING HUMAN-WILDLIFE CONFLICT: THE CASE OF TAITA COMMUNITY, KENYA. *International Journal of Current Research*, *4*, 26.

Myneni, R. B., Hall, F. G., Sellers, P. J., & Marshak, A. L. (1995). The interpretation of spectral vegetation indexes. *IEEE Transactions on Geoscience and Remote Sensing*, *33*(2), 481–486. https://doi.org/10.1109/TGRS.1995.8746029

Na, X., Zhang, S., Li, X., Yu, H., & Liu, C. (2010). Improved Land Cover Mapping using Random Forests Combined with Landsat Thematic Mapper Imagery and Ancillary Geographic Data. *Photogrammetric Engineering & Remote Sensing*, *76*(7), 833–840. https://doi.org/10.14358/PERS.76.7.833

Naha, D., Sathyakumar, S., Dash, S., Chettri, A., & Rawat, G. S. (2019). Assessment and prediction of spatial patterns of human-elephant conflicts in changing land cover scenarios of a human-dominated landscape in North Bengal. *PLOS ONE*, *14*(2), e0210580. https://doi.org/10.1371/journal.pone.0210580

Naughton-Treves, L. (1998). Predicting Patterns of Crop Damage by Wildlife around Kibale National Park, Uganda. *Conservation Biology*, *12*(1), 156–168. https://doi.org/10.1111/j.1523-1739.1998.96346.x

Naughton-Treves, L., & Treves, A. (2005). Socio-ecological factors shaping local support for wildlife: Crop-raiding by elephants and other wildlife in Africa. In R. Woodroffe, S. Thirgood, & A. Rabinowitz (Eds.), *People and Wildlife, Conflict Or Co-existence?* (pp. 252–277). Cambridge University Press.

Ncube, H. (2019). A call to embrace adaptive management for effective elephant conservation in Zimbabwe. *South African Journal of Science*, *115*(3–4), 1–3. https://doi.org/10.17159/sajs.2019/5413

Ndlovu, M., Devereux, E., Chieffe, M., Asklof, K., & Russo, A. (2016). Responses of African elephants towards a bee threat: Its application in mitigating human-elephant conflict. *South African Journal of Science*, *112*(1–2), 01–05. https://doi.org/10.17159/sajs.2016/20150058

Nencini, F., Garzelli, A., Baronti, S., & Alparone, L. (2007). Remote sensing image fusion using the curvelet transform. *Information Fusion*, *8*(2), 143–156. https://doi.org/10.1016/j.inffus.2006.02.001

Newbold, T., Hudson, L. N., Hill, S. L. L., Contu, S., Lysenko, I., Senior, R. A., Börger, L., Bennett, D. J., Choimes, A., Collen, B., Day, J., De Palma, A., Díaz, S., Echeverria-Londoño, S., Edgar, M. J., Feldman, A., Garon, M., Harrison, M. L. K., Alhusseini, T., … Purvis, A. (2015). Global effects of land use on local terrestrial biodiversity. *Nature*, *520*(7545), 45–50. https://doi.org/10.1038/nature14324

Nigussie, D., Zurita-Milla, R., & Clevers, J. G. P. W. (2011). Possibilities and limitations of artificial neural networks for subpixel mapping of land cover. *International Journal of Remote Sensing*, *32*(22), 7203–7226. https://doi.org/10.1080/01431161.2010.519740

Ntukey, L. T., Munishi, L. K., Kohi, E., & Treydte, A. C. (2022). Land Use/Cover Change Reduces Elephant Habitat Suitability in the Wami Mbiki–Saadani Wildlife Corridor, Tanzania. *Land*, *11*(2), Article 2. https://doi.org/10.3390/land11020307

O'Connell-Rodwell, C. E., Rodwell, T., Rice, M., & Hart, L. A. (2000). Living with the modern conservation paradigm: Can agricultural communities co-exist with elephants? A five-year case study in East Caprivi, Namibia. *Biological Conservation*, *93*(3), 381–391. https://doi.org/10.1016/S0006-3207(99)00108-1

Ollinger, S. V. (2011). Sources of variability in canopy reflectance and the convergent properties of plants. *New Phytologist*, *189*(2), 375–394. https://doi.org/10.1111/j.1469-8137.2010.03536.x

Omeja, P. A., Jacob, A. L., Lawes, M. J., Lwanga, J. S., Rothman, J. M., Tumwesigye, C., & Chapman, C. A. (2014). Changes in Elephant Abundance Affect Forest Composition or Regeneration? *Biotropica*, *46*(6), 704–711. https://doi.org/10.1111/btp.12154

Oppong, S., Danquah, E., & Sam, M. (2008). An update on crop-raiding by elephants at Bia Conservation Area, Ghana from 2004 to 2006. *Pachyderm*, *44*, 59–64. https://pachydermjournal.org/index.php/pachyderm/article/view/148

Osborn, F. V. (2002). Capsicum Oleoresin as an Elephant Repellent: Field Trials in the Communal Lands of Zimbabwe. *The Journal of Wildlife Management*, *66*(3), 674–677. https://doi.org/10.2307/3803133

Osborn, F. V. (2004). Seasonal variation of feeding patterns and food selection by crop-raiding elephants in Zimbabwe. *African Journal of Ecology*, *42*(4), 322–327.

Osborn, F. V. (2010). Mitigating measures to reduce human-elephant conflict: What do we know? In L. Braack & R. Smuts (Eds.), *Towards Rationalizing Transboundary Elephant Management and Human Needs in the Kavango/mid-Zambezi Region*. Centre for Biodiversity Conservation, Kirstenbosch Botanical Gardens,.

Owen-Smith, R. N. (1988). *Megaherbivores: The influence of very large body size on ecology*. Cambridge University Press.

Pandit, V. R., & Bhiwani, R. J. (2021). Morphology-based spatial filtering for efficiency enhancement of remote sensing image fusion. *Computers & Electrical Engineering*, *89*, 106945. https://doi.org/10.1016/j.compeleceng.2020.106945

Pardo-Igúzquiza, E., Chica-Olmo, M., & Atkinson, P. M. (2006). Downscaling cokriging for image sharpening. *Remote Sensing of Environment*, *102*(1–2), 86–98.

Pardo-Iguzquiza, E., Rodríguez-Galiano, V. F., Chica-Olmo, M., & Atkinson, P. M. (2011). Image fusion by spatially adaptive filtering using downscaling cokriging. *ISPRS Journal of Photogrammetry and Remote Sensing*, *66*(3), 337–346.

Parker, G. E., & Osborn, F. V. (2001). Dual-season crop damage by elephants in eastern Zambezi Valley, Zimbabwe. *Pachyderm*, *30*, 49–56.

Parker, G. E., Osborn, F. V., Hoarse, R. E., & Niskanen, L. S. (2007). *Human-elephant conflict mitigation: A training course for community-based approaches in Africa* [Training Manual].

Pelgrum, H. (2000). *Spatial aggregation of land surface characteristics: Impact of resolution of remote sensing data on land surface modelling* (p.) [Phd]. https://library.wur.nl/WebQuery/wurpubs/65791

Peng, J., Loew, A., Merlin, O., & Verhoest, N. E. C. (2017). A review of spatial downscaling of satellite remotely sensed soil moisture. *Reviews of Geophysics*, *55*(2), 341–366. https://doi.org/10.1002/2016RG000543

Phan, T. N., Kuch, V., & Lehnert, L. W. (2020). Land Cover Classification using Google Earth Engine and Random Forest Classifier—The Role of Image Composition. *Remote Sensing*, *12*(15), Article 15. https://doi.org/10.3390/rs12152411

Platts, P. J., Mason, S. C., Palmer, G., Hill, J. K., Oliver, T. H., Powney, G. D., Fox, R., & Thomas, C. D. (2019). Habitat availability explains variation in climate-driven range shifts across multiple taxonomic groups. *Scientific Reports*, *9*(1), 15039. https://doi.org/10.1038/s41598-019-51582-2

Plumptre, A. j. (1994). The effects of trampling damage by herbivores on the vegetation of the Pare National des Volcans, Rwanda. *African Journal of Ecology*, *32*(2), 115–129. https://doi.org/10.1111/j.1365-2028.1994.tb00563.x

Poggio, L., Gimona, A., & Brewer, M. J. (2013). Regional scale mapping of soil properties and their uncertainty with a large number of satellite-derived covariates. *Geoderma*, *209–210*, 1–14. https://doi.org/10.1016/j.geoderma.2013.05.029

Polansky, L., Kilian, W., & Wittemyer, G. (2015). Elucidating the significance of spatial memory on movement decisions by African savannah elephants using state–space models. *Proceedings of the Royal Society B: Biological Sciences*, *282*(1805), 20143042. https://doi.org/10.1098/rspb.2014.3042

Posit team. (2023). *RStudio: Integrated Development Environment for R.* Posit Software, PBC. http://www.posit.co/

Powers, R. P., & Jetz, W. (2019). Global habitat loss and extinction risk of terrestrial vertebrates under future land-use-change scenarios. *Nature Climate Change*, *9*(4), Article 4. https://doi.org/10.1038/s41558-019-0406-z

Pozo, R. A., Coulson, T., McCulloch, G., Stronza, A. L., & Songhurst, A. C. (2017). Determining baselines for human-elephant conflict: A matter of time. *PLOS ONE*, *12*(6), e0178840. https://doi.org/10.1371/journal.pone.0178840

Pozo, R. A., Cusack, J. J., McCulloch, G., Stronza, A., Songhurst, A., & Coulson, T. (2018). Elephant space-use is not a good predictor of crop-damage. *Biological Conservation*, *228*, 241–251. https://doi.org/10.1016/j.biocon.2018.10.031

Presotto, A., Fayrer-Hosken, R., Curry, C., & Madden, M. (2019). Spatial mapping shows that some African elephants use cognitive maps to navigate the core but not the periphery of their home ranges. *Animal Cognition*, *22*(2), 251–263. https://doi.org/10.1007/s10071-019-01242-9

Prestele, R., Alexander, P., Rounsevell, M. D. A., Arneth, A., Calvin, K., Doelman, J., Eitelberg, D. A., Engström, K., Fujimori, S., Hasegawa, T., Havlik, P., Humpenöder, F., Jain, A. K., Krisztin, T., Kyle, P., Meiyappan, P., Popp, A., Sands, R. D., Schaldach, R., … Verburg, P. H. (2016). Hotspots of uncertainty in land-use and land-cover change projections: A global-scale model comparison. *Global Change Biology*, *22*(12), 3967–3983. https://doi.org/10.1111/gcb.13337

Raj, R., Hamm, N. A. S., & Kant, Y. (2013). Analysing the effect of different aggregation approaches on remotely sensed data. *International Journal of Remote Sensing*, *34*(14), 4900–4916. https://doi.org/10.1080/01431161.2013.781289

Ranchin, T., Aiazzi, B., Alparone, L., Baronti, S., & Wald, L. (2003). Image fusion—The ARSIS concept and some successful implementation schemes. *ISPRS Journal of Photogrammetry and Remote Sensing*, *58*(1), 4–18. https://doi.org/10.1016/S0924-2716(03)00013-3

Reiner, F., Brandt, M., Tong, X., Skole, D., Kariryaa, A., Ciais, P., Davies, A., Hiernaux, P., Chave, J., Mugabowindekwe, M., Igel, C., Oehmcke, S., Gieseke, F., Li, S., Liu, S., Saatchi, S., Boucher, P., Singh, J., Taugourdeau, S., … Fensholt, R. (2023). More than one quarter of Africa's tree cover is found outside areas previously classified as forest. *Nature Communications*, *14*(1), Article 1. https://doi.org/10.1038/s41467-023-37880-4

Revill, A., Florence, A., MacArthur, A., Hoad, S., Rees, R., & Williams, M. (2020). Quantifying Uncertainty and Bridging the Scaling Gap in the Retrieval of Leaf Area Index by Coupling Sentinel-2 and UAV Observations. *Remote Sensing*, *12*(11), Article 11. https://doi.org/10.3390/rs12111843

Richardson, C. J. (2005). The Loss of Property Rights and the Collapse of Zimbabwe. *Cato Journal, 25*, 541. https://heinonline.org/HOL/Page?handle=hein.journals/catoj25&id=549&div=&collection=

Riitters, K. H., O'Neill, R. V., & Jones, K. B. (1997). Assessing habitat suitability at multiple scales: A landscape-level approach. *Biological Conservation*, *81*(1–2), 191–202.

Rodriguez-Galiano, V. F., & Chica-Rivas, M. (2014). Evaluation of different machine learning methods for land cover mapping of a Mediterranean area using multi-seasonal Landsat images and Digital Terrain Models. *International Journal of Digital Earth*, *7*(6), 492–509. https://doi.org/10.1080/17538947.2012.748848

Rose, R. A., Byler, D., Eastman, J. R., Fleishman, E., Geller, G., Goetz, S., Guild, L., Hamilton, H., Hansen, M., & Headley, R. (2015). Ten ways remote sensing can contribute to conservation. *Conservation Biology*, *29*(2), 350–359.

Rosenqvist, A., Shimada, M., Ito, N., & Watanabe, M. (2007). ALOS PALSAR: A Pathfinder Mission for Global-Scale Monitoring of the Environment. *IEEE Transactions on Geoscience and Remote Sensing*, *45*(11), 3307–3316. https://doi.org/10.1109/TGRS.2007.901027

Rouse, J. W., Haas, R. H., Schell, J. A., & Deering, D. W. (1974). Monitoring vegetation systems in the Great Plains with ERTS. *NASA Spec. Publ*, *351*(1), 309.

Ruggiero, R. G. (1992). Seasonal forage utilization by elephants in central Africa. *African Journal of Ecology*, *30*(2), 137–148. https://doi.org/10.1111/j.1365-2028.1992.tb00487.x

Sachikonye, L. M. (2003). From 'Growth with Equity' to 'Fast-Track' Reform: Zimbabwe's Land Question. *Review of African Political Economy*, *30*(96), 227–240. https://doi.org/10.1080/03056244.2003.9693496

Sala, O. E., Stuart Chapin, F., III, Armesto, J. J., Berlow, E., Bloomfield, J., Dirzo, R., Huber-Sanwald, E., Huenneke, L. F., Jackson, R. B., Kinzig, A., Leemans, R., Lodge, D. M., Mooney, H. A., Oesterheld, M., Poff, N. L., Sykes, M. T., Walker, B. H., Walker, M., & Wall, D. H. (2000). Global Biodiversity Scenarios for the Year 2100. *Science*, *287*(5459), 1770–1774. https://doi.org/10.1126/science.287.5459.1770

Sanare, J. E., Valli, D., Leweri, C., Glatzer, G., Fishlock, V., & Treydte, A. C. (2022). A Socio-Ecological Approach to Understanding How Land Use Challenges Human-Elephant Coexistence in Northern Tanzania. *Diversity*, *14*(7), Article 7. https://doi.org/10.3390/d14070513

Saura, S. (2004). Effects of remote sensor spatial resolution and data aggregation on selected fragmentation indices. *Landscape Ecology*, *19*(2), 197–209. https://doi.org/10.1023/B:LAND.0000021724.60785.65

Saura, S., & Castro, S. (2007). Scaling functions for landscape pattern metrics derived from remotely sensed data: Are their subpixel estimates really accurate? *ISPRS Journal of Photogrammetry and Remote Sensing*, *62*(3), 201–216. https://doi.org/10.1016/j.isprsjprs.2007.03.004

Scharsich, V., Mtata, K., Hauhs, M., Lange, H., & Bogner, C. (2017). Analysing land cover and land use change in the Matobo National Park and surroundings in Zimbabwe. *Remote Sensing of Environment*, *194*, 278–286. https://doi.org/10.1016/j.rse.2017.03.037

Schipper, E. L. F., Ensor, J., Mukherji, A., Mirzabaev, A., Fraser, A., Harvey, B., Totin, E., Garschagen, M., Pathak, M., Antwi-Agyei, P., Tanner, T., & Shawoo, Z. (2021). Equity in climate

scholarship: A manifesto for action. *Climate and Development*, *13*(10), 853–856. https://doi.org/10.1080/17565529.2021.1923308

Schlossberg, S., Chase, M. J., & Sutcliffe, R. (2019). Evidence of a Growing Elephant Poaching Problem in Botswana. *Current Biology*, *29*(13), 2222-2228.e4. https://doi.org/10.1016/j.cub.2019.05.061

Schneider, D. (2009). *Quantitative Ecology: Measurements, Models and Scaling* (2nd ed.). Academic Press.

Seo, S., Choi, J.-S., Lee, J., Kim, H.-H., Seo, D., Jeong, J., & Kim, M. (2020). UPSNet: Unsupervised Pan-Sharpening Network With Registration Learning Between Panchromatic and Multi-Spectral Images. *IEEE Access*, *8*, 201199–201217. https://doi.org/10.1109/ACCESS.2020.3035802

Shaban, M. A., & Dikshit, O. (2001). Improvement of classification in urban areas by the use of textural features: The case study of Lucknow city, Uttar Pradesh. *International Journal of Remote Sensing*, *22*(4), 565–593. https://doi.org/10.1080/01431160050505865

Shah, V. P., Younan, N. H., & King, R. L. (2008). An Efficient Pan-Sharpening Method via a Combined Adaptive PCA Approach and Contourlets. *IEEE Transactions on Geoscience and Remote Sensing*, *46*(5), 1323–1335. https://doi.org/10.1109/TGRS.2008.916211

Shannon, G., Page, B. R., Mackey, R. L., Duffy, K. J., & Slotow, R. (2008). Activity Budgets and Sexual Segregation in African Elephants (Loxodonta africana). *Journal of Mammalogy*, *89*(2), 467–476. https://doi.org/10.1644/07-MAMM-A-132R.1

Sharifi, E., Saghafian, B., & Steinacker, R. (2019). Downscaling Satellite Precipitation Estimates With Multiple Linear Regression, Artificial Neural Networks, and Spline Interpolation Techniques. *Joumal of Geophysical Research: Atmospheres*, *124*(2), 789–805. https://doi.org/10.1029/2018JD028795

Shimada, M., Itoh, T., Motooka, T., Watanabe, M., Shiraishi, T., Thapa, R., & Lucas, R. (2014). New global forest/non-forest maps from ALOS PALSAR data (2007–2010). *Remote Sensing of Environment*, *155*, 13–31. https://doi.org/10.1016/j.rse.2014.04.014

Shoko, C., Dube, T., Sibanda, M., & Bangamwabo, V. (2016). Quantifying the spatial and temporal changes in forested landcover using landscape metrics derived from remotely sensed data in rural parts of Zimbabwe. *Transactions of the Royal Society of South Africa*, *71*(1), 105–113. https://doi.org/10.1080/0035919X.2015.1121934

Sibanda, M., Dube, T., Mubango, T., & Shoko, C. (2016). The utility of earth observation technologies in understanding impacts of land reform in the eastern region of Zimbabwe. *Journal of Land Use Science*, *11*(4), 384–400. https://doi.org/10.1080/1747423X.2015.1130756

Sillero, N., & Barbosa, A. M. (2021). Common mistakes in ecological niche models. *International Journal of Geographical Information Science*, *35*(2), 213–226. https://doi.org/10.1080/13658816.2020.1798968

Sitati, N. W., Walpole, M. J., & Leader-Williams, N. (2005). Factors affecting susceptibility of farms to crop raiding by African elephants: Using a predictive model to mitigate conflict. *Journal of Applied Ecology*, *42*(6), 1175–1182. https://doi.org/10.1111/j.1365-2664.2005.01091.x

Soares, J. V., Rennó, C. D., Formaggio, A. R., da Costa Freitas Yanasse, C., & Frery, A. C. (1997). An investigation of the selection of texture features for crop discrimination using SAR imagery. *Remote Sensing of Environment*, *59*(2), 234–247. https://doi.org/10.1016/S0034-4257(96)00156-3

Song, H., Liu, Q., Wang, G., Hang, R., & Huang, B. (2018). Spatiotemporal Satellite Image Fusion Using Deep Convolutional Neural Networks. *IEEE Journal of Selected Topics in Applied Earth Observations and Remote Sensing*, *11*(3), 821–829. https://doi.org/10.1109/JSTARS.2018.2797894

Songhurst, A., & Coulson, T. (2014). Exploring the effects of spatial autocorrelation when identifying key drivers of wildlife crop-raiding. *Ecology and Evolution*, *4*(5), 582–593. https://doi.org/10.1002/ece3.837

Su, Y.-F. (2019). Integrating a scale-invariant feature of fractal geometry into the Hopfield neural network for super-resolution mapping. *International Journal of Remote Sensing*, *40*(23), 8933–8954. https://doi.org/10.1080/01431161.2019.1624865

Swetnam, R. D., & Reyers, B. (2011). Meeting the challenge of conserving Africa's biodiversity: The role of GIS, now and in the future. *Landscape and Urban Planning*, *100*(4), 411–414. https://doi.org/10.1016/j.landurbplan.2011.02.002

Tan, K.-C. (2021). Just conservation: The question of justice in global wildlife conservation. *Philosophy Compass*, *16*(2), e12720. https://doi.org/10.1111/phc3.12720

Tanyanyiwa, V. I., & Madobi, R. (2021). Challenges to the Effective Teaching and Learning of Geography through ODeL at the Zimbabwe Open University. *Journal of Learning for Development*, *8*(2), Article 2. https://doi.org/10.56059/jl4d.v8i2.427

Tfwala, S. S., & Wang, Y.-M. (2016). Estimating Sediment Discharge Using Sediment Rating Curves and Artificial Neural Networks in the Shiwen River, Taiwan. *Water*, *8*(2), Article 2. https://doi.org/10.3390/w8020053

Thant, Z. M., May, R., & Røskaft, E. (2021). Pattern and distribution of human-elephant conflicts in three conflict-prone landscapes in Myanmar. *Global Ecology and Conservation*, *25*, e01411.

Thapa, S., Garcia Millan, V. E., & Eklundh, L. (2021). Assessing Forest Phenology: A Multi-Scale Comparison of Near-Surface (UAV, Spectral Reflectance Sensor, PhenoCam) and Satellite (MODIS, Sentinel-2) Remote Sensing. *Remote Sensing*, *13*(8), Article 8. https://doi.org/10.3390/rs13081597

Theobald, D. M., Harrison-Atlas, D., Monahan, W. B., & Albano, C. M. (2015). Ecologically-Relevant Maps of Landforms and Physiographic Diversity for Climate Adaptation Planning. *PLOS ONE*, *10*(12), e0143619. https://doi.org/10.1371/journal.pone.0143619

Thouless, C., Dublin, H. T., Blanc, J., Skinner, D., Daniel, T., Taylor, R., Maisels, F., Frederick, H., & Bouché, P. (2016). African elephant status report 2016. *An Update from the African Elephant Database*.

Tian, Y., Wang, Y., Zhang, Y., Knyazikhin, Y., Bogaert, J., & Myneni, R. B. (2003). Radiative transfer based scaling of LAI retrievals from reflectance data of different resolutions. *Remote Sensing of Environment*, *84*(1), 143–159. https://doi.org/10.1016/S0034-4257(02)00102-5

Tiller, L. N., Humle, T., Amin, R., Deere, N. J., Lago, B. O., Leader-Williams, N., Sinoni, F. K., Sitati, N., Walpole, M., & Smith, R. J. (2021). Changing seasonal, temporal and spatial crop-raiding trends over 15 years in a human-elephant conflict hotspot. *Biological Conservation*, *254*, 108941. https://doi.org/10.1016/j.biocon.2020.108941

Timberlake, J. R., Nobanda, N., & Mapaure, I. (1993). Vegetation survey of the communal lands, North and West Zimbabwe. *Kirkia*, *14*(2), 171–270. https://www.jstor.org/stable/44657292

Townsend, P. A., Lookingbill, T. R., Kingdon, C. C., & Gardner, R. H. (2009). Spatial pattern analysis for monitoring protected areas. *Remote Sensing of Environment*, *113*(7), 1410–1420. https://doi.org/10.1016/j.rse.2008.05.023

Treves, A. (2008). Human–wildlife conflicts around protected areas. In M. J. Manfredo, J. J. Vaske, P. J. Brown, D. J. Decker, & E. A. Duke, *Wildlife and society: The science of human dimensions* (pp. 214–228). Island Press.

Tsalyuk, M., Kilian, W., Reineking, B., & Getz, W. M. (2019). Temporal variation in resource selection of African elephants follows long-term variability in resource availability. *Ecological Monographs*, *89*(2), e01348. https://doi.org/10.1002/ecm.1348

Tshipa, A., Valls-Fox, H., Fritz, H., Collins, K., Sebele, L., Mundy, P., & Chamaillé-Jammes, S. (2017). Partial migration links local surface-water management to large-scale elephant conservation in the world's largest transfrontier conservation area. *Biological Conservation*, *215*, 46–50. https://doi.org/10.1016/j.biocon.2017.09.003

Tucker, C. J. (1979). Red and photographic infrared linear combinations for monitoring vegetation. *Remote Sensing of Environment*, *8*(2), 127–150. https://doi.org/10.1016/0034-4257(79)90013-0

Turner, M. G. (Ed.). (1987). *Landscape Heterogeneity and Disturbance* (Vol. 64). Springer Verlag, Inc.

Turner, M. G. (1989). Landscape Ecology: The Effect of Pattern on Process. *Annual Review of Ecology and Systematics*, *20*(1), 171–197. https://doi.org/10.1146/annurev.es.20.110189.001131

Turner, M. G., Dale, V. H., & Gardner, R. H. (1989). Predicting across scales: Theory development and testing. *Landscape Ecology*, *3*(3), 245–252.

Turner, M. G., O'Neill, R. V., Gardner, R. H., & Milne, B. T. (1989). Effects of changing spatial scale on the analysis of landscape pattern. *Landscape Ecology*, *3*(3), 153–162. https://doi.org/10.1007/BF00131534

Turner, W., Rondinini, C., Pettorelli, N., Mora, B., Leidner, A. K., Szantoi, Z., Buchanan, G., Dech, S., Dwyer, J., Herold, M., Koh, L. P., Leimgruber, P., Taubenboeck, H., Wegmann, M., Wikelski, M., & Woodcock, C. (2015). Free and open-access satellite data are key to biodiversity conservation. *Biological Conservation*, *182*, 173–176. https://doi.org/10.1016/j.biocon.2014.11.048

Urbazaev, M., Thiel, C., Mathieu, R., Naidoo, L., Levick, S. R., Smit, I. P. J., Asner, G. P., & Schmullius, C. (2015). Assessment of the mapping of fractional woody cover in southern African savannas using multi-temporal and polarimetric ALOS PALSAR L-band images. *Remote Sensing of Environment*, *166*, 138–153. https://doi.org/10.1016/j.rse.2015.06.013

Useya, J., Chen, S., & Murefu, M. (2019). Cropland Mapping and Change Detection: Toward Zimbabwean Cropland Inventory. *IEEE Access*, *7*, 53603–53620. https://doi.org/10.1109/ACCESS.2019.2912807

Valeix, M., Fritz, H., Sabatier, R., Murindagomo, F., Cumming, D., & Duncan, P. (2011). Elephant-induced structural changes in the vegetation and habitat selection by large herbivores in an African savanna. *Biological Conservation*, *144*(2), 902–912. https://doi.org/10.1016/j.biocon.2010.10.029

Van Wyk, P. (2013). *Trees of Southern Africa*. Struik Nature.

Vapnik, V. (1999). *The Nature of Statistical Learning Theory*. Springer Science & Business Media. https://books.google.com/books/about/The_Nature_of_Statistical_Learning_Theor.html?id=sna9BaxVbj8C

Vincent, V., & Thomas, R. G. (1960). *An agroecological Survey of Southern Rhodesia Part 1: Agro-ecological Survey*. Government Publisher.

Vogel, S. M., Lambert, B., Songhurst, A. C., McCulloch, G. P., Stronza, A. L., & Coulson, T. (2020). Exploring movement decisions: Can Bayesian movement-state models explain crop consumption behaviour in elephants (Loxodonta africana)? *Journal of Animal Ecology*, *89*(4), 1055–1068. https://doi.org/10.1111/1365-2656.13177

Wang, X., Blanchet, F. G., & Koper, N. (2014). Measuring habitat fragmentation: An evaluation of landscape pattern metrics. *Methods in Ecology and Evolution*, *5*(7), 634–646. https://doi.org/10.1111/2041-210X.12198

Wang, Y., Xie, D., Liu, S., Hu, R., Li, Y., & Yan, G. (2016). Scaling of FAPAR from the Field to the Satellite. *Remote Sensing*, *8*(4), 310. https://doi.org/10.3390/rs8040310

Waters, C. N., Zalasiewicz, J., Summerhayes, C., Barnosky, A. D., Poirier, C., Gałuszka, A., Cearreta, A., Edgeworth, M., Ellis, E. C., Ellis, M., Jeandel, C., Leinfelder, R., McNeill, J. R., Richter, D. deB, Steffen, W., Syvitski, J., Vidas, D., Wagreich, M., Williams, M., … Wolfe, A. P. (2016). The Anthropocene is functionally and stratigraphically distinct from the Holocene. *Science*, *351*(6269). https://doi.org/10.1126/science.aad2622

Welch, G., & Bishop, G. (1997). *An Introduction to the Kalman Filter*.

Welch, R., Madden, M., & Doren, R. (1999). Mapping the Everglades. *Photogrammetric Engineering and Remote Sensing*, *65*, 163–170.

Wellmann, T., Lausch, A., Andersson, E., Knapp, S., Cortinovis, C., Jache, J., Scheuer, S., Kremer, P., Mascarenhas, A., Kraemer, R., Haase, A., Schug, F., & Haase, D. (2020). Remote sensing in urban planning: Contributions towards ecologically sound policies? *Landscape and Urban Planning*, *204*, 103921. https://doi.org/10.1016/j.landurbplan.2020.103921

Western, D., & Mose, V. (2023). Cascading effects of elephant–human interactions and the role of space and mobility in sustaining biodiversity -. *Ecosphere*, *14*(5). https://doi.org/10.1002/ecs2.4512

White, E. V., & Roy, D. P. (2015). A contemporary decennial examination of changing agricultural field sizes using Landsat time series data. *Geo: Geography and Environment*, *2*(1), 33–54. https://doi.org/10.1002/geo2.4

Wiens, J. A. (1989). Spatial Scaling in Ecology. *Functional Ecology*, *3*(4), 385–397. https://doi.org/10.2307/2389612

Wiens, J., Sutter, R., Anderson, M., Blanchard, J., Barnett, A., Aguilar-Amuchastegui, N., Avery, C., & Laine, S. (2009). Selecting and conserving lands for biodiversity: The role of remote sensing. *Remote Sensing of Environment*, *113*(7), 1370–1381. https://doi.org/10.1016/j.rse.2008.06.020

Williamson, B. R. (1983). *The condition and nutrition of elephant in Wankie National Park*. National Museums and Monuments of Rhodesia.

Worldwide broadband speed league 2022. (2022). [Data set]. https://doi.org/h

Wu, H., & Li, Z.-L. (2009). Scale Issues in Remote Sensing: A Review on Analysis, Processing and Modeling. *Sensors*, *9*(3), Article 3. https://doi.org/10.3390/s90301768

Wu, J. (2004). Effects of changing scale on landscape pattern analysis: Scaling relations. *Landscape Ecology*, *19*(2), 125–138. https://doi.org/10.1023/B:LAND.0000021711.40074.ae

Wu, J. (2007). Scale and scaling: A cross-disciplinary perspective. In *Key Topics in Landscape Ecology* (pp. 115–142). Cambridge University Press. https://asu.pure.elsevier.com/en/publications/scale-and-scaling-a-cross-disciplinary-perspective

Wu, J. (2013). Key concepts and research topics in landscape ecology revisited: 30 years after the Allerton Park workshop. *Landscape Ecology*, *28*(1), 1–11. https://doi.org/10.1007/s10980-012-9836-y

Wu, J., & Hobbs, R. (2002). Key issues and research priorities in landscape ecology: An idiosyncratic synthesis. *Landscape Ecology*, *17*(4), 355–365. https://doi.org/10.1023/A:1020561630963

Wu, J., Shen, W., Sun, W., & Tueller, P. T. (2002). Empirical patterns of the effects of changing scale on landscape metrics. *Landscape Ecology*, *17*(8), 761–782. https://doi.org/10.1023/A:1022995922992

Wu, L., Liu, X., Zheng, X., Qin, Q., Ren, H., & Sun, Y. (2015). Spatial scaling transformation modeling based on fractal theory for the leaf area index retrieved from remote sensing imagery. *Journal of Applied Remote Sensing*, *9*(1), 096015. https://doi.org/10.1117/1.JRS.9.096015

Wyatt, J. R., & Eltringham, S. K. (1974). The daily activity of the elephant in the Rwenzori National Park, Uganda. *African Journal of Ecology*, *12*(4), 273–289. https://doi.org/10.1111/j.1365-2028.1974.tb01037.x

Xu, C., Zhao, S., & Liu, S. (2020). Spatial scaling of multiple landscape features in the conterminous United States. *Landscape Ecology*, *35*(1), 223–247. https://doi.org/10.1007/s10980-019-00937-1

Yang, C., Zhan, Q., Lv, Y., & Liu, H. (2019). Downscaling Land Surface Temperature Using Multiscale Geographically Weighted Regression Over Heterogeneous Landscapes in Wuhan, China. *IEEE Journal of Selected Topics in Applied Earth Observations and Remote Sensing*, *12*(12), 5213–5222. https://doi.org/10.1109/JSTARS.2019.2955551

Yang, J., Fu, X., Hu, Y., Huang, Y., Ding, X., & Paisley, J. (2017). PanNet: A Deep Network Architecture for Pan-Sharpening. *2017 IEEE International Conference on Computer Vision (ICCV)*, 1753–1761. https://doi.org/10.1109/ICCV.2017.193

Yoo, E.-H., & Kyriakidis, P. C. (2006). Area-to-point kriging with inequality-type data. *Journal of Geographical Systems*, *8*(4), 357–390.

Young, J. C., Marzano, M., White, R. M., McCracken, D. I., Redpath, S. M., Carss, D. N., Quine, C. P., & Watt, A. D. (2010). The emergence of biodiversity conflicts from biodiversity impacts: Characteristics and management strategies. *Biodiversity and Conservation*, *19*(14), 3973–3990. https://doi.org/10.1007/s10531-010-9941-7

Yu, L., Wang, J., & Gong, P. (2013). Improving 30 m global land-cover map FROM-GLC with time series MODIS and auxiliary data sets: A segmentation-based approach. *International Journal of Remote Sensing*, *34*(16), 5851–5867. https://doi.org/10.1080/01431161.2013.798055

Zarco-González, M. M., Monroy-Vilchis, O., & Alaníz, J. (2013). Spatial model of livestock predation by jaguar and puma in Mexico: Conservation planning. *Biological Conservation*, *159*, 80–87. https://doi.org/10.1016/j.biocon.2012.11.007

Zhang, L., Zhang, L., & Du, B. (2016). Deep Learning for Remote Sensing Data: A Technical Tutorial on the State of the Art. *IEEE Geoscience and Remote Sensing Magazine*, *4*(2), 22–40. https://doi.org/10.1109/MGRS.2016.2540798

Zhang, Y., Du, Y., Ling, F., Fang, S., & Li, X. (2014). Example-Based Super-Resolution Land Cover Mapping Using Support Vector Regression. *IEEE Journal of Selected Topics in Applied Earth Observations and Remote Sensing*, *7*(4), 1271–1283. https://doi.org/10.1109/JSTARS.2014.2305652

Zhu, X., Cai, F., Tian, J., & Williams, T. K.-A. (2018). Spatiotemporal Fusion of Multisource Remote Sensing Data: Literature Survey, Taxonomy, Principles, Applications, and Future Directions. *Remote Sensing*, *10*(4), Article 4. https://doi.org/10.3390/rs10040527

Zhu, Z., & Woodcock, C. E. (2014). Continuous change detection and classification of land cover using all available Landsat data. *Remote Sensing of Environment*, *144*, 152–171. https://doi.org/10.1016/j.rse.2014.01.011

Zhu, Z., Wulder, M. A., Roy, D. P., Woodcock, C. E., Hansen, M. C., Radeloff, V. C., Healey, S. P., Schaaf, C., Hostert, P., Strobl, P., Pekel, J.-F., Lymburner, L., Pahlevan, N., & Scambos, T. A. (2019). Benefits of the free and open Landsat data policy. *Remote Sensing of Environment*, *224*, 382–385. https://doi.org/10.1016/j.rse.2019.02.016

Zimbabwe. (2023). In *The World Factbook*. Central Intelligence Agency. https://www.cia.gov/the-world-factbook/countries/zimbabwe/

Zimbabwe Livelihoods Zone Profiles (pp. 1–90). (2010). Zimbabwe Vulnerability Assessment Committee. https://fews.net/sites/default/files/documents/reports/zw_profile_en%20Dec%202010.pdf

Zimbabwe National Elephant Management Plan: 2015-2020 (pp. 1–67). (2016). Zimbabwe Parks and Wildlife Management Authority.

ZIMBABWE NATIONAL ELEPHANT MANAGEMENT PLAN (2021 – 2025) (pp. 1–88). (2021). [National Legislation]. Zimbabwe Parks and Wildlife Management Authority. https://www.cms.int/sites/default/files/document/cms_nlp_zwe_plan_elephant_2021.pdf

Zimbabwe's Fifth National Report to the Convention on Biodiversity (p. 48). (2015). Ministry of Environment, Water and Climate Republic of Zimbabwe. https://www.cbd.int/doc/world/zw/zw-nr-05-en.pdf

Zimmermann, A., Simon, P., Linnell, J., Glickman, J., Marchini, S., Hill, C., & Sandstrom, C. (2023). Introduction. In *IUCN SSC guidelines on human-wildlife conflict and coexistence* (First). IUCN.

ZimStats. (2022). *2022 Population & Housing Census-Preliminary* [Census Preliminary Report]. National Statistics Agency. https://zimbabwe.opendataforafrica.org/anjlptc/2022-population-housing-census-preliminary

APPENDICES

Appendix A

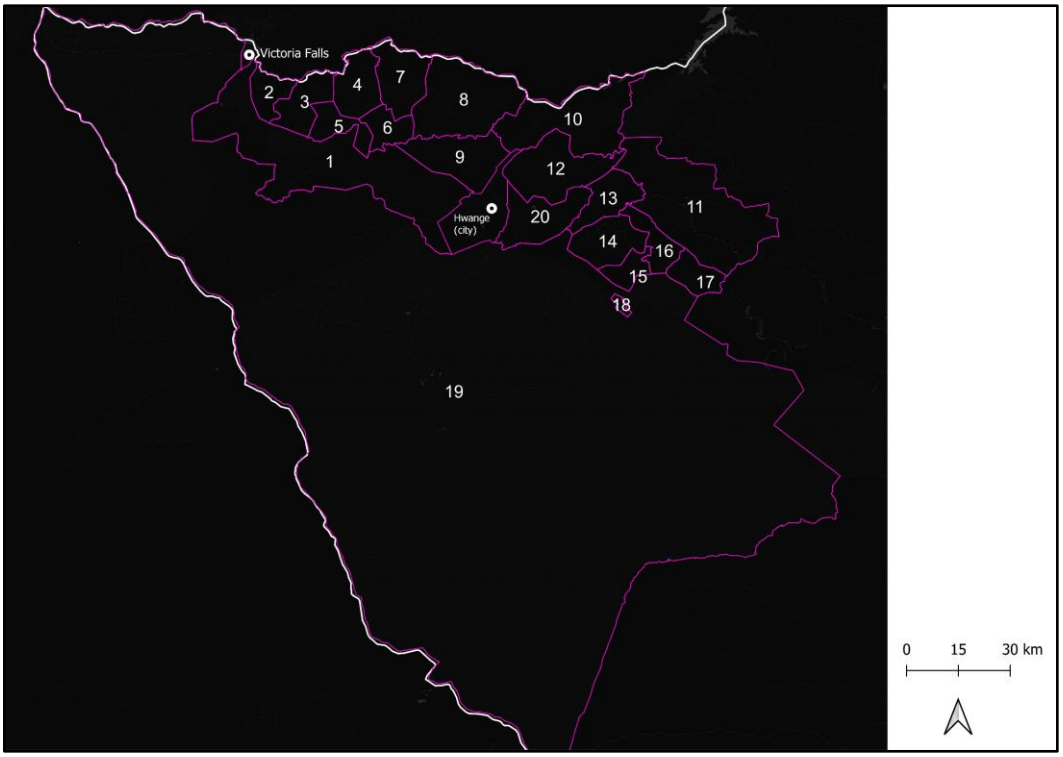

Figure 1.5. Wards of Hwange District. Rural District Wards are identified by number. The cities of Victoria Falls and Hwange are indicated by white circles encasing a black dot.

Table 1.1. Updated Agro-Ecological Zones for Zimbabwe (Manatsa et al., 2020)

Region	Climatic Conditions	Recommend Land Use and Management
I	Annual rainfall > 1000mm but possible to get amounts less than 1000, Probability of exceeding 500mm at least 95%, length of rainfall season > 130days and maximum temperature between 21 and 25C	Suitable for forestry plantations, banana apples, macadamia nuts, coffee, and tea in addition to intensive livestock production. The region is also suitable for long season (late maturing) maize varieties - requiring >130 days to maturity), Irish potato, field peas and soya beans. [Terracing is highly recommended along steep terrains to minimize soil erosion considering the soils are susceptible to erosion due to a weakly developed crumb structure. The soils require regular soil pH monitoring].

IIa	Annual rainfall between 750 and 1000mm (it is not unusual to get amounts below 750 and above 1000 mm in places), Probability of exceeding 500mm at least 90%, length of rainfall season between 120 and 130 days and maximum temperature between 23 and 27C	Suitable for maize varieties requiring 120-130 days to maturity, flue-cured tobacco, groundnuts, Irish potato, cotton and soybean. Barley and wheat are grown under irrigation in the winter and drier months, Intensive livestock production (beef, dairy and poultry) (based on pastures and pen fattening) is also recommended.
IIb	Annual rainfall between 750 and 1000mm (it is not unusual to get amounts below 750 and above 1000 mm in places), Probability of exceeding 500mm at least 80%, length of rainfall season between 115 and 120 days and maximum temperature between 25 and 28C	Suitable for maize varieties requiring 115-120 days to maturity, Cotton, Irish potato, barley, flue-cured tobacco, groundnuts, sorghum, sugar beans, coffee and horticultural crops can be successfully grown. Winter wheat is also grown under irrigation. Intensive livestock production is also recommended in this region.
III	Annual rainfall between 650 and 800mm while some places may receive amounts exceeding 800mm, Probability of exceeding 500mm between 75 and 80%, length of rainfall season between 110 and 120 days and maximum temperature between 25 and 28C	Suitable for maize varieties requiring 110-120 days to maturity. Soybean, groundnuts, cotton and sunflower are also suitable crops in this region. Supplementary irrigation is critical for successful crop production. The region is also suitable for semi-intensive livestock production (beef, dairy and small stock (e.g goats and poultry).
IV	Annual rainfall between 450 and 650mm which may be exceeded in some places within the region, Probability of exceeding 500mm between 60 and 80%, length of rainfall season between 105 and	Suitable for maize varieties requiring 105-120 days to maturity. However, in the absence of irrigation farmers are advised to grow drought tolerant crops such as sorghum (finger millet, pearl millet, water melons and cowpeas. Extensive cattle ranching, rearing of small stock (e.g. goats and poultry) and wildlife are

	120 days and maximum temperature between 27 and 29C	ideal farming systems for this region. [Rainwater harvesting techniques are required to capture the little moisture in the region].
Va	Annual rainfall less than 650mm in the southern areas while Region Va areas in the Zambezi Valley to the north of the country mostly exceed this amount, Probability of exceeding 500mm between 60 and 80%, length of rainfall season between 100 and 120 days and maximum temperature between 28 and 30C	Suitable for extensive cattle ranching and goat production. The region is marginal for drought tolerant crops such as sorghum, finger millet, pearl millet and cowpeas. Sugarcane is an ideal crop under irrigation, particularly in the vertisol and siallitic soils. Tree plantations, mainly oranges, lemons and lime are also recommended where irrigation is available. This region is also suitable for extensive game-ranching and tourism.
Vb	Annual rainfall below 600mm, Probability of exceeding 500mm less than 60%, length of rainfall season less than 110 days and maximum temperature between 28 and 32C	Tree plantations, mainly oranges, lemons and lime are recommended where irrigation is available. This region is also suitable for extensive cattle ranching, goats and wildlife tourism.

Appendix B

Table 1.0 Advantages and limitations of scaling methods.

Scaling method	Advantages	Limitations	References
<u>Upscaling</u>			
Mean and Median Aggregation	Simple to implement. No additional data needed.	Distorts complex shapes. Ignores spatial heterogeneity and correlation.	(Raj et al., 2013; Riitters et al., 1997)7/19/2023 7:46:00 AM
Majority Rules Aggregation	Simple to understand and implement. No additional data needed.	Assumes within-pixel values are homogenous. Small effects can be magnified. Rare land covers may be eliminated. Often produces clumpy landscapes. Ignores spatial correlation.	(Frazier, 2014; Frazier et al., 2021; He et al., 2002; Holt et al., 1996; Raj et al., 2013; Xu et al., 2020)
Central Pixel Resampling	Simple to understand and implement. No additional data needed.	Ignores spatial heterogeneity and correlation.	(Bian & Butler, 1999; Raj et al., 2013)
Random Rule-Based Aggregation	Maintains land cover type proportions. No additional data needed. Maintains spatial patterns.	Assumes within-pixel values are homogenous. Disaggregates categories. Ignores spatial correlation.	(He et al., 2002, p. 200)
Moving Window Data Aggregation	Preserves information about the spatial structure of underlying heterogeneity. No additional data needed.	Very fine grains across global extents have a high computational demand.	(L. J. Graham et al., 2019)
Point-Centered Distance-Weighted Moving Window	Maintains proportion of land cover types. Spatial correlation can be included. No additional data needed.	Optimizing parameters is challenging.	(Gardner et al., 2008; Raj et al., 2013)

Object-Specific Upscaling (OSU)	Object-specific spatial information considered. Multiscale spatial thresholds defined.	Ignores spatial correlation.	(Hay et al., 2001)
OSU w/Moran's Index	Extracts features using the Moran index.	Considers spatial correlation.	(Bihamta Toosi et al., 2020)
Fractals	Useful for scaling resistance surfaces. No additional data needed.	Complex to understand. Variation must be independent of scale. Features obtained at one scale cannot be generalized to other scales.	(Galpern & Manseau, 2013) (Galpern & Manseau, 2013)
Downscaling			
Resampling (bilinear, cubic convolution, etc.)	Simple to understand and implement. No additional data needed.	Uncertainties and biases present in the original data are propagated into models. Can falsely suggest a higher level of heterogeneity is present.	(Frazier et al., 2021; Sillero & Barbosa, 2021)
Intensity, Hue, and Saturation Pansharpening	Simple to understand and implement. No additional data needed.	Spectral distortions possible. Can create spatial artifacts.	(Gillespie et al., 1987; Haydn et al., 1982)
Deep Learning Pansharpening	Produces fewer distortions and artifacts.	Requires additional data. High computational demand. Large number of training data required. Higher-level machine learning expertise needed.	(Azarang & Ghassemian, 2017; W. Huang et al., 2015; Seo et al., 2020; J. Yang et al., 2017)
Bayesian Pansharpening	Accounts for uncertainty. Potential for greater accuracy than linear regression-based methods.	Requires additional data. High computational demand. Higher-level machine learning expertise needed. Must identify an appropriate statistical model for image representation.	(Pandit & Bhiwani, 2021)
Kalman Filtering	Integrates observations and their uncertainties. Does not require explicit parameter tuning.	Requires additional data. More complex to implement and understand.	(G. Welch & Bishop, 1997)

	Considers spatial autocorrelation.		
Taylor Series Expansion Methods, including PSM	Simple to understand.	Unwieldy with many variables. Challenging to compute.	(Malenovský et al., 2007; Pelgrum, 2000; H. Wu & Li, 2009)
Spatial Area-to-Point (ATP) Kriging	No additional data needed. Can report uncertainty estimates. Can consider heterogeneity in samples.	Involved process for calculating the punctual semivariogram required.	(Goovaerts, 2006; Kyriakidis, 2004; Yoo & Kyriakidis, 2006)
Geographically Weighted ATP Regression Kriging	Considers spatial correlation. Handles spatial heterogeneity.	Requires additional data. Computationally intensive.	(Jin et al., 2018)
Multiscale Geographically Weighted Regression Kriging	Enriches spatial details/information.	Complex and time-consuming. Slight smoothing effect.	(C. Yang et al., 2019)
Super-Resolution Mapping	Consider mixed pixels. Use theories of maximum spatial dependency to guide sub-pixel placement.	Requires additional data. Challenging to compute. Does not consider the local details or the structure of coarse patches.	(Frazier, 2015c; X. Li et al., 2014)
Generalized Additive Modeling	Accommodates complex and nonlinear patterns.	Requires additional data.	(Hoskins et al., 2016)
Multinomial Logistic Regression and Bayes Theorem	Accommodates nonlinear patterns.	Requires additional data. Determining probability of priors can be challenging.	(Dendoncker et al., 2006)
Regression-Based Methods, Including Machine Learning	Can be simple to understand and implement, although this varies. Some methods are particularly adept at handling noise.	Require additional data. Statistical assumptions should be met.	(Kaheil et al., 2008; Sharifi et al., 2019)

Fractals	Useful for scaling resistance surfaces. No additional data needed.	Complex to understand. Variation must be independent of scale. Features obtained at one scale cannot be generalized to other scales.	(Galpern & Manseau, 2013)

Appendix C

Table 3.8. Satellite sensors and their respective bands and reflectance captured.

Satellite sensor	Band number	Spectral band	Central wavelength
Planet	1	Blue	
	2	Green	
	3	Red	
Sentinel-2 MSI Level 2A	1	Aerosols	443.9nm (S2A) / 442.3nm (S2B)
	2	Blue	496.6nm (S2A) / 492.1nm (S2B)
	3	Green	560nm (S2A) / 559nm (S2B)
	4	Red	664.5nm (S2A) / 665nm (S2B)
	5	Red Edge 1	703.9nm (S2A) / 703.8nm (S2B)
	6	Red Edge 2	740.2nm (S2A) / 739.1nm (S2B)
	7	Red Edge 3	782.5nm (S2A) / 779.7nm (S2B)
	8	NIR	835.1nm (S2A) / 833nm (S2B)
	8A	Red Edge 4	864.8nm (S2A) / 864nm (S2B)
	9	Water vapor	945nm (S2A) / 943.2nm (S2B)
	11	SWIR 1	1613.7nm (S2A) / 1610.4nm (S2B)
	12	SWIR 2	2202.4nm (S2A) / 2185.7nm (S2B)

Landsat 8 OLI SR product, level 2	1	Ultra blue, coastal aerosol	443nm
	2	Blue	483nm
	3	Green	560nm
	4	Red	660nm
	5	NIR	865nm
	6	SWIR 1	1650nm
	7	SWIR 2	2220nm

Table 3.9. Vegetation indices used in land cover classification.

Index	Formula	Source
NDVI	$\frac{NIR - Red}{NIR + Red}$	(Rouse et al., 1974)
Normalized difference red edge index (NDRE)	$\frac{NIR - Red\,Edge}{NIR + Red\,Edge}$	(Barnes et al., 2000)
Normalized difference in green/red index (NGRDI)	$\frac{Green - Red}{Green - Red}$	(Tucker, 1979)

Table 3.10. Error matrices for top-performing land cover classifications.

Landsat 2019 Wet									
	Ag	Thicket	Soil	Water	Lowland vegetation	Open Forest	Closed Forest	Burn	Total
Ag	31		1						32
Thicket		25	1						26
Soil	1	2	19						22
Water				33					33
Lowland vegetation					30				30
Open Forest						30	1		31
Closed Forest						1	33		34
Burn									0
Total	32	27	21	33	30	31	34	0	208
Planet 2019 Wet									
	Ag	Thicket	Soil	Water	Lowland vegetation	Open Forest	Closed Forest	Burn	Total

Ag	28	1	3						32
Thicket	1	25							26
Soil	1	1	20						22
Water				28	1	3	`		32
Lowland vegetation					30				30
Open Forest				1		30			31
Closed Forest		1			1	1	31		34
Burn									0
Total	30	28	23	29	32	34	31	0	207
Landsat 2019 Dry									
	Ag	Thicket	Soil	Water	Lowland vegetation	Open Forest	Closed Forest	Burn	Total
Ag	31		1				2		34
Thicket		24							24
Soil	1		29		1			1	32
Water				29					29
Lowland vegetation		1			27				28
Open Forest						28	1		29
Closed Forest							28		28
Burn								32	32
Total	32	25	30	29	28	28	31	33	236
Sentinel 2019 Dry									
	Ag	Thicket	Soil	Water	Lowland vegetation	Open Forest	Closed Forest	Burn	Total
Ag	31		1				2		34
Thicket		24							24
Soil	3	1	27					1	32
Water				29					29
Lowland vegetation	2				23		2		27
Open Forest						29			29
Closed Forest		1					27		28
Burn							1	31	32
Total	36	26	28	29	23	29	32	32	235

Table 3.11. Area of top performing land cover classification models.

Square kilometers	Land cover class	Season	Satellite

252.225674	Agriculture	Wet	Landsat
541.764942	Shrubland	Wet	Landsat
128.586093	Soil	Wet	Landsat
4.110761	Water	Wet	Landsat
38.492769	Lowland vegetation	Wet	Landsat
203.765858	OpenCanopyForest	Wet	Landsat
903.986187	ClosedCanopyForest	Wet	Landsat
143.356101	Agriculture	Wet	Planet
461.391357	Shrubland	Wet	Planet
143.335283	Soil	Wet	Planet
24.648489	Water	Wet	Planet
135.075866	Lowland vegetation	Wet	Planet
153.468355	OpenCanopyForest	Wet	Planet
1012.354692	ClosedCanopyForest	Wet	Planet
180.351044	Agriculture	Dry	Landsat
416.345408	Shrubland	Dry	Landsat
123.320256	Soil	Dry	Landsat
4.538535	Water	Dry	Landsat
75.83907	Lowland vegetation	Dry	Landsat
104.740063	OpenCanopyForest	Dry	Landsat
1120.659285	ClosedCanopyForest	Dry	Landsat
47.142927	Burn	Dry	Landsat
145.333862	Soil	Dry	Sentinel
3.234742	Water	Dry	Sentinel
79.81083	Lowland vegetation	Dry	Sentinel
92.130851	OpenCanopyForest	Dry	Sentinel
1094.652954	ClosedCanopyForest	Dry	Sentinel
75.251358	Burn	Dry	Sentinel

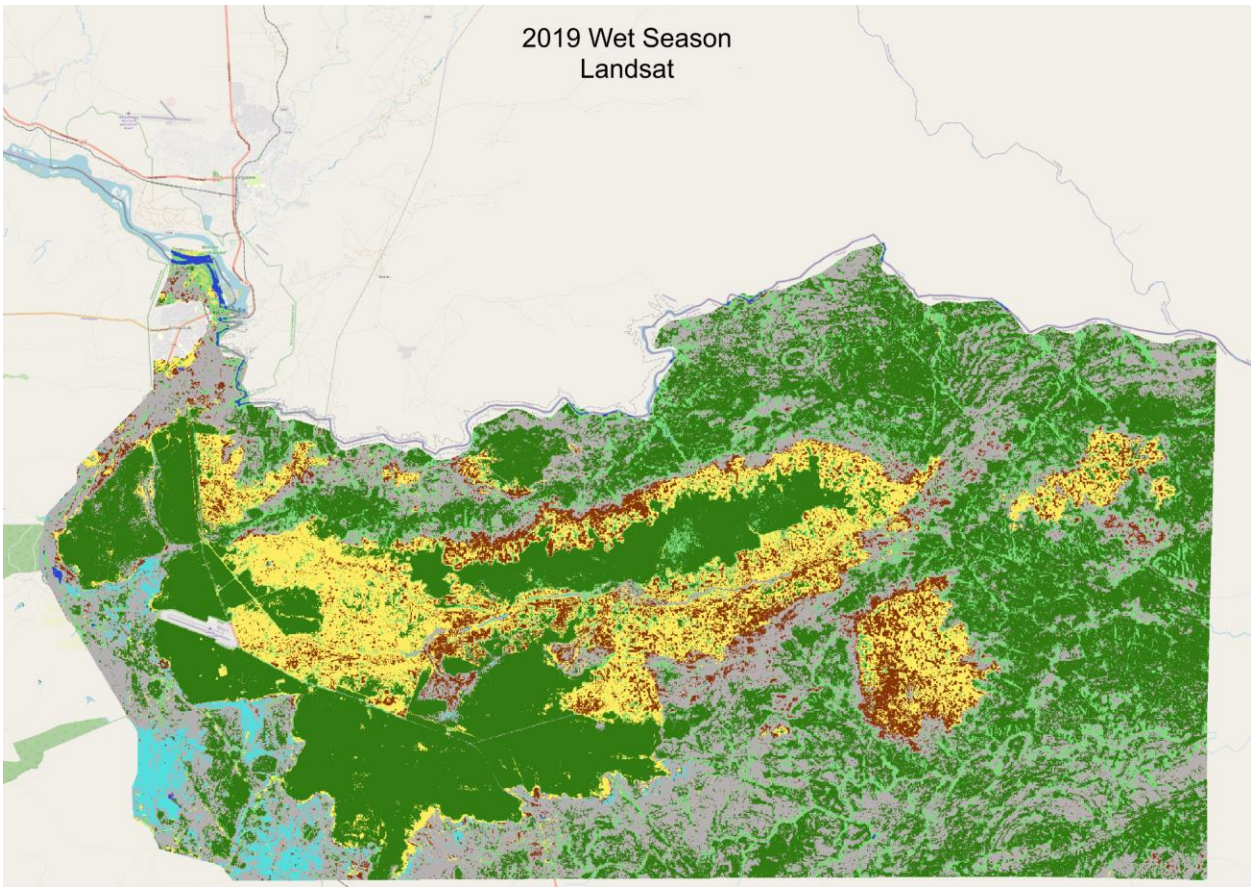

Figure 3.11. 2019 Wet Season Classified using Landsat Imagery. Cropland is in yellow, bare soil in brown, closed canopy forest in dark green, open canopy forest in light green, shrubland/thicket in gray, water in dark blue, and lowland vegetation in light blue.

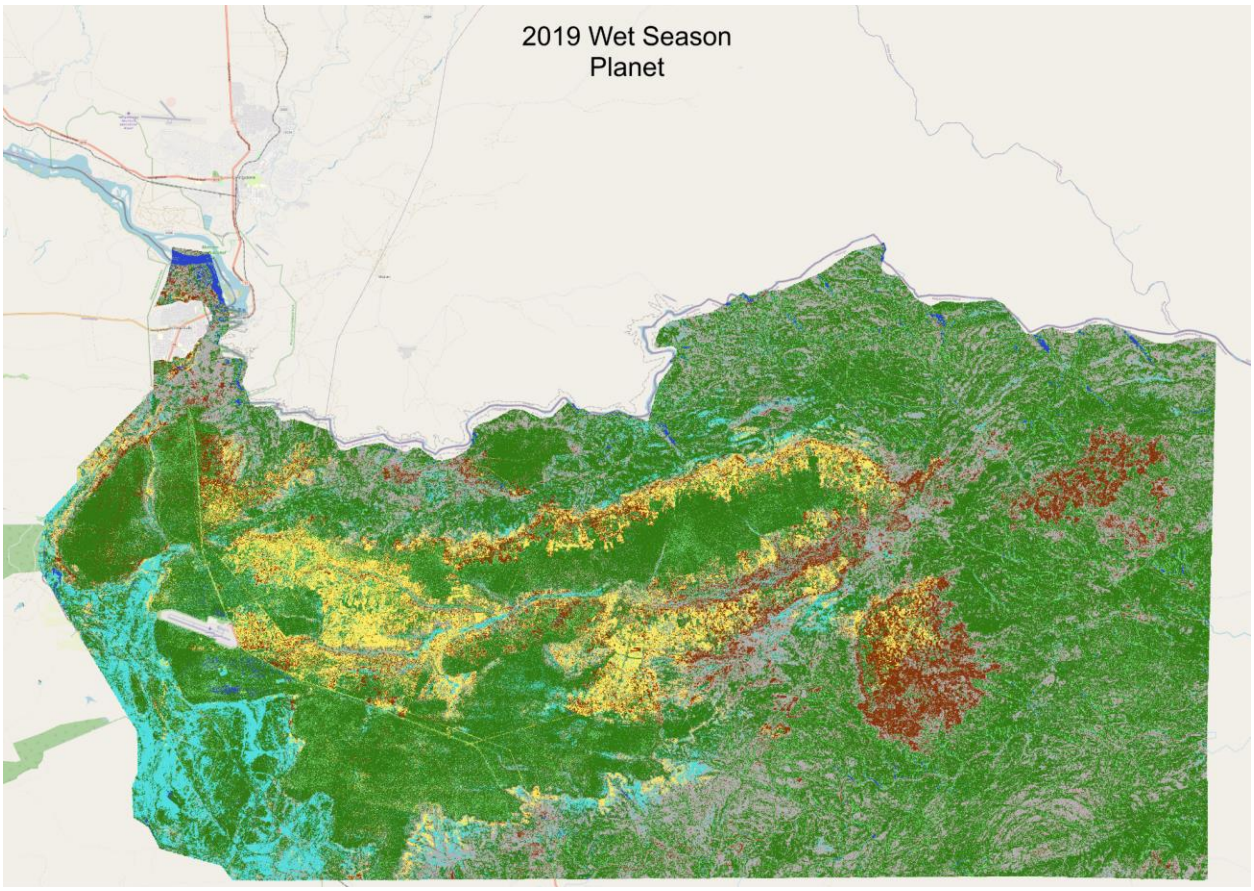

Figure 3.12. 2019 Wet Season Classified using Planet Imagery. Cropland is in yellow, bare soil in brown, closed canopy forest in dark green, open canopy forest in light green, shrubland/thicket in gray, water in dark blue, and lowland vegetation in light blue.

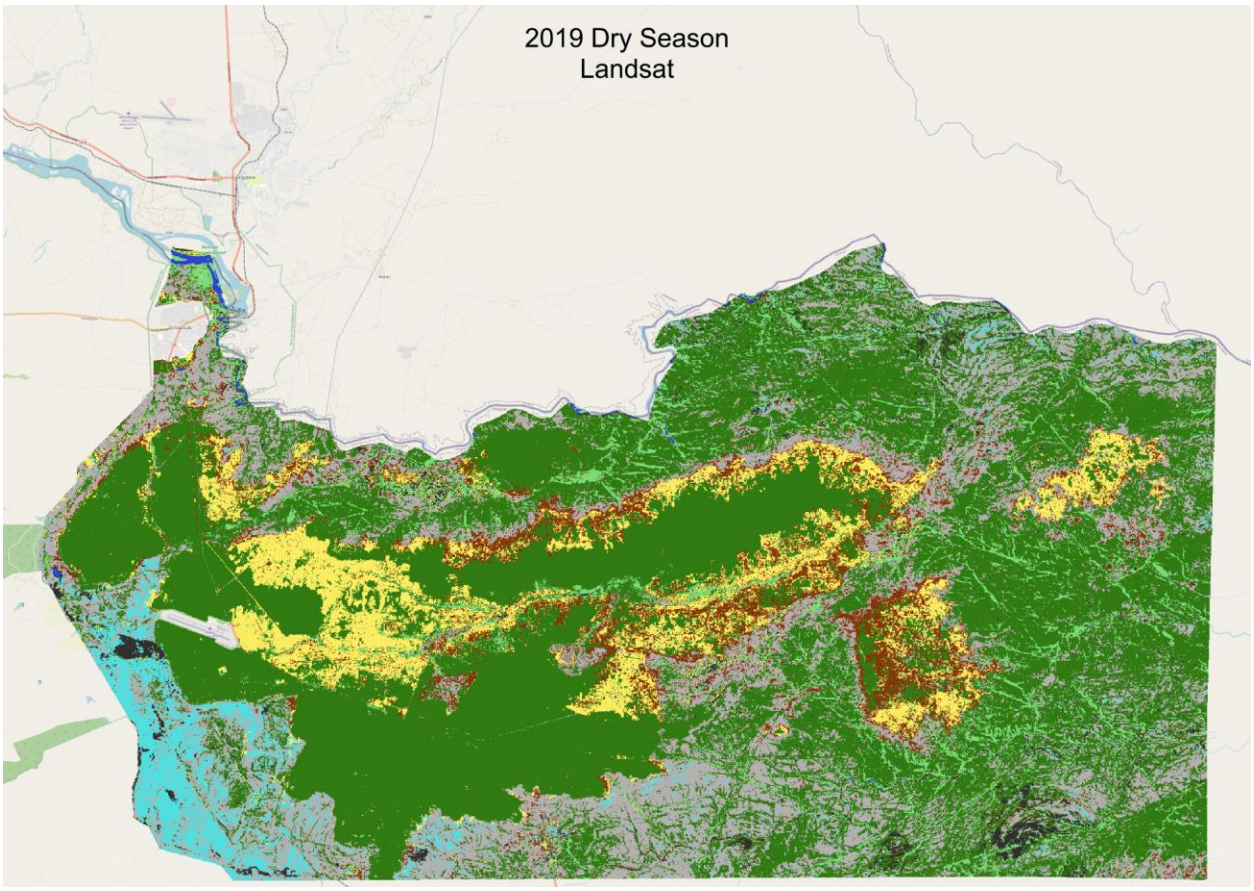

Figure 3.13. 2019 Dry Season Classified using Landsat Imagery. Cropland is in yellow, bare soil in brown, closed canopy forest in dark green, open canopy forest in light green, shrubland/thicket in gray, water in dark blue, and lowland vegetation in light blue. Burn scars are in black.

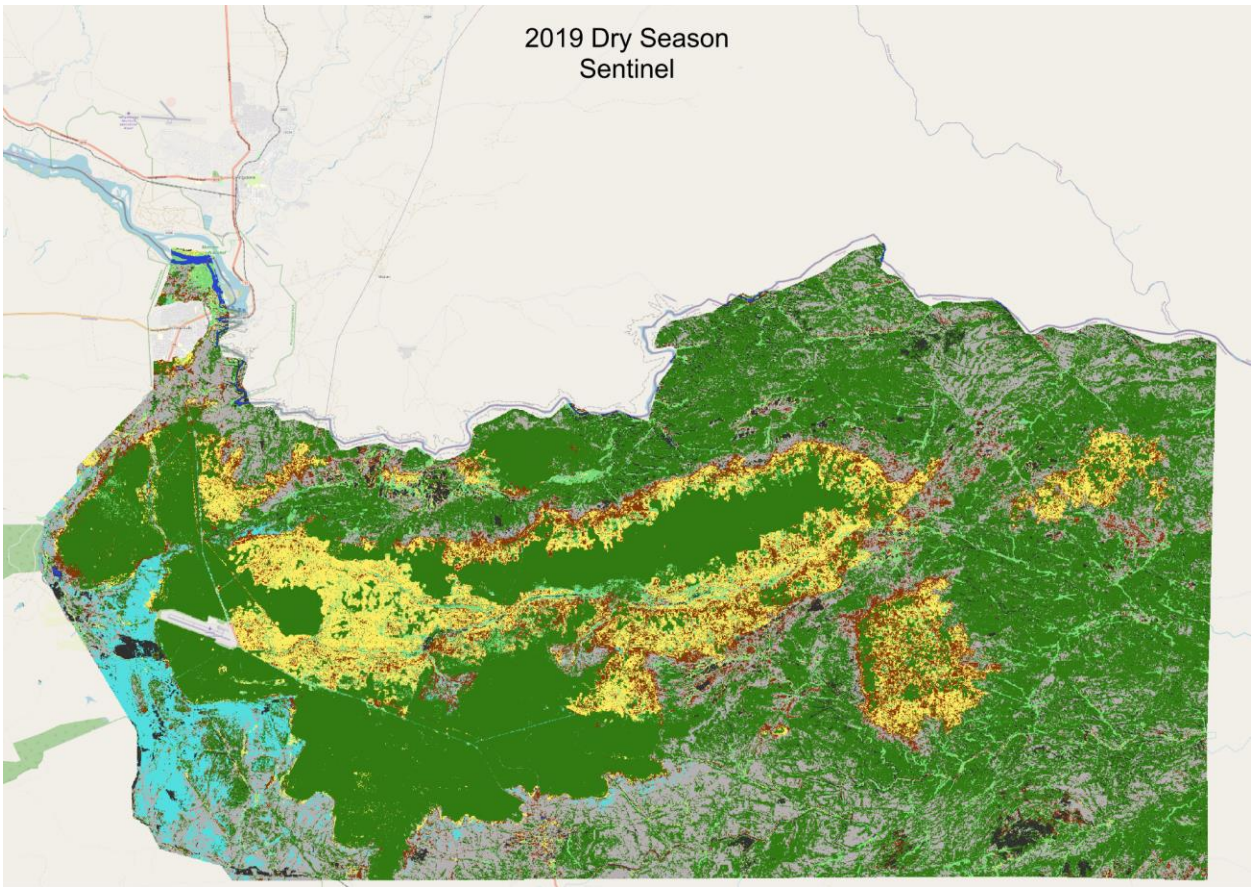

Figure 3.14. 2019 Dry Season Classified using Sentinel Imagery. Cropland is in yellow, bare soil in brown, closed canopy forest in dark green, open canopy forest in light green, shrubland/thicket in gray, water in dark blue, and lowland vegetation in light blue. Burn scars are in black.

Table 3.12. NGRDI values of central tendency for respective land cover classifications of top performing models. Index spans from -1.0 to 1.0.

Season	Satellite	Class	MIN	MAX	RANGE	MEDIAN
Dry	Sentinel	Ag	0.075	0.493	0.419	0.261
Dry	Sentinel	Thicket	0.059	0.478	0.419	0.208
Dry	Sentinel	Bare soil	0.092	0.854	0.762	0.202
Dry	Sentinel	Water	0.003	0.306	0.303	0.014
Dry	Sentinel	Lowland vegetation	0.058	0.389	0.331	0.224
Dry	Sentinel	Forest	0.069	0.589	0.520	0.186
Dry	Sentinel	Burn	0.027	0.343	0.316	0.120
Dry	Landsat	Ag	0.073	0.518	0.445	0.269
Dry	Landsat	Thicket	0.096	0.356	0.260	0.172
Dry	Landsat	Bare soil	0.041	0.532	0.491	0.272
Dry	Landsat	Water	0.004	0.236	0.232	0.013
Dry	Landsat	Lowland vegetation	0.035	0.370	0.335	0.192
Dry	Landsat	Forest	0.024	0.424	0.401	0.162
Dry	Landsat	Burn	0.022	0.354	0.332	0.131

Wet	Planet	Ag	-0.287	0.436	0.723	-0.156
Wet	Planet	Thicket	-0.333	0.469	0.803	-0.088
Wet	Planet	Bare soil	-0.478	0.193	0.671	-0.179
Wet	Planet	Water	-0.247	1.000	1.247	0.207
Wet	Planet	Lowland vegetation	-0.253	0.542	0.795	-0.060
Wet	Planet	Forest	-1.000	1.000	2.000	0.024
Wet	Landsat	Ag	0.052	0.390	0.337	0.128
Wet	Landsat	Thicket	0.035	0.478	0.443	0.116
Wet	Landsat	Bare soil	0.005	0.762	0.757	0.152
Wet	Landsat	Water	0.003	0.342	0.339	0.105
Wet	Landsat	Lowland vegetation	0.004	0.272	0.268	0.102
Wet	Landsat	Forest	0.024	0.218	0.194	0.091

Table 3.13. Agricultural and forested areas' NDVI measures for top performing models. Note Planet Quarterly Basemaps used for classification do not include a near infrared band at this time, thus NDVI can not be calculated using this land cover model. NDVI ranges from -1 to 1 with higher values indicating greater greenness or vegetation health.

			Mean	StDev	Max	Min
Wet						
	L8	Forest	0.70815	0.047624	0.912206	0.073436558
	L8	Ag	0.569624	0.067376	0.84635	-0.50423777
Dry						
	L8	Forest	0.34326	0.047817	0.852888	-0.39529926
	L8	Ag	0.296195	0.053476	0.66482	-0.06607163
	S2	Forest	0.339785	0.049023	0.852888	-0.27344242
	S2	Ag	0.306048	0.059946	0.705849	-0.06351516